DISSERTATION

DISCOVERY AND CHARACTERIZATION OF THE SLAC COMPLEX AND ITS ROLE IN

ACTIN POLYMERIZATION DURING CLATHRIN-MEDIATED ENDOCYTOSIS

Submitted by

Daniel Feliciano

Department of Biochemistry and Molecular Biology

In partial fulfillment of the requirements

For the Degree of Doctor of Philosophy

Colorado State University

Fort Collins, Colorado

Summer 2013

Doctoral Committee:

    Advisor: Santiago Di Pietro

    James Bamburg
    Norman Curthoys
    Chaoping Chen
    Noreen Reist

ABSTRACT

DISCOVERY AND CHARACTERIZATION OF THE SLAC COMPLEX AND ITS ROLE IN

ACTIN POLYMERIZATION DURING CLATHRIN-MEDIATED ENDOCYTOSIS

Endocytosis is the process by which cells control the lipid and transmembrane protein compositions in order to comply with certain requirements essential for cellular function. The different forms of endocytosis provide the cell with a discriminatory system where specific cargoes are selected, packed and internalized when there is a particular physiological demand. Given the importance of endocytic internalization routes for a variety of cellular processes, it is not surprising that defects in the protein machinery involved in these pathways leads to pathologies. Examples of some metabolic disorders associated to defects in adaptor or receptor function include autosomal recessive and familial hypercholesterolemia. In other cases, mutations in actin regulatory proteins, such as WASp, can cause many blood disorders that include primary immunodeficiency and thrombocytopenia.

Clathrin-mediated endocytosis (CME) is a fundamental pathway conserved from yeast to humans that proceeds by forming a clathrin coat at the plasma membrane followed by the recruitment of proteins that promote membrane curvature, actin polymerization, and scission. CME is the mayor route for nutrient uptake, distribution of membrane components, and receptor internalization. During CME, branched actin polymerization nucleated by the Arp2/3 complex provides force needed to drive vesicle internalization. Las17 (WASp) is the strongest activator of the Arp2/3 complex in yeast cells, it is not autoinhibited, and arrives to endocytic sites 20 seconds before actin polymerization begins. One of the most outstanding questions in the field

has been how Las17 is inhibited during the initial 20 seconds after its arrival to sites of endocytosis.

In this dissertation, the discovery and characterization of a stable complex between Las17 and the clathrin adaptor Sla1 is described, in which Las17 is inhibited. This interaction is direct, multivalent, and strong, and was mapped to novel Las17 polyproline motifs that are simultaneously class I (RxxPxxP) and class II (PxxPxR). *In vitro* pyrene-actin polymerization assays established that Sla1 inhibition of Las17 activity depends on a new class I/II Las17 polyproline motifs. The inhibition is based on competition between Sla1 and monomeric actin for binding to sequences comprising a novel G-actin binding site in Las17 that is also characterized. The Las17 novel G-actin binding module 1 (LGM1) requires two sets of arginine-rich sites for normal Las17 function *in vitro* and *in vivo*.

Furthermore, live cell imaging showed the interaction with Sla1 is important for normal Las17 recruitment to endocytic sites, its inhibition during the initial 20 seconds, and for efficient endocytosis. Within this complex, Las17 requires full length Bzz1, a membrane tubulation protein, for its activation *in vitro* through a mechanism that does not depend on complex dissociation. Since Sla1 and Las17 regulate actin polymerization during clathrin-mediated endocytosis, this complex has been named SLAC.

The discovery and characterization of the SLAC complex help to define the negative and positive mechanisms regulating Las17 activity and answer one of the most outstanding questions in the field. This work also sets the stage to decipher the roles of other WASp homologues in mammalian cells. Overall, findings reported here advance our understanding of the regulation of actin polymerization by Las17 during clathrin-mediated endocytosis.

ACKNOWLEDGMENTS

TABLE OF CONTENTS

LIST OF FIGURES

CHAPTER 1

INTRODUCTION

1.1 Overview

The main goal of this dissertation is to understand how the Arp2/3 complex nucleation promoting factor Las17 is regulated to provide the cell with a well-timed mechanism for actin assembly at sites of endocytosis. The studies presented here identify and characterize different aspects of Las17 control including novel binding sequences and protein regulators.

The actin cytoskeleton is essential for a variety of functions in eukaryotic cells. Some important processes requiring actin assembly include cytokinesis, cell motility and endocytosis. Clathrin-mediated endocytosis (CME) is a fundamental endocytic process due to its importance in down regulation of signal transduction events, virus internalization, and nutrient uptake. During CME proteins mediating membrane curvature and regulating the organization of the actin cytoskeleton have essential roles in generating invaginations of the plasma membrane at endocytic sites. This is essential for the formation of a clathrin coated pit that concentrates cargo, and the internalization and scission of vesicles from the plasma membrane. Given the importance of actin polymerization during endocytic internalization it is not surprising that defects in protein machineries involved in these pathways lead to pathologies.

The primary cellular factor involved in actin nucleation in endocytosis is the Arp2/3 complex. The Arp2/3 complex requires the interaction with nucleation promoting factors (NPFs) for its activation to nucleate actin filaments. The strength with which these NPFs stimulate actin

polymerization by Arp2/3 complex, ranges greatly with Las17 reported to be the strongest in *saccharomyces cerevisiae*. Las17 arrives to endocytic sites with the same timing as other components of the coat module, about 20 seconds before actin assembly is initiated. To understand the regulation of the actin cytoskeleton in endocytosis, it is essential to determine the mechanism that restricts actin assembly to late stages of the endocytic internalization pathway.

This dissertation, reports the discovery of a large biochemically stable complex termed SLAC, and its relevance for normal regulation of actin polymerization and endocytosis in live cells (Chapter 2). These findings on which I am the first author were published in the Molecular Biology of the Cell (MBoC) in 2012. Also included here is the characterization of a novel G-actin binding module in Las17 as a key component of SLAC positive and negative regulation, and a model for the mechanism of SLAC activation dependent on Bzz1 (Chapter 3). In addition, a protocol is included for the analysis of clathrin-adaptor interactions in yeast published as a methods article on which I am first author in the Journal of Visualized Experiments (JoVE) in 2011 (Appendix). This methods article is based on work I did as a third author in a study that established Sla1, one of the SLAC complex components, as a bona fide clathrin adaptor, which was published in the European Molecular Biology Organization (EMBO) Journal in 2010.

To understand the findings presented in this dissertation, certain general concepts of endocytic trafficking and regulation of actin polymerization will be discussed. Different routes of endocytosis and their functions in yeast and mammalian cells for cargo uptake will be discussed. Then, the mechanisms put in place by the cell to maintain the balance between the monomeric actin pool and the actin filaments used for membrane remodeling events will be discussed. The importance of understanding the control of Las17 NPF activity as model for the regulation of WASp in mammals will also be established (Chapter 1). A list of acronyms and abbreviations is

provided to simplify the reading of this dissertation (Appendix). Most of the content of this dissertation will present the discovery of the SLAC complex (Chapter 2) and new insights on the regulation of the SLAC complex and the characterization of a novel G-actin binding motif in Las17 (Chapter 3). A summary of the findings will be presented in Chapter 4.

1.2 Endocytic trafficking

Eukaryotic cells are internally organized by forming a well-structured membrane-bound compartmentalized system suitable for communication between the inner and the outer world. This allows a strict control of what is coming in or out of the cell. The extracellular-leaflet of the plasma membrane is the platform used by cells to communicate with the environment that surrounds them, and that is why its composition must be highly regulated. Endocytosis is the process by which cells control the lipid and transmembrane protein compositions to comply with certain requirements essential for cellular function. This process encompasses the *de novo* formation of an internal membrane-bound microenvironment or vesicle originated from the plasma membrane. In this way lipids, integral proteins, small particles, pathogens and extracellular fluids become fully internalized by the cell. The fate of each cargo in these vesicles is pre-determined by sorting signals that control the recruitment of diverse proteins that orchestrate trafficking of the vesicular components within the cell.

Compartments such as the endosome and lysosome play important roles during the sorting, recycling and disposal of endocytic cargoes. In some cases, extracellular components are internalized by endocytosis, processed inside the cell and later secreted or re-exposed at the plasma membrane through a morphological opposite pathway known as exocytosis. A good example of this mechanism occurs for the amyloid precursor protein (APP). APP is internalized

through clathrin-mediated endocytosis and cleaved inside of neurons to produce the amyloid beta (Aβ), which is later exocytosed/secreted in the brain [1]. The internalization of pathogens, which are processed and presented on the surface by immune cells, is another example of a route involving the endosomal trafficking system. Transcytosis in polarized cells, such as epithelial cells, allows the transport of cargoes from the apical side to the basolateral side of the cell. The equilibrium between endo-and exocytosis maintains the size of the cell, and the control of this equilibrium allows the communication between the cell and its environment to be precisely regulated.

Down regulation of signal transduction events mediated by endocytosis of transmembrane receptors, which can interact with extracellular ligands, can adjust the sensitivity of cells to external signals. Nevertheless, the role for endocytosis is not restricted to simply block the interactions of the cell with the outer world, but is also essential for a broader spectrum of physiological processes. Some of the key processes regulated by endocytosis include but are not limited to nutrient uptake, reorganization of plasma membrane lipid components, cell migration and antigen presentation. Furthermore, pathogens such as viruses often take advantage of this pathway to mediate their internalization to infect cells [2]. In addition, endocytosis is known to play key roles in the activation of many intracellular signalling cascades [3]. Despite the knowledge we have about the critical functions of endocytosis many question about its regulation remain unanswered.

There are many routes of endocytic uptake employed by cells and these can be grouped by the type of cargo internalized. In addition, different modes of endocytosis can be classified if the vesicles that are formed require a coat protein, or are independent of a coat. Some of the most common endocytic routes include caveolin-associated endocytosis, clathrin-independent

4

endocytic pathways such as macropinocytosis and phagocytosis, and clathrin-dependent endocytosis. Clathrin-dependent pathways have been studied in both mammalian cells and yeast and this dissertation will focus on the latter system.

1.2.1 Routes for endocytosis

The different forms of endocytosis provide the cell with a discriminatory system where specific cargoes are selected, packed and internalized when there is a particular physiological demand. Although most routes of endocytosis are used by the cell for defined cargo transport, constitutive endocytosis also occurs. The requirement of a clathrin coat simplifies the classification of endocytic pathways into those that internalize extracellular material through clathrin-dependent endocytosis (CDE) or clathrin-independent endocytosis (CIE). Caveolin-dependent endocytosis is a form of endocytosis independent of clathrin, but the use of caveolin to form a coat-like structure permits its classification independent from CIE routes into those that are caveolae-associated endocytic pathways (Figure 1.1).

Despite the different forms of endocytic internalization, all of these go through the same basic stages (Figure 1.2). These steps include cargo detection and/or accumulation, coat recruitment (not precent in CIE routes), actin polymerization and plasma membrane curvature, and vesicular scission. In yeast and mammals, plasma membrane curvature and scission are linked to actin polymerization regulation. In yeast, scission proteins such as Rvs161/167p (amphiphysins) and Vps1 (dynamin) influence the organization of actin at the cell cortex and
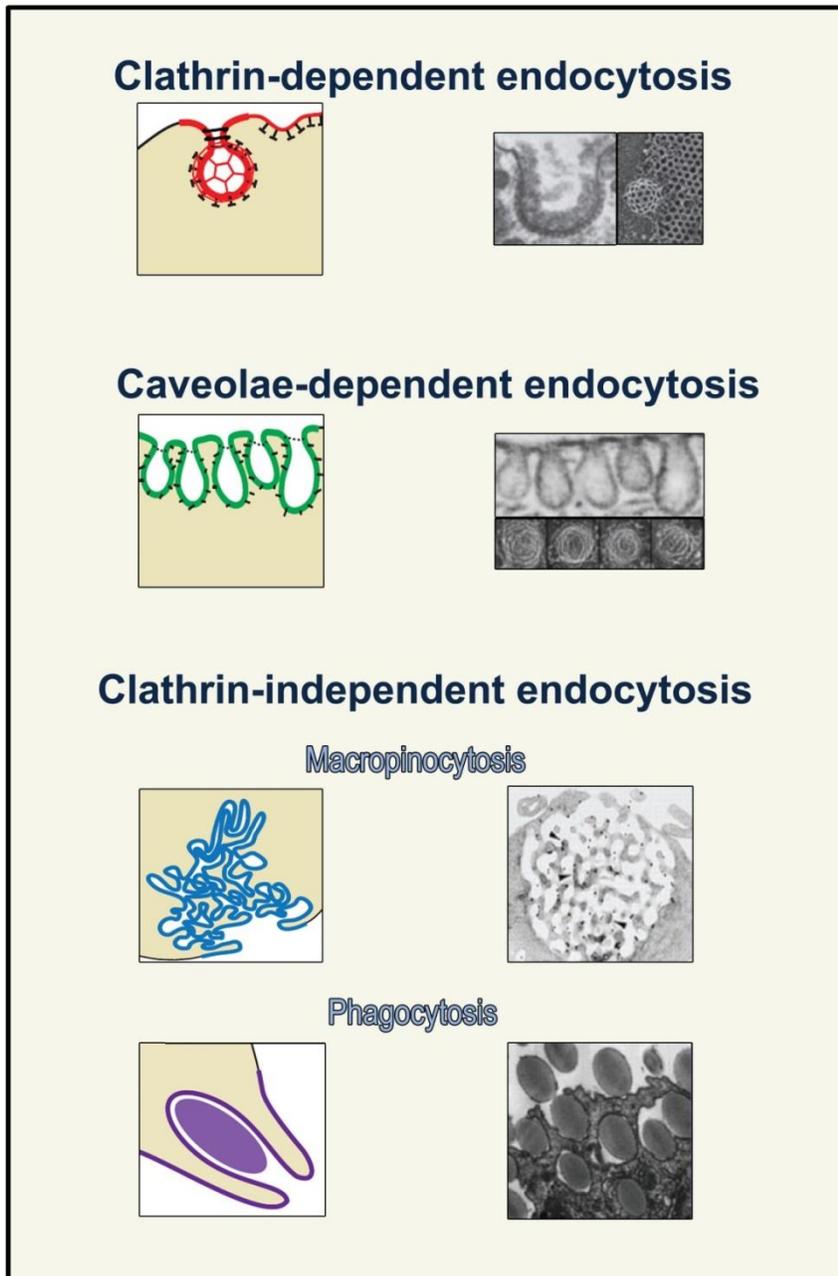
Figure 1. 1
Most commonly studied endocytic portals. Transmission and scanning electron micrographs of several endocytic structures. Cartoons [8] and microscopy images are modified from the following sources: Clathrin-dependent endocytosis [9], Caveolae-dependent endocytosis [10], phagocytosis[8], macropinocytosis [11].The arrowheads in the macropinocytic picture indicate cytoskeletal elements.

6
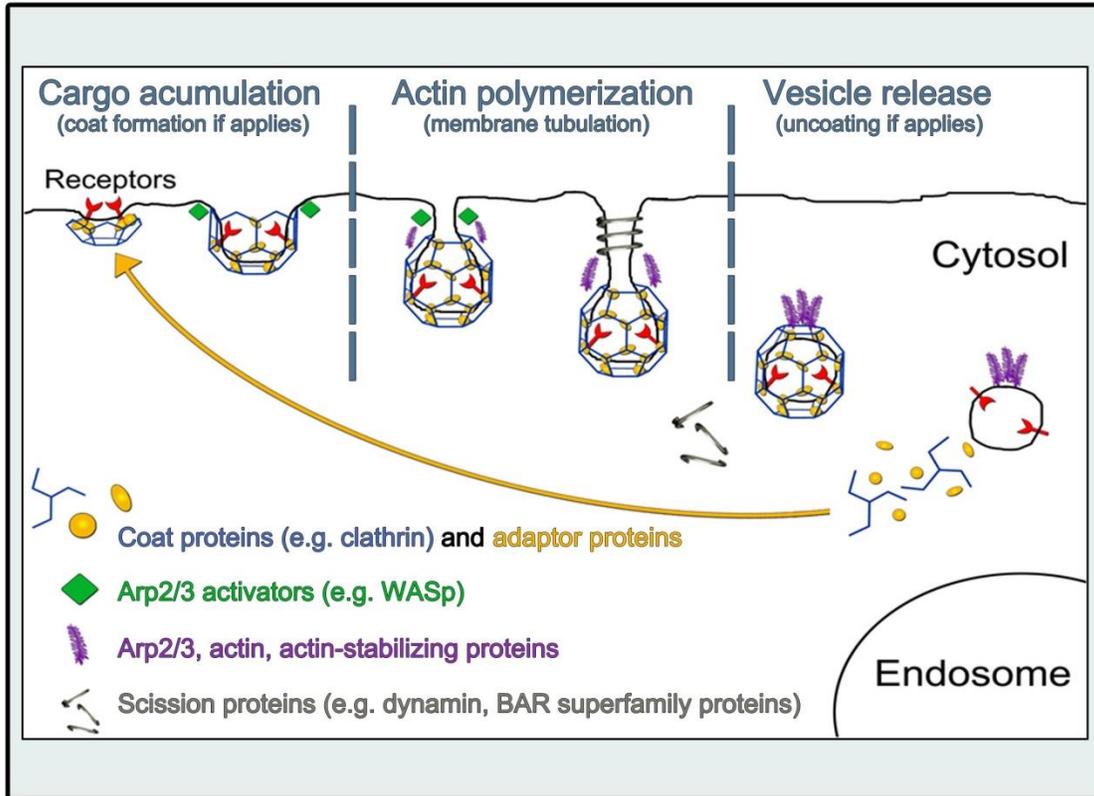
Figure 1. 2
Basic stages for clathrin-dependent or clathrin-independent endocytic internalization. *First*, cargo is detected and accumulated during coat formation (coat formation does not happens in clathrin-independent pathways). *Second*, Arp2/3 and its activators promote actin polymerization and membrane tubulation occurs. *Third*, scission proteins are recruited and cargo containing vesicles are released. In clathrin-dependent pathways vesicle release precede coat disassembly.

work in vesicle scission at the plasma membrane (Figure 1.2) [4-6]. In mammals, the GTPase dynamin olygomerizes to form plasma membrane tubular structures that form the vesicle neck and promote fission and vesicle release [7]. The importance of dynamin for vesicle release has been observed in caveolae and clathrin dependent pathways but its role in CIE is less understood.

Clathrin-dependent endocytosis, also known as clathrin-mediated endocytosis (CME), is a fundamental mode of endocytosis due to its role in down regulation of signal transduction events, virus internalization, distribution of membrane components, and nutrient uptake. The most common forms of CME are receptor-mediated endocytosis and one of the routes used for extracellular fluid uptake known as pinocytosis. Several diseases are caused by mutation of protein components involved in this pathway; however, little is known about the regulation of CME. This process is characterized by the formation of a protein coat of clathrin and adaptors surrounding the forming vesicle (Figure 1.1, 1.2, 1.3). The clathrin coat is assembled during endocytic vesicle formation from individual clathrin "triskelia", which is an hexameric protein complex made of 3 light and 3 heavy chains (Figure 1.2, 1.3) [12, 13]. Clathrin-binding adaptors connect clathrin to the membrane through their association to lipids and/or membrane proteins (Figure 1.3) [14]. The protein-lipid network established by clathrin adaptors is highly dynamic, allowing the coat to assemble and disassemble in a regulated manner [13, 14]. Adaptors also package transmembrane protein cargo, such as receptors, during endocytic clathrin-coated vesicle (CCV) formation. This process is mediated by binding of specific sorting signals in the protein cytoplasmic tail by the adaptor protein [14]. In addition, adaptors contain a multidomain structure that allows them to function as scaffold proteins capable of controlling and organizing protein-lipid and protein-protein interactions through different domains (Figure 1.3).
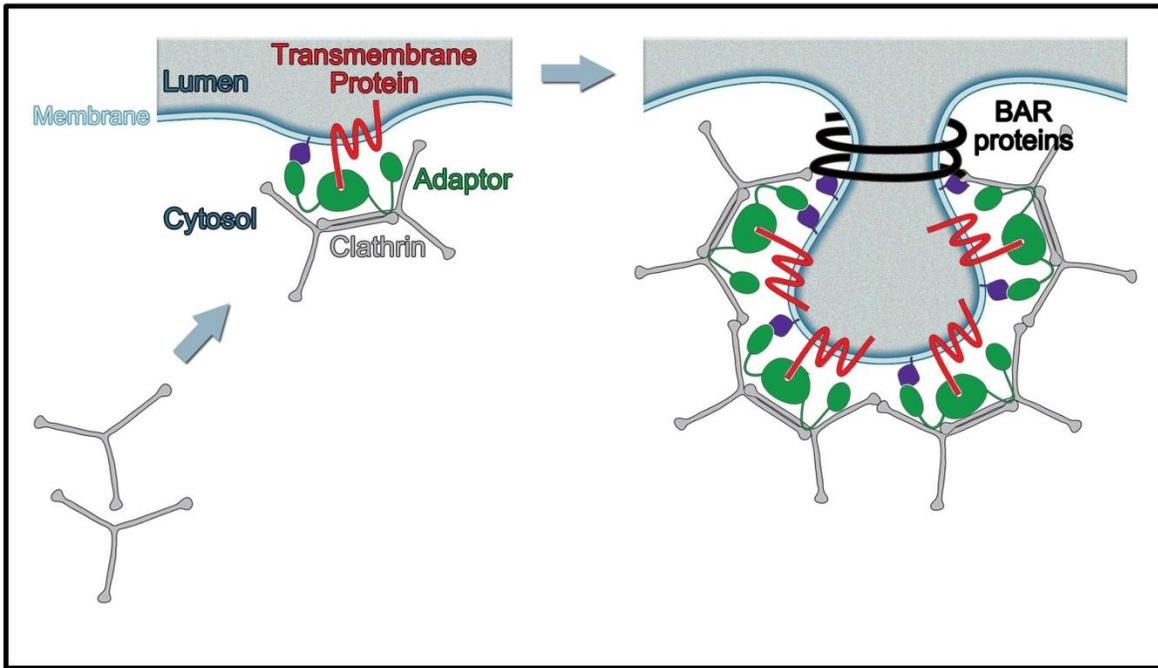
Figure 1. 3
Coat formation during clathrin-mediated endocytosis. Recruitment of clathrin triskelions (*grey*) requires their binding to clathrin-adaptors (*green*) which recognize sorting signals in cargo proteins (transmembrane protein in *red*) or lipids (*purple*) at the plasma membrane. This allows the concentration of cargo within clathrin bound structures. Recruitment of tubulation proteins such as BAR containing proteins allows the formation of clathrin coated pits.

Identification of these adaptor domains and characterization of their roles in coat formation is essential to understand the molecular mechanisms that regulate endocytosis.

Clathrin binding sequences are arranged as short interaction motifs within adaptors and accessory proteins. These sequences are believed to be critical for clathrin recruitment and CCV formation. Two distinct motifs have been identified and named as the clathrin-box (CB) and the W-box (WB) [14]. The consensus CB sequence was identified as L[L/I][D/E/N][L/F][D/E]. Nevertheless, variants of this sequence have been discovered [15, 16]. In addition, the consensus sequence of WB was identified as PWxxW [14, 17]. These motifs (CB and WB) bind to the clathrin heavy chain terminal domain allowing normal vesicle internalization. The networking ability of adaptor proteins facilitates simultaneous recruitment of cargo and clathrin to endocytic sites and regulation of later stages of vesicle internalization. However, the significance of adaptor-clathrin interactions for coat formation has not been clearly established *in vivo.*

An interesting feature of the recognition mechanism by adaptors is the fact that an eukaryotic cell can express several adaptors that only recognize specific types of sorting signals. The most common example of endocytic clathrin adaptor protein is Adaptor Protein-2 (AP-2), which is conserved in all eukaryotes. AP-2 recognizes the sorting signals YXXΦ or (D/E)XXXL(L/I) in transmembrane proteins such as the transferrin receptor but not the NPXY signal in proteins such as the LDL receptor family [18]. In budding yeast, Synthetic Lethal with Actin binding protein-1 (Sla1), an endocytic clathrin adaptor binds the NPFXD endocytic sorting signal [19]. Sla1 was originally identified as an actin associated protein necessary for normal cortical actin cytoskeleton assembly. Besides its actin cytoskeleton regulatory properties, Sla1 also has several features characteristic of endocytic clathrin adaptors. Sla1 has typical adaptor characteristics such as a multidomain structure, is recruited at early stages of endocytic vesicle

formation, and is required for clathrin- and actin-dependent internalization of cargoes containing the NPFXD endocytic sorting signals [4, 20-22]. Sla1 is an important component of the SLAC complex, where it inhibits the function of the yeast WASp homologue, fine tuning the temporal regulation of actin polymerization. **Section 1.3** will discuss the role of actin assembly during endocytosis and **Chapter 2** will describe the importance of the SLAC complex during clathrin-mediated endocytosis.

Caveolae-dependent endocytosis is the most commonly studied mode of clathrin-independent endocytosis that forms a coat-like structure made of the specific lipid raft caveolae (Figure 1.1). Caveolae, or "little caves", are 60–80 nm in diameter flask-shaped invaginations of the plasma membrane lined by caveolin that in some mammalian cell types, such as adipocytes, fibroblasts, type I pneumocytes, endothelial and smooth muscle cells, can constitute about a third of the plasma membrane area [23].Three mammalian caveolin proteins have been described. Caveolin-1 and -2 are commonly found in nonmuscle cells. In contrast, caveolin-3 is muscle specific. Caveolin-1 has been shown to be enriched in caveolae where it forms high-order oligomers of about 100-200 molecules [10, 24]. In addition, caveolin-1 is palmitoylated, and binds fatty acids and cholesterol to stabilize oligomer formation [25, 26]. Cholesterol reduction at the plasma membrane flattens caveolae and enhances the mobility of caveolin-1 structures [10].

Uptake of only very few cellular markers has been shown to be caveolin-1 dependent [9, 27]. Transcytosis in polarized cells, such as endothelial cells, is currently the most convincing trafficking process believed to occur in a caveolae-dependent fashion [28]. In addition, caveolae are the port of entry for several viruses, including the simian virus-40 [29]. The process of caveolin-1 dependent endocytosis includes clustering of plasma membrane lipid raft components

11

into caveolae and the subsequent signaling events leading to invagination and internalization [30]. In mammalian cells, local actin polymerization complements the formation of caveolae and is believed to promote their internalization [31]. The caveolin- rich vesicles are transported in a Rab5 dependent manner to both classical early endosome as well as pre-existing caveolin-1-enriched organelles known as caveosomes [30, 32]. The caveosome has been described as a cholesterol-rich structure on which markers of the classical endocytic pathways are absent [30].

Clathrin-independent endocytosis comprises those modes of endocytosis not dependent on the clathrin coat protein for cargo uptake. In contrast to clathrin- and claveolin-dependent pathways, this endocytic route, in most cases, does not require dynamin for vesicle internalization. Only few endogenous proteins associated with clathrin-independent endocytic pathways have been discovered and little is known about their contribution to endocytosis. There are several forms of clathrin-independent endocytosis, but for simplicity only macropinocytosis and phagocytosis will be discussed (Figure 1.1).

Macropinocytosis is the bulk uptake of extracellular fluid through large ruffles- or goblet-shaped invaginations. Ruffled extensions of the plasma membranes form around extracellular fluid with subsequent internalization of this region (Figure 1.1) [8] . These pathways involve the internalization of larger membrane areas than clathrin- or caveolin-dependent endocytosis. The generation of large endocytic vesicles of around 5um in diameter is belived to be a Rac1 and actin dependent process, but some variations of these requirements have been found [33, 34]. An example of this is the NKG2A inhibitory receptor which has been found to be internalized by a Rac1-dependent-actin-independent macropinocytic process [33]. PAK1, a kinase that binds and is activated by Rac1, is a sufficient and necessary component for the induction of the macropinocytic pathway [35, 36]. Cholesterol is required for the recruitment of activated Rac1 to

micropinocytic sites, which allow the classification of macropinocytosis as a cholesterol dependent process [37].

After internalization, the large vesicles formed at the plasma membrane are fused into an internal organelle known as macropinosome. Macropinocytic structures are not electron-dense regions and thus it has been difficult to analyze them by electron microscopy methods. However, these pathways can be analyzed in real-time by the use of fluorescently-tagged cargo proteins and phase contrast microscopy [27]. The morphological and mechanistic properties of macropinocytosis resemble those observed in another form of clathrin-independent endocytosis known as phagocytosis.

Phagocytosis is an inducible mode of endocytosis involving the active protrusion of lamellipodia around a particle or pathogen that is engulfed by specialized cells (Figure 1.1). Professional phagocytic cells, such as neutrophils, monocytes and/or macrophages use this clathrin-independent pathway for the internalization of C3b or immunoglobulin opsonized particles and pathogens. Upon binding of Fc receptors to the Fc region of immunoglobulins, phagocytic cells produce cytoplasmic projections that extend beyond the leading edge of lamellipodia around the particle in a cdc42-dependent manner, but afterwards depend on Rac1 for its internalization [38-41]. Actin polymerization is necessary for phagocytosis to occur [42]. During this process the cortical actin nucleator Arp2/3 complex and its activator N-WASp are recruited to the phagocytic membranes [42]. Uptake of particles opsonized with the complement protein fragment C3b, occurs upon binding to the C3b receptor (CR3) in a RhoA-dependent manner [43, 44]. Despite Arp2/3 complex recruitment, membrane protrusions are not frequently observed during C3b induced phagocytosis [42]. Newly formed phagosomes, which are the

largest forms of endosomes, are driven by an actin comet tail towards the cell center where the particles and pathogens that have been phagocytosed are processed [45].

1.2.2 Endosomal-lysosomal system

The endosomal system serves as a major connection between extracellular and intracellular environments [46]. Endocytosis is the starting point for the delivery of extracellular material to membrane-bound compartments inside the cell. 65-95 nm diameter structures known as vesicles are formed from the plasma membrane through actin dependent mechanisms and are utilized by the cell to transport cargo to internal organelles called early endosomes (Figure 1.4).

Early endosomes, also known as sorting endosomes, are heterogeneous port compartments where cargo containing vesicles anchor and fuse soon after being formed and released from the plasma membrane. One of the main functions of early endosomes is to serve as hubs for intracellular trafficking and cargo sorting to other organelles. Several routes used in early endosomal trafficking include retrograde transport to the trans-golgi network, trafficking to other endosomal organelles, and delivery of cargo to lysosomes for protein degradation (Figure 1.4) [47, 48]. In addition, some of these early endosomes, known as recycling endosomes, redirect integral protein receptors that were endocytosed back to the plasma membrane for their reutilization (Figure 1.4) [49]. Early endosomes contain a moderately acidic environment with an average pH 6.5, which is maintained by vacuolar-type proton pump ATPases (V-ATPase). The low pH permits the dissociation of soluble-intraluminal ligands from their receptors allowing their transport out of the endosomes into the cytoplasm or their transport to other organelles. The constant organelle remodeling and vesicular trafficking is responsible for the maintenance
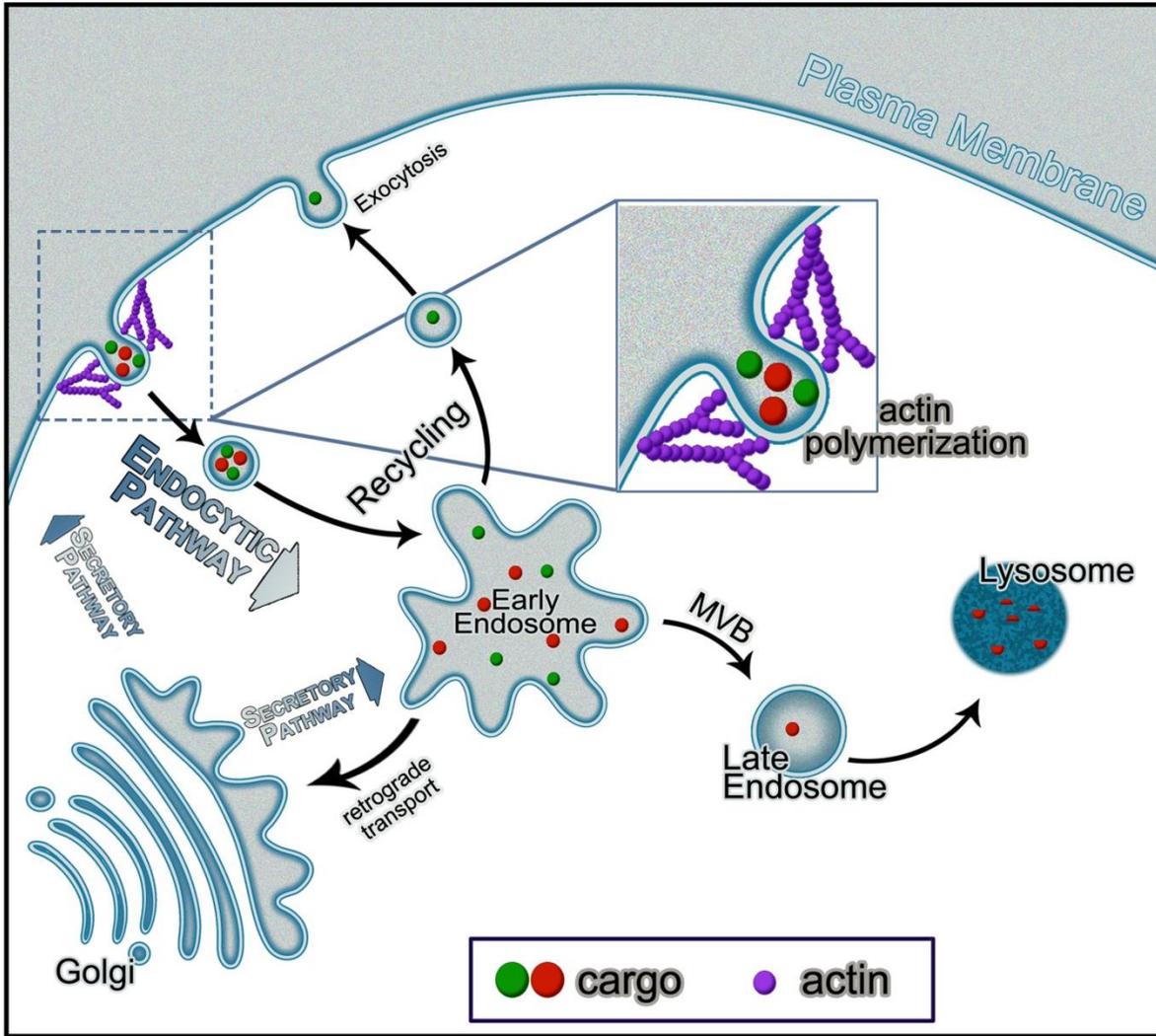
Figure 1. 4
Diagram of the Endosomal-Lysosomal system. Cargo (*green* and *red*) is packed in vesicles that are internalized through actin (*purple*) dependent mechanisms. After internalization, vesicles dock and fuse to early endosomes where they dump their content. From early endosomes cargo can be delivered back to the plasma membrane (*green*) or sent to late endosomes for it further delivery to lysosomes for degradation (*red*). Other pathways such as the secretory and retrograde transports are utilized for cargo trafficking in and out of early endosomes.

and maturation of endosomes [50]. Changes in the intraluminal membrane protein content, lipid composition, luminal pH, and morphology are essential for endosome function and maturation from early endosomes to late endosomes, which can further mature to lysosomes [48, 51-53].

Lysosomes are specialized organelles in charge of the degradation of proteins, carbohydrate, lipids, extracellular pathogens, waste material, and cellular debris [53]. The creation of intraluminal vesicles within late endosomes lead to the formation of multivesicular bodies. Delivery of lytic acid hydrolases to multivesicular bodies and late endosome, followed by further acidification of the lumen, aids in the transition between endosomes to degradative lysosomes [53]. The highly acidic property, close to pH 5, of the lysosome luminal environment allows active hydrolases to function in the degradation processes [53].

1.2.3 The endocytic recycling pathway

Cells internalize plasma membrane proteins and extracellular material by endocytosis. Endosomal recycling pathways return a pool of the endocytosed proteins and lipids back to the plasma membrane (Figure 1.4). The balance between endocytic removal and recycling fine-tunes the composition of the plasma membrane and is necessary for diverse cellular processes including cytokinesis, cell adhesion and junction formation, cell migration, signal transduction and cell polarity. Cells internalize their entire plasma membrane between one and five times per hour, necessitating a robust and coordinated regulation of recycling pathways [54].

Endocytosis occurs by a variety of modes that can be grouped into those that are clathrin-dependent and those that are clathrin-independent [8, 55]. In CDE, the cytoplasmic sorting signals of transmembrane proteins are specifically recognized by adaptor proteins and ultimately packaged into clathrin-coated vesicles that are internalized. The receptor for low-density

16

lipoprotein (LDL) particles is a well characterized example of a CDE cargo protein. Another example is the transferrin receptor, a broadly used marker of the endocytic recycling pathway. Among clathrin-independent processes, macropinocytosis and phagocytosis are specialized pathways that are stimulated and, as CDE, are dependent on actin assembly at the cell cortex [56-59].

The early endosome receives endocytosed material from primary vesicles generated by CIE and CDE. Phosphatidylinositol-3-phosphate (PtdIns3P), small GTPases and other proteins mark the early endosome and are required for its function. The intraluminal environment of endosomes is mildly acidic allowing ligand release from receptors by conformational changes [60]. An example of this is the transferrin-receptor, which uses the increased acidification at recycling endosomes to release bound ions and facilitate recycling of the transferrin receptor back to the plasma membrane.

For recycling of clathrin-independent endocytic cargoes and signaling receptors, positive selection processes may be involved. In contrast, some CDE cargoes such as the transferrin receptor and the LDL receptor (LDLR) are recycled back to the plasma membrane by a default recycling mode independent of any specific cytoplasmic sequences for recognition and sorting [60].

Protein trafficking regulation and recycling depends on small GTPases (Rab and Arf proteins) and their effectors, the scaffolding proteins from the RME-1 family of C-terminal Eps15 homology domain proteins (EHD1–4), tubulation of the membrane, membrane fission, and motor proteins [61, 62]. Genetic analysis of *C. elegans* and yeast systems has provided a great deal of knowledge that has expanded our understanding of endocytosis and recycling [63, 64]. The recycling pathway can be classified into fast or slow recycling. The formation of

tubules emanating from endosomes and the distribution of lipids and membrane proteins from luminal content permit the transfer to a juxtanuclear endocytic recycling compartment from which recycling endosomes emerge, and also can lead to fast recycling pathways. The fast recycling transport back to the plasma membrane from the early endosome has been well described for glycosphingolipids and the transferrin receptor [60, 65]. These pathways require a series of proteins including the small GTPases Rab4 and Rab35 which are used as markers of this rapid mode of recycling [65-67]. Studies on Rab35 have shown that this small GTPase localizes to early endosomes as well to the plasma membrane and is recognized as an important component for rapid recycling of the *C. elegans* LDLR-like yolk receptor and the mammalian transferrin receptor [68]. The slow recycling pathway is less understood but, morphologically, in this route endocytic recycling compartments are described as tubular compartments largely deprived of fluid, that acquire EHD1, and the small GTPase Rab11 after losing Rab5 [69].

1.3 Actin assembly during endocytosis.

The actin cytoskeleton is essential for a variety of functions in eukaryotic cells. Some important processes requiring actin assembly include cytokinesis, cell motility and endocytosis (Figure 1.4). During cytokinesis eukaryotic cells use actin filaments, together with the motor protein myosin, to form the acto-myosin ring that help to pinch off and separate cells during cell division [70]. Another important function of the actin cytoskeleton is to drive locomotion by the extension of various structures such as pseudopods. In multicellular organisms, different processes depend on cell motility, including fibroblast migration during wound healing, remodeling of the nervous system, and stimulated movements of immune cells [71-73]. Membrane remodeling events, such as endocytosis, also depend on the actin cytoskeleton. In

18

yeast, actin polymerization at the cell cortex has been implicated in endocytosis and there is a great deal of evidence demonstrating that its role for vesicle internalization is essential [70, 74-77]. In mammalian cells, it is clear that the actin cytoskeleton is critical to form membrane protrusions during micropinocytosis and phagocytosis [78, 79]. This section will focus on the basic requirements for actin polymerization and their role during endocytosis.

1.3.2 Formation of actin filaments

Microfilaments, known as actin filaments, are protein polymers made up of two helical intertwined strands of actin subunits that display a polarized arrangement. Based on the arrowhead pattern created when myosin binds actin filaments, the pointed end is the slowest growing end of the filament. In contrast, the rapidly growing end of the filament is called the barbed end. These ends can also be named based on the presence of bound ATP or ADP. The ATP bound site of actin filaments is known as the "+ end" (barbed end) while the ADP bound site of the filament is called the "- end" (pointed end). The polarized properties of actin filaments and dynamic recycling of actin monomers allow processes such as treadmilling, and the conversion of chemical energy to mechanical force for cellular functions [80].

Actin nucleation is the initiation of a new filament by assembly from actin monomers. Intrinsic or spontaneous nucleation of actin filaments is an unfavorable process due to the instability of actin dimers and trimers, which are intermediates required for filament elongation [80]. Cells maintain a pool of monomer sequestering proteins which prevent spontaneous nucleation of actin filaments. Elongation of actin filaments is a rapid and diffusion limited reaction. Although intrinsic nuclei formation is a slow process, under physiological salt conditions, pure actin can assemble into dimers and trimers and filaments can elongate in a concentration dependent manner [80].

Auxiliary proteins can stimulate or hinder elongation. Inhibition of the elongation can be accomplished when the barbed end is capped by specialized proteins. In contrast, the processes of filament uncapping or severing can expose barbed ends, thus promoting elongation. The critical concentrations (Cc), equivalent to the filament monomer dissociation constant (Kd), is the concentration of monomeric globular actin (G-actin) in equilibrium with actin filaments (F-actin) [80]. The critical concentration differs for pointed and barbed ends of actin (see below). Elongation of actin filaments depends on the actin critical concentrations for their pointed and barbed ends.

Spontaneous nucleation of actin filaments in the cell is extremely rare. Actin polymerization appears to be initiated de novo by assembly of nuclei from actin monomers, which requires actin nucleators. There are several actin nucleators including the formins, Spire and the Arp2/3 complex [80-82]. The roles of these nucleators are diverse, involving the formation of different actin structures. In yeast, there are three actin structures including "patches" (endocytosis), "cables" (vesicular trafficking and cell polarization) and "rings" (cytokinesis) [70]. Yeast formins, such as Bni1, are capable of nucleating actin filaments and aid in the formation of actin cables which are used for vesicular trafficking to endosomal compartments [83, 84].   However, the formation of cortical actin filaments involved in plasma membrane remodeling events, such as endocytosis, is dependent on the Arp2/3 complex. Here the discussion of actin nucleation will be focused on the Arp2/3 complex and its nucleation promoting factors.

1.3.3 Maintenance of G-actin subunits in the cell

Polymerization of actin filaments requires an available pool of actin monomers. This pool of monomeric actin can be used to elongate pre-existing actin filaments that have been uncapped or severed, in addition to form actin nuclei upon recruitment and/or activation of actin nucleators. Cells maintain a high concentration of unpolymerized actin with concentrations as high as 300 uM, in unactivated neutrophils [80, 85]. Given the low Ca^{2+} (micromolar) and the high Mg^{2+} (millimolar) physiological concentration, most of the monomeric actin pool is presumably in the form of Mg-ATP-bound G-actin [86]. Elongation of an actin filament is a bimolecular event that can be regulated by controlling the ability of actin monomers for binding to the filament ends. During elongation, actin monomers are added to both ends of the filament in a concentration dependent manner. The critical concentration, under physiological conditions, for the barbed and pointed ends are 0.1 μM and 0.6 μM respectively [80]. Evolution has provided cells with ways for maintaining this pool of actin monomers unpolymerized while being above the critical concentration. These mechanisms include G-actin binding proteins that sequester monomers and modify their ability to polymerize, and capping proteins that block the addition of monomers to filament ends [80]. In vertebrate cells, the main proteins binding and maintaining the pool of actin monomers are thymosin proteins and profilin.

Profilin, an actin-binding protein involved in the dynamic turnover and restructuring of the actin cytoskeleton, maintains the pool of Mg-ATP-actin monomers available to elongate any actin filament with exposed barbed ends. Profiling binding to G-actin opens the nucleotide binding pocket and allows nucleotide exchange from ADP to ATP [87-91]. Cells maintain their ATP/ADP ratio of 10:1 therefore actin monomers coming off of filaments with ADP bound will be recharged with ATP. In addition to promote elongation of actin filaments at the barbed end,

profilin also increases the rate of filament turnover at the pointed end by working synergistically with the pointed-end-severing-protein ADF/cofilin [92-94]. ADF/cofilin binds preferentially to ADP actin subunits in F-actin and severs filaments to increase the ADP actin monomer pool. By exchanging ADP for ATP in G-actin, ADF/cofilin is recycled to bind to F-actin. Profilin is the primary protein binding actin monomers in many organisms including yeast [80]. The affinity of profilin for actin filaments is low; however, the binding affinity for actin monomers bound to ADP (Kd = 500 nM) or ATP (Kd = 100 nM) is much stronger [95-97]. Despite the effect of profilin lowering the critical concentration at barbed ends, high levels of profilin may lead to sequestration and reduces barbed end elongation [92, 98, 99].

Thymosin-β4, the predominant form of beta thymosins in mammalian cells, is a 43 residue long peptide known to compete with profilin for binding to G-actin [100, 101]. Thymosin- β4 is a sequestering protein that binds ATP- actin with a Kd =1.4 μM [92, 97, 102]. Budding yeast has no thymosin gene, and uses profilin for actin sequestering fuctions [103]. In cells with thymosin-β4, profilin functions as a transporter between the thymosin-bound actin pool and the barbed end of an actin filament [92]. The exchange of G-actin between thymosin-β4 and profilin increases the ATP-actin-profilin pool that can be used for nucleated polymerization or elongation of uncapped filaments.

Capping proteins block the addition of actin monomers to barbed ends protecting the cellular G-actin pool from rapid depletion. The percentage of cellular actin filaments with free barbed ends is unknown, but the high affinity for barbed ends (Kd = 0.1 nM) and the micromolar concentration of capping protein in the cell are believed to be enough to cap most barbed ends [85, 104, 105]. The addition of uncapped filaments to cell extracts containing high concentrations of G-actin results in fast polymerization of the actin pool [85, 104]. However,

further addition of capping proteins to these extracts inhibits the elongation of actin filaments [104].

Overall, cells use two mechanisms to maintain the high levels of actin monomer in the cytoplasm that depend on G-actin-binding and barbed-end-binding proteins. G-actin-binding proteins, such as profilin and thymosin-β4, are used to keep ATP-actin in its monomeric form, while capping proteins block barbed ends from elongating to protect the G-actin pool from depletion through their continuous addition into filaments. On their own, these mechanisms are not efficient, but their combination builds a large pool of unpolymerized actin that, when free barbed ends are generated in the cell, is used for a fast and explosive growth of actin filaments.

1.3.4 G-actin binding sequences

Actin structures are an integral part of the cytoskeleton of all eukaryotes. Actin exists in both monomeric and filamentous form. Monomers are bound to ATP or ADP and their nucleotide state can affect their biochemical properties. Actin polymerization is an active process regulated by a vast number of actin-binding proteins. These proteins can interact with actin through several actin-binding motifs which in turn can bind F-actin (calponin homology domain), G-actin (Thymosin-β4/WASp homology domain 2) or both (ADF homology and gelsolin homology domains) [106-110].

The thymosin-β (Tβ) and WASp homology 2 (WH2) domains are small G-actin binding sequences present in a number of different proteins [111]. The functions of these G-actin binding sequences can include G-actin sequestration, actin filament growth, and nucleation and in some cases severing [112]. These monomeric actin binding domains are believed to be part of a similar family but obvious differences have been observed [113]. For example, these motifs have low

sequence similarity, despite the conservation of some important basic sequences, and there is evidence suggesting that Tβ and WH2 domains have different biological roles [111]. The conserved structure of WH2 domains includes an N-terminus alpha helix (α-helix1) followed by a highly conserved LKKT/V sequence (Figure 1.5) [111, 114, 115]. Although, Tβ contains an N-terminus alpha helix (α-helix 1) and a conserved basic sequence (LKKT/V), these two components are separated by a five amino acid long linker in the Tβ motif (Figure 1.5) [116, 117]. A C-terminus alpha helix (α-helix 2), not present in WH2 domains, is also conserved among Tβ containing proteins (Figure 1.5) [111]. The WH2 domain has a variable length, ranging from 17 to 27 amino acids, allowing its classification into short or long motifs [111]. Despite the sequence variability between Tβ and WH2 domains, both display an analogous fold and binding pattern when their N-terminal alpha helix and central LKKT/V sequence are bound to G-actin [101, 111, 114, 118-121].

There is a large range for the actin binding affinities of Tβ and WH2 domains with fluctuating dissociation constants from 0.05 to more than 100 μM [111]. However, several studies consistently demonstrate that Tβ binds actin with 10 fold less affinity than WH2 sequences [111, 122-124]. Differences in binding affinities among WH2 domains have also been observed. For example, it has been shown that the WH2 in WAVE, a member of the WASp family proteins, has the strongest binding affinity for G-actin (Kd = 0.05 ± 0.003 μM), approximately 5 fold higher than WASp WH2 [111]. A proposed explanation for these differences, among WH2 domains, is the presence of two Arg residues in the basic sequence of WAVE (LRRV) (Figure 1.5), which can form salt bridges with actin [111].

Several WH2 domain-containing proteins have been identified among different species, including yeast and humans [113]. Humans have eighteen different WH2 domain-containing

Sequence comparison between Tβ and WH2 motif
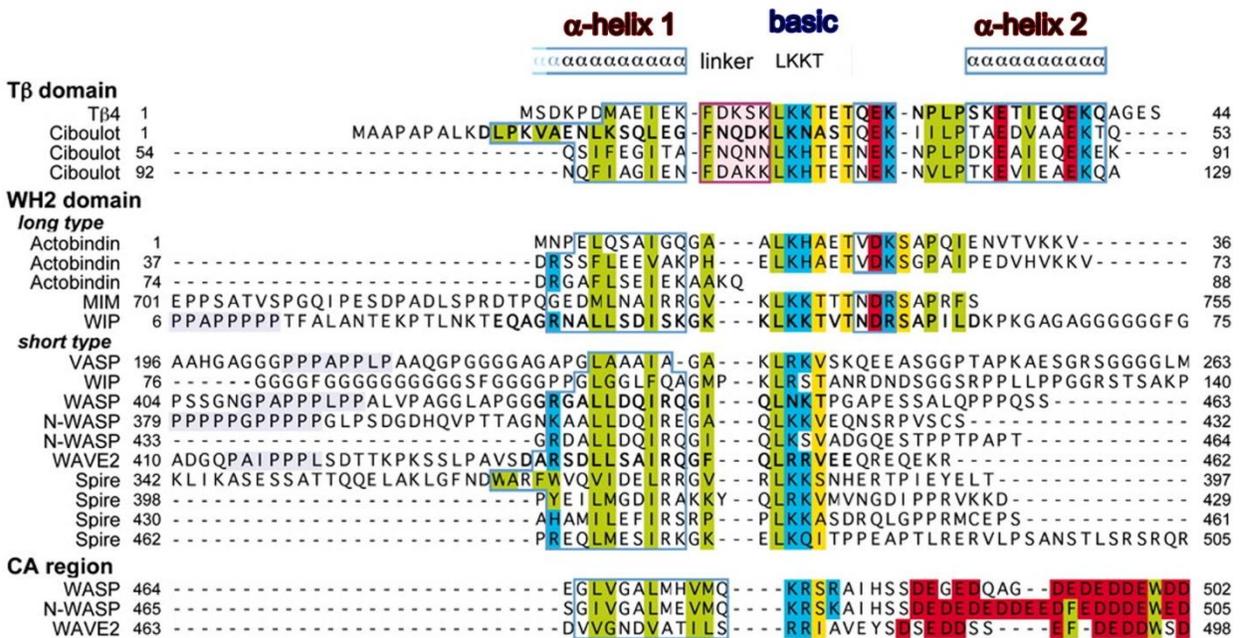
Figure 1. 5
Sequence alignment of WH2 and Tβ motifs of various G-actin binding proteins. The sequence accession numbers for each are: Q546P5 (Tβ4), O97428 (ciboulot), P18281 (actobindin), O43312 (MIM), Q53TA9 (WIP), P50552 (VASP), P42768 (WASP), and O00401 (N-WASP), Q9Y6W5 (WAVE2), and Q9U4F1 (Spire). Conserved amino acids are colored according to their chemical characteristics (*green*, nonpolar; *blue*, basic; *yellow*, small or polar amino amino acid). Proline-rich sequences are highlighted in *light-purple*. The linker region of Tβ is shown in *pink*. The acidic amino acids in the c̲entral and a̲cidic (CA) domain are in *red*. This figure is adapted from *Chereau D et al. (2005)* [111].

proteins, while *saccharomyces cerevisiae* has only three [113]. In addition to eukaryotes, WH2 domains and related sequences are also present in bacteria and viruses [113]. These domains have been identified in a group of baculoviral capsid proteins, where are believed to regulate actin assembly during infection [113]. The ActA protein, expressed and used by Listeria to generate actin comet tails for propulsion and motility, contains sequences related to the WH2 domain [111]. Although the sequences in ActA are involved in binding and regulation of the host cell actin pool, they lack some of the essential and functional key residues conserved in WH2 domains [111]. The variable nature of actin binding proteins, in terms of their sequence and function, reveal the possibility of potential actin binding modules that have not been discovered and might be involved in key cellular functions.

Recently, studies performed in yeast have described novel actin binding sequences with important roles in cell polarity, bundling of actin filaments, regulation of clathrin-mediated endocytosis, and de novo actin nucleation processes independent of the Arp2/3 complex [125-129]. Together, these observations demonstrate the importance of identifying and characterizing new actin binding sequences. **Chapter 3** will discuss the new findings on the characterization of a novel G-actin binding sequence in Las17, and its role regulating the SLAC complex during endocytosis.

1.3.5 Regulation of the Arp2/3 complex by nucleation promoting factors

Membrane remodeling events, such as endocytosis, require dynamic actin polymerization at the cell cortex. Nucleation is the rate limiting step during actin polymerization and is mediated by actin nucleators. The Arp2/3 complex is the main actin nucleator responsible for the regulation of cortical actin assembly. The Arp2/3 complex is a heteroheptameric stable complex

formed by two actin-related proteins, Arp2 and Arp3, and five other subunits [80]. Purified Arp2/3 nucleates filaments with free barbed ends but this process is extremely inefficient [104]. Cellular regulatory mechanisms have been put in place to increase the Arp2/3 complex activity. Nucleation promoting factors (NPF), such as the WASp family members, are the primary activators of the Arp2/3 complex both in yeast and mammals. The Listeria protein ActA is another type of Arp2/3 activator that promotes Arp2/3 mediated actin polymerization during the infectious phase of listeriosis [130]. Secondary Arp2/3 activators, such as preformed actin filaments, can enhance Arp2/3 recruitment and activity and promote actin filament branching [80].

WASp family proteins, such as WAVE, WASH, WASp and N-WASp, bind and activate the Arp2/3 complex through their VCA domain. The VCA, also known as WCA, is an Arp2/3 regulatory module that contains a WH2 domain (also known as verproline homology domain) that binds to G-actin, and the central (also known as connector domain) and acidic domain (CA) that binds to Arp2/3 [131-134]. Recombinant proteins containing only the WCA domain of different members of the WASp family are sufficient to bind and activate Arp2/3 [135-137].

The mechanism for Arp2/3 activation requires a conformational change upon binding to the CA domain of NPFs. The change in conformation allows the Arp2 and Arp3 subunits to resemble an actin dimer that later can interact with an actin monomer bound to the WH2, thus forming a stable trimer or actin nucleus [104]. Under optimal conditions, two WCA domains can bind to and activate the Arp2/3 complex to initiate a new filament [132, 138, 139]. However, overexpression of WCA in vertebrates perturbs the normal Arp2/3 complex localization and affects actin organization [133]. After nucleation, Arp2/3 remains attached to the pointed end of the filament forming part of the actin filament network [140]. The Arp2/3 complex can also

anchor onto a preformed filament where it can form new filament branches at a fixed angle of 70° [140, 141]. The combination of nucleation and branching can explain the morphology of the leading edge but differs from the regulatory mechanism used in the formation of filopodia, which consist of parallel bundles of actin filaments rather than a branching network [80, 142].

In addition to the WCA module, the WASp subfamily proteins have an amino-terminal WASp homology 1 (WH1) domain (also known as EVH1 domain) that binds to the WASp interacting protein (WIP) and when mutated can lead to Wisckott-Aldrich syndrome (WAS) [134]. In contrast, WAVE subfamily proteins contain a WAVE homology domain (WHD) (also known as SHD) located at the amino terminus. Both WASp and WAVE proteins have a central nonstructured polyproline stretch important for many processes, including the regulation of their NPF activity [143, 144]. An important variation between WASp and WAVE proteins is the presence of a GTPase-binding domain (GBD), also known as CDC42/Rac-interactive binding (CRIB) domain, in WASp [145]. The GBD is known to interact with the WCA at the C-terminal and this intramolecular interaction leads to the autoinhibition of WASp NPF activity [145-147]. This autoinhibitory intramolecular interaction can be released by the competitive binding of GTP-bound Cdc42 to the GBD, which exposes the WCA leading to activation of the Arp2/3 complex [134, 145-147]. In contrast, WAVE 1 is active in isolation but is normally found as part of an heteropentameric stable complex that maintains it inhibited, and its activation was proposed to be dependent on its interaction with the small GTPase Rac [148, 149].

WASp and WAVE homologs have been discovered in a wide variety of eukaryotic species including *Dictyostelium discoideum, Caenorhabditis elegans*, *Drosophila melanogaster* and mammals [150-155]. The plant *Arabidopsis thaliana* has four WAVE homologs, but no WASps [152]. In contrast, *Saccharomyces cerevisiae* has only one WASp homolog (Las17), but

no apparent WAVE gene has been identified [150, 151]. Despite the classification of Las17 as member of the WASp subfamily, Las17 does not have the GBD and it is not autoinhibited. **Chapter 2** will discuss the mechanism by which Las17 is inhibited as part of the SLAC complex.

1.3.6 Role of actin polymerization during endocytosis

The actin cytoskeleton is utilized by the cell for diverse processes including down-regulation of signal transduction, cell motility, cytokinesis and membrane remodeling. It is regulated by a series of accessory proteins that promote nucleation and regulate actin dynamics. Localized sites of actin polymerization at the cell cortex, also known as actin patches, correspond to endocytic sites in both yeast and mammals. During endocytosis, actin polymerization generates a network of actin branches that drives the inward movement of the newly formed vesicle from the plasma membrane [20, 156, 157]. Proteins involved in this process localize to the endocytic site and can be readily detected by fluorescence microscopy [4, 20, 75, 76, 143, 144, 151]. Some of these proteins include the Arp2/3 complex and NPFs, capping protein, cofilin, actin bundling proteins, and Fes/CIP4 homology-Bin/Amphiphysin/Rvsp (F-BAR) domain containing proteins [156, 158-163].

The Arp2/3 complex is the primary actin nucleator at sites of endocytosis, and defects in its actin regulatory function result in abnormal patch organization [156, 158]. The nucleation activity of Arp2/3 requires binding to NPFs, which also localize at endocytic sites [164]. All five yeast NPFs, including the only WASp homolog Las17, localize to actin patches, while in mammals, only the WASp and WAVE family proteins activate Arp2/3 during plasma membrane remodeling events [143, 144, 165].

Capping of barbed ends, which is essential for maintaining the G-actin pool, is also implicated in endocytosis. It has been suggested that capping proteins can funnel the monomeric actin pool to barbed ends that are rapidly elongating while capping nondynamic peripheral filaments and branches [4, 156]. Deletion of capping protein genes significantly reduces the rate of inward patch movement, leading to prolonged time of membrane invagination [74]. Under these conditions, there is less G-actin being delivered to growing barbed ends, thus decreasing the efficiency of invagination [4, 156]. In addition to regulating growing barbed ends, recent evidence has determined the importance of capping proteins during post-scission membrane movement [74].

Turnover of actin filaments is an important part of endocytosis. Proteins involved in actin filament disassembly, such as coronin and cofilin, are present at endocytic patches [166-168]. Consistent with a role in actin turnover, these proteins arrive right after actin polymerization initiates and mutations affecting their function can lead to defects in actin depolymerization [159, 169-171]. Defects in coronin function, similar to what is observed for cofilin mutants, extend the time of actin patches at the plasma membrane before internalization, and also increase the distance the patch moves into the cytoplasm after scission [170, 172].

Actin bundling also has an important role during endocytosis. The yeast fimbrin, Sac6, is an actin bundling protein associated with actin cables that has been linked with actin polymerization events that occur during endocytosis [173, 174]. Deletion of Sac6 has been shown to disrupt the actin cytoskeleton in yeast cells leading to a very poor rate of endocytic internalization [174, 175]. There is evidence demonstrating that in these cells the movement of endocytic patches away from the plasma membrane is impaired [4]. The yeast homolog of SM22, Scp1, is another bundling protein that localizes to endocytic patches [176, 177]. These

findings support the idea that actin bundling proteins are also important components of the endocytic machinery with roles in vesicular internalization events.

Ample evidence demonstrates the existence of many protein-protein interactions between the actin cytoskeleton and some endocytic adaptors. One of these protein interactions is mediated by the mammalian orthologue of the yeast adaptor Sla2, Hip1R. During membrane remodeling, Hip1R binds cortactin, clathrin and actin filaments to regulate actin polymerization at clathrin-dependent endocitic sites [178]. In yeast, Sla2 is associated with actin filaments and also binds to the clathrin light chain. In cells carrying a deletion of the SLA2 gene, actin comet tails are observed and endocytic internalization is affected [20]. Other proteins, such as transducer of Cdc42-dependent actin assembly 1 (Toca-1), SNX9 and the F-BAR-domain containing protein syndapin (Bzz1 in yeast), connect dynamin to N-WASp linking the actin cytoskeleton with the vesicular scission processes [75]. Inhibition of Arp2/3 complex-mediated actin polymerization has also been observed after the addition of the BAR domain containing protein PICK1 in *in vitro* studies [179]. In yeast and mammals, proteins from the BAR domain superfamily, including BAR and F-BAR containing proteins, can sense or induce membrane curvature which is also a process coupled to actin polymerization at the plasma membrane (Figure 1.3).

Many F-BAR proteins have been related to actin regulation in clathrin-mediated endocytosis (Figure 1.3). Some of these are the FCHo1 and FCHo2 (Syp1 in yeast), CIP4 (also known as Toca-1), and syndapin [162, 180, 181]. These proteins participate in early invagination events that are important for the formation of tubules within clathrin coated pits in yeast and mammals [77]. Initial membrane curvature and recruitment of clathrin has been linked to the recruitment of FCHo1 (Syp1) to sites of clathrin dependent endocytosis [77]. There is evidence indicating that regulation of the actin cytoskeleton is directly related to membrane curvature

through F-Bar domain containing proteins. In yeast, Syp1 negatively regulates Las17 (WASp) *in vitro* and *in vivo*, while another F-BAR containing protein, Bzz1, has been shown to activate it *in vitro* [182]. These results suggest a mechanism where F-BAR domain containing proteins work as sensors, and the actin filament organization is tailored depending on the stage of membrane curvature.

1.4 Las17 as a model to study WASp NPF activity regulation by SH3-containing proteins

Given the importance of endocytic internalization routes for a variety of cellular processes, it is not surprising that defects in protein machineries involved in these pathways lead to pathologies. Many diseases are related to defects in specific stages of plasma membrane remodeling events. These include mutations in receptor or adaptor proteins used for cargo accumulation and defects in actin regulatory proteins such as Arp2/3 complex nucleation promoting factors. Examples of metabolic disorders associated to defects in adaptor or receptor function include autosomal recessive hypercholesterolemia (mutation in the adaptor protein ARH) and familial hypercholesterolemia (mutation in the LDL receptor) [8, 183]. In these illnesses high levels of cholesterol are present in the blood and if these levels persist can ultimately cause secondary cardiovascular diseases [8, 183]. In other cases, mutation in actin regulatory proteins, such as WASp, can promote blood disorders that can include primary immunodeficiency and thrombocytopenia, which are characteristic symptoms present in Wiskott-Aldrich syndrome patients.

1.4.2 Thrombocytopenia and Wiskott Aldrich Syndrome

Hematopoietic cells are multipotent stem cells produced in the bone marrow responsible for giving rise to different cell types in blood, such as lymphoid and myeloid cell lines (including megakaryocytes and platelets). Platelets, together with erythrocytes and plasma, form a major proportion of human blood. Platelets are produced from very large cells called megakaryocytes that undergo a process of fragmentation resulting in the release of over 1,000 platelets per megakaryocyte. Platelets play fundamental roles in the antihemorrhagic process including detection of vascular lesions, adherence at sites of injury, recruitment of additional platelets, and consolidation into a haemostatic plug [184, 185].Thrombocytopenia (lower than normal platelets counts) or impaired platelet function have been associated with moderate to severe bleeding [186, 187]. Thrombocytopenia can be caused by failure of the bone marrow to produce normal numbers of megakaryocytes or by increased destruction of platelets. Several factors are responsible for platelet destruction; such as Immune Thrombocytopenic Purpura (ITP), which recent evidence has placed as a key pathology associated with the Wiskott Aldrich Syndrome (WAS) [188]. WAS is an X-linked disease caused by mutations in the Wiskott-Aldrich syndrome protein gene (*WASP*). The clinical characteristics of this disease include frequent infections caused by immunodeficiency, eczema, increased incidence of autoimmune manifestations, thrombocytopenia and platelets of small size [189-191]. As a consequence of the platelet defect, the majority (89%) of patients with WAS have a history of bleeding, including epistaxis and oral bleeding [190, 191]. In WAS patients, hematopoietic cells suffer from dysfunctional organization of the actin cytoskeleton, which is believed to be the main reason for the manifestations observed in this disease [190].

1.4.3 WASp regulatory mechanisms

WASp is a 64 KDa protein expressed in hematopoietic cells with a very important role in regulating actin polymerization nucleation [79, 192, 193]. Actin branches, formed in the cell cortex, are built up by the actin filament nucleation activity of the Arp2/3 complex. These structures are known to be critical for membrane remodeling processes and proper functional control of cell morphology [183]. Cortical actin dynamics in hematopoietic cells is o*rchestrated* by WASp, which binds and activates Arp2/3 complex initiating actin polymerization. In addition to being a nucleation promoting factor (NPF), WASp has also been postulated to be a scaffold protein capable of interacting with different cytoskeletal regulatory molecules involved in membrane remodeling. These interactions are thought to be mediated through the binding of the polyproline (PxxP) motifs in WASp to Src homology 3 (SH3) domains of signaling molecules [193-197]. Several proteins involved in membrane remodeling, such as intersectin and syndapin, also contain SH3 domains that bind WASp, linking it to the membrane remodeling machinery (Figure 1.6) [198-200]. All the mechanisms by which WASp is activated are not fully understood. One of the better known machanisms, probably not indispensable, of WASp activation is through its interaction with the small GTPase Cdc42, mediated by the WASp GBD domain [201-203]. In addition to this GDB-Cdc42 interaction, Toca-1 is essential for proper Cdc42-dependent actin polymerization [204]. Another mechanism by which WASp is believed to be regulated is through phosphorylation-dephosphorylation cycles [195, 205]. Finally, a less well understood mechanism of WASp regulation is by its possible inhibition or activation through interactions with SH3-containing proteins that can also maintain the spatio-temporal distribution of WASp in the cell [143, 144, 151, 193-197]. In yeast, the SH3-containing protein Sla1 (intersectin) and Bzz1 (syndapin) interact with Las17 (WASp), and *in vitro* studies have
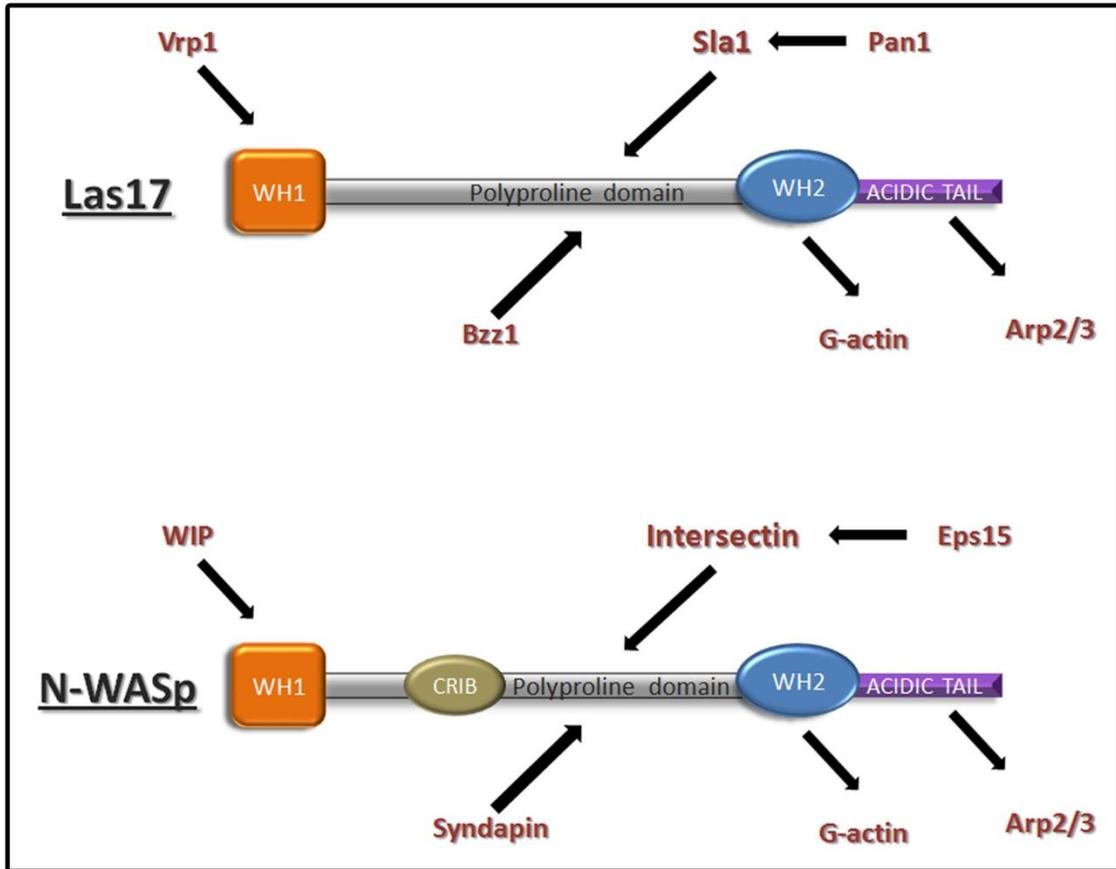
Figure 1. 6
Diagram of Las17 and N-WASp domains. Here are presented several Las17 binding proteins (*top*) and their homologues in mammal (*bottom*). Arrows represent possible protein interactions.

suggested that these proteins can potentially regulate Las17 NPF activity by a mechanism involving SH3-PxxP interaction [143, 144] (Figure 1.6).

The involvement of the actin cytoskeleton in cell migration and trafficking of hematopoietic cells makes these cells very sensitive to mutations or any minor disruption in the *WASP* gene. The fact that WAS affects the normal number of platelets in blood also suggest that WASp may have a unique and essential role in platelet production and functional regulation through signal events that affect cortical actin assembly in megakaryocytes [206-208]. In order to better undertand the relationship between actin assembly aberrations and WAS, it is imperative to understand the different mechanisms by which WASp and its homologues are regulated.

1.4.4 Las17 regulation by SH3-containing proteins.

WASp homologues share several functional domains. The carboxy-terminal domain known as WCA domain is a critical common feature of WASp/WAVE proteins with the key role of activating the Arp2/3 complex (Figure 1.6) [80]. The central region is a proline–rich stretch essential for multiple interactions with SH3-containinig proteins (Figure 1.6) [143, 144, 193-197], and potentially a target domain for WASp regulation (Figure 1.6). The amino terminal domain, WH1, is known to bind <u>W</u>ASp <u>I</u>nteracting <u>P</u>rotein (WIP/Vrp1), an essential protein with a key role in WASp stability (Figure 1.6) [209]. WASp and some WASp homologues, also contain a CRIB domain important for autoinhibition. Some members of the WASp family, however, are not autoinhibited by a GBD domain mechanism. The only WASp homolog and strongest NPF in yeast, Las17 belongs to this group (Figure 1.6) [143, 144, 151].

It has been suggested that Sla1 (intersectin) interacts with and inhibits Las17 NPF activity *in vitro,* and its interaction is required for proper Las17 localization to the plasma

36

membrane *in vivo* [143, 144, 151]. Different groups have shown that Las17 and Sla1 arrive to membrane remodeling sites about 20 seconds before actin polymerization begins [20, 144]. Therefore, it is relevant to ask: How is Las17 kept inactive during the initial 20 seconds before actin polymerization is initiated? **Chapter 2** will describe in detail the discovery and characterization of SLAC, a stable complex between Sla1 and Las17. The identification of this complex is consistent with *in vitro* studies mentioned previously and explains why Las17 NPF activity is not detected during the initial 20 seconds after arrival to the plasma membrane. Bzz1 (Syndapin), has been shown to arrive to Las17 patches right before actin filaments are detected suggesting its possible involvement in Las17 regulation by releasing Sla1 inhibition [143, 144]. In **Chapter 3** new insights for the Bzz1 role in Las17 regulation will be presented. These interactions are also conserved in mammalian cells, which validate the use of *S. cerevisiae* and Las17 to study this Cdc42-independent mechanism for WASp regulation (Figure 1.6).

 S.cerevisiae cells carrying a deletion of the LAS17 gene (*Las17Δ*) show growth defects due to deficiency of actin assembly [80, 151]. Importantly*, Las17Δ* cells co-transformed with human WASp and WIP constructs show suppression of the growth phenotype [210]. This also suggests that the WIP-WASp and Vrp1-Las17 functions are conserved and demonstrates the validity of using S. cerevisiae as model system (Figure 1.6).

 Together, this dissertation will present the discovery and characterization of a novel actin regulatory complex involved in CME and will authenticate the SLAC complex as a model to study a novel molecular mechanism of WASp regulation by SH3-PxxP interactions.

REFERENCES

1.   Wu, F. and P.J. Yao, *Clathrin-mediated endocytosis and Alzheimer's disease: an update.* Ageing Res Rev, 2009. **8**(3): p. 147-9.
2.   Schelhaas, M., *Come in and take your coat off - how host cells provide endocytosis for virus entry.* Cell Microbiol, 2010. **12**(10): p. 1378-88.
3.   Hoeller, D., S. Volarevic, and I. Dikic, *Compartmentalization of growth factor receptor signalling.* Curr Opin Cell Biol, 2005. **17**(2): p. 107-11.
4.   Kaksonen, M., C.P. Toret, and D.G. Drubin, *A modular design for the clathrin- and actin-mediated endocytosis machinery.* Cell, 2005. **123**(2): p. 305-20.
5.   Yu, X. and M. Cai, *The yeast dynamin-related GTPase Vps1p functions in the organization of the actin cytoskeleton via interaction with Sla1p.* J Cell Sci, 2004. **117**(Pt 17): p. 3839-53.
6.   Peter, B.J., et al., *BAR domains as sensors of membrane curvature: the amphiphysin BAR structure.* Science, 2004. **303**(5657): p. 495-9.
7.   Roux, A., et al., *GTP-dependent twisting of dynamin implicates constriction and tension in membrane fission.* Nature, 2006. **441**(7092): p. 528-31.
8.   Doherty, G.J. and H.T. McMahon, *Mechanisms of endocytosis.* Annu Rev Biochem, 2009. **78**: p. 857-902.
9.   Roth, T.F. and K.R. Porter, *Yolk Protein Uptake in the Oocyte of the Mosquito Aedes Aegypti. L.* J Cell Biol, 1964. **20**: p. 313-32.
10.   Rothberg, K.G., et al., *Caveolin, a protein component of caveolae membrane coats.* Cell, 1992. **68**(4): p. 673-82.
11.   Shao, Y., et al., *Pincher, a pinocytic chaperone for nerve growth factor/TrkA signaling endosomes.* J Cell Biol, 2002. **157**(4): p. 679-91.
12.   Kirchhausen, T., *Clathrin.* Annu Rev Biochem, 2000. **69**: p. 699-727.
13.   Brodsky, F.M., et al., *Biological basket weaving: formation and function of clathrin-coated vesicles.* Annu Rev Cell Dev Biol, 2001. **17**: p. 517-68.
14.   Owen, D.J., B.M. Collins, and P.R. Evans, *Adaptors for clathrin coats: structure and function.* Annu Rev Cell Dev Biol, 2004. **20**: p. 153-91.
15.   Dell'Angelica, E.C., et al., *Association of the AP-3 adaptor complex with clathrin.* Science, 1998. **280**(5362): p. 431-4.
16.   Dell'Angelica, E.C., *Clathrin-binding proteins: got a motif? Join the network!* Trends Cell Biol, 2001. **11**(8): p. 315-8.
17.   Miele, A.E., et al., *Two distinct interaction motifs in amphiphysin bind two independent sites on the clathrin terminal domain beta-propeller.* Nat Struct Mol Biol, 2004. **11**(3): p. 242-8.
18.   Keyel, P.A., et al., *A single common portal for clathrin-mediated endocytosis of distinct cargo governed by cargo-selective adaptors.* Mol Biol Cell, 2006. **17**(10): p. 4300-17.
19.   Mahadev, R.K., et al., *Structure of Sla1p homology domain 1 and interaction with the NPFxD endocytic internalization motif.* EMBO J, 2007. **26**(7): p. 1963-71.
20.   Kaksonen, M., Y. Sun, and D.G. Drubin, *A pathway for association of receptors, adaptors, and actin during endocytic internalization.* Cell, 2003. **115**(4): p. 475-87.
21.   Howard, J.P., et al., *Sla1p serves as the targeting signal recognition factor for NPFX(1,2)D-mediated endocytosis.* J Cell Biol, 2002. **157**(2): p. 315-26.
22.   Piao, H.L., I.M. Machado, and G.S. Payne, *NPFXD-mediated endocytosis is required for polarity and function of a yeast cell wall stress sensor.* Mol Biol Cell, 2007. **18**(1): p. 57-65.
23.   Parton, R.G. and K. Simons, *The multiple faces of caveolae.* Nat Rev Mol Cell Biol, 2007. **8**(3): p. 185-94.

24.   Pelkmans, L. and M. Zerial, *Kinase-regulated quantal assemblies and kiss-and-run recycling of caveolae.* Nature, 2005. **436**(7047): p. 128-33.

25.   Dietzen, D.J., W.R. Hastings, and D.M. Lublin, *Caveolin is palmitoylated on multiple cysteine residues. Palmitoylation is not necessary for localization of caveolin to caveolae.* J Biol Chem, 1995. **270**(12): p. 6838-42.

26.   Monier, S., et al., *Oligomerization of VIP21-caveolin in vitro is stabilized by long chain fatty acylation or cholesterol.* FEBS Lett, 1996. **388**(2-3): p. 143-9.

27.   Kirkham, M. and R.G. Parton, *Clathrin-independent endocytosis: new insights into caveolae and non-caveolar lipid raft carriers.* Biochim Biophys Acta, 2005. **1746**(3): p. 349-63.

28.   Heltianu, C., et al., *Evidence for thyroxine transport by the lung and heart capillary endothelium.* Microvasc Res, 1989. **37**(2): p. 188-203.

29.   Tagawa, A., et al., *Assembly and trafficking of caveolar domains in the cell: caveolae as stable, cargo-triggered, vesicular transporters.* J Cell Biol, 2005. **170**(5): p. 769-79.

30.   Pelkmans, L. and A. Helenius, *Insider information: what viruses tell us about endocytosis.* Curr Opin Cell Biol, 2003. **15**(4): p. 414-22.

31.   Pelkmans, L., D. Puntener, and A. Helenius, *Local actin polymerization and dynamin recruitment in SV40-induced internalization of caveolae.* Science, 2002. **296**(5567): p. 535-9.

32.   Pelkmans, L., et al., *Caveolin-stabilized membrane domains as multifunctional transport and sorting devices in endocytic membrane traffic.* Cell, 2004. **118**(6): p. 767-80.

33.   Masilamani, M., et al., *Uncommon endocytic and trafficking pathway of the natural killer cell CD94/NKG2A inhibitory receptor.* Traffic, 2008. **9**(6): p. 1019-34.

34.   Swanson, J.A. and C. Watts, *Macropinocytosis.* Trends Cell Biol, 1995. **5**(11): p. 424-8.

35.   Dharmawardhane, S., et al., *Regulation of macropinocytosis by p21-activated kinase-1.* Mol Biol Cell, 2000. **11**(10): p. 3341-52.

36.   Knaus, U.G., et al., *Structural requirements for PAK activation by Rac GTPases.* J Biol Chem, 1998. **273**(34): p. 21512-8.

37.   Grimmer, S., B. van Deurs, and K. Sandvig, *Membrane ruffling and macropinocytosis in A431 cells require cholesterol.* J Cell Sci, 2002. **115**(Pt 14): p. 2953-62.

38.   Massol, P., et al., *Fc receptor-mediated phagocytosis requires CDC42 and Rac1.* EMBO J, 1998. **17**(21): p. 6219-29.

39.   Castellano, F., P. Montcourrier, and P. Chavrier, *Membrane recruitment of Rac1 triggers phagocytosis.* J Cell Sci, 2000. **113 (Pt 17)**: p. 2955-61.

40.   Hoppe, A.D. and J.A. Swanson, *Cdc42, Rac1, and Rac2 display distinct patterns of activation during phagocytosis.* Mol Biol Cell, 2004. **15**(8): p. 3509-19.

41.   Chimini, G. and P. Chavrier, *Function of Rho family proteins in actin dynamics during phagocytosis and engulfment.* Nat Cell Biol, 2000. **2**(10): p. E191-6.

42.   May, R.C., et al., *Involvement of the Arp2/3 complex in phagocytosis mediated by FcgammaR or CR3.* Nat Cell Biol, 2000. **2**(4): p. 246-8.

43.   Caron, E. and A. Hall, *Identification of two distinct mechanisms of phagocytosis controlled by different Rho GTPases.* Science, 1998. **282**(5394): p. 1717-21.

44.   Olazabal, I.M., et al., *Rho-kinase and myosin-II control phagocytic cup formation during CR, but not FcgammaR, phagocytosis.* Curr Biol, 2002. **12**(16): p. 1413-18.

45.   Southwick, F.S., et al., *Actin-based endosome and phagosome rocketing in macrophages: activation by the secretagogue antagonists lanthanum and zinc.* Cell Motil Cytoskeleton, 2003. **54**(1): p. 41-55.

46.   Wieffer, M., T. Maritzen, and V. Haucke, *SnapShot: endocytic trafficking.* Cell, 2009. **137**(2): p. 382 e1-3.

47.   Clague, M.J., *Molecular aspects of the endocytic pathway.* Biochem J, 1998. **336 (Pt 2)**: p. 271-82.

48.   Jovic, M., et al., *The early endosome: a busy sorting station for proteins at the crossroads.* Histol Histopathol, 2010. **25**(1): p. 99-112.

49.   Hao, M. and F.R. Maxfield, *Characterization of rapid membrane internalization and recycling.* J Biol Chem, 2000. **275**(20): p. 15279-86.

50.   Gruenberg, J., G. Griffiths, and K.E. Howell, *Characterization of the early endosome and putative endocytic carrier vesicles in vivo and with an assay of vesicle fusion in vitro.* J Cell Biol, 1989. **108**(4): p. 1301-16.

51.   Presley, J.F., et al., *Bafilomycin A1 treatment retards transferrin receptor recycling more than bulk membrane recycling.* J Biol Chem, 1997. **272**(21): p. 13929-36.

52.   Mellman, I., *Endocytosis and molecular sorting.* Annu Rev Cell Dev Biol, 1996. **12**: p. 575-625.

53.   Huotari, J. and A. Helenius, *Endosome maturation.* EMBO J, 2011. **30**(17): p. 3481-500.

54.   Steinman, R.M., et al., *Endocytosis and the recycling of plasma membrane.* J Cell Biol, 1983. **96**(1): p. 1-27.

55.   Conner, S.D. and S.L. Schmid, *Regulated portals of entry into the cell.* Nature, 2003. **422**(6927): p. 37-44.

56.   Mayor, S. and R.E. Pagano, *Pathways of clathrin-independent endocytosis.* Nat Rev Mol Cell Biol, 2007. **8**(8): p. 603-12.

57.   Sandvig, K., et al., *Clathrin-independent endocytosis: from nonexisting to an extreme degree of complexity.* Histochem Cell Biol, 2008. **129**(3): p. 267-76.

58.   Swanson, J.A., *Shaping cups into phagosomes and macropinosomes.* Nat Rev Mol Cell Biol, 2008. **9**(8): p. 639-49.

59.   Donaldson, J.G., N. Porat-Shliom, and L.A. Cohen, *Clathrin-independent endocytosis: a unique platform for cell signaling and PM remodeling.* Cell Signal, 2009. **21**(1): p. 1-6.

60.   Maxfield, F.R. and T.E. McGraw, *Endocytic recycling.* Nat Rev Mol Cell Biol, 2004. **5**(2): p. 121-32.

61.   Grant, B.D. and S. Caplan, *Mechanisms of EHD/RME-1 protein function in endocytic transport.* Traffic, 2008. **9**(12): p. 2043-52.

62.   Daumke, O., et al., *Architectural and mechanistic insights into an EHD ATPase involved in membrane remodelling.* Nature, 2007. **449**(7164): p. 923-927.

63.   Balklava, Z., et al., *Genome-wide analysis identifies a general requirement for polarity proteins in endocytic traffic.* Nat Cell Biol, 2007. **9**(9): p. 1066-73.

64.   Shaw, J.D., et al., *Yeast as a model system for studying endocytosis.* Exp Cell Res, 2001. **271**(1): p. 1-9.

65.   Choudhury, A., et al., *Elevated endosomal cholesterol levels in Niemann-Pick cells inhibit rab4 and perturb membrane recycling.* Mol Biol Cell, 2004. **15**(10): p. 4500-11.

66.   van der Sluijs, P., et al., *The small GTP-binding protein rab4 controls an early sorting event on the endocytic pathway.* Cell, 1992. **70**(5): p. 729-40.

67.   Deneka, M., et al., *Rabaptin-5alpha/rabaptin-4 serves as a linker between rab4 and gamma(1)-adaptin in membrane recycling from endosomes.* EMBO J, 2003. **22**(11): p. 2645-57.

68.   Kouranti, I., et al., *Rab35 regulates an endocytic recycling pathway essential for the terminal steps of cytokinesis.* Curr Biol, 2006. **16**(17): p. 1719-25.

69.   Sonnichsen, B., et al., *Distinct membrane domains on endosomes in the recycling pathway visualized by multicolor imaging of Rab4, Rab5, and Rab11.* J Cell Biol, 2000. **149**(4): p. 901-14.

70.   Moseley, J.B. and B.L. Goode, *The yeast actin cytoskeleton: from cellular function to biochemical mechanism.* Microbiol Mol Biol Rev, 2006. **70**(3): p. 605-45.

71.   Conrad, P.A., et al., *Relative distribution of actin, myosin I, and myosin II during the wound healing response of fibroblasts.* J Cell Biol, 1993. **120**(6): p. 1381-91.

72.   Hu, J., et al., *Septin-driven coordination of actin and microtubule remodeling regulates the collateral branching of axons.* Curr Biol, 2012. **22**(12): p. 1109-15.

73.   Ananthakrishnan, R. and A. Ehrlicher, *The forces behind cell movement.* Int J Biol Sci, 2007. **3**(5): p. 303-17.

74.   Robertson, A.S., E. Smythe, and K.R. Ayscough, *Functions of actin in endocytosis.* Cell Mol Life Sci, 2009. **66**(13): p. 2049-65.

75.   Galletta, B.J., O.L. Mooren, and J.A. Cooper, *Actin dynamics and endocytosis in yeast and mammals.* Curr Opin Biotechnol, 2010. **21**(5): p. 604-10.

76.   Galletta, B.J. and J.A. Cooper, *Actin and endocytosis: mechanisms and phylogeny.* Curr Opin Cell Biol, 2009. **21**(1): p. 20-7.

77.   Mooren, O.L., B.J. Galletta, and J.A. Cooper, *Roles for actin assembly in endocytosis.* Annu Rev Biochem, 2012. **81**: p. 661-86.

78.   May, R.C. and L.M. Machesky, *Phagocytosis and the actin cytoskeleton.* J Cell Sci, 2001. **114**(Pt 6): p. 1061-77.

79.   Welch, M.D. and R.D. Mullins, *Cellular control of actin nucleation.* Annu Rev Cell Dev Biol, 2002. **18**: p. 247-88.

80.   Pollard, T.D., L. Blanchoin, and R.D. Mullins, *Molecular mechanisms controlling actin filament dynamics in nonmuscle cells.* Annu Rev Biophys Biomol Struct, 2000. **29**: p. 545-76.

81.   Graziano, B.R., et al., *Mechanism and cellular function of Bud6 as an actin nucleation-promoting factor.* Mol Biol Cell, 2011. **22**(21): p. 4016-28.

82.   Ducka, A.M., et al., *Structures of actin-bound Wiskott-Aldrich syndrome protein homology 2 (WH2) domains of Spire and the implication for filament nucleation.* Proc Natl Acad Sci U S A, 2010. **107**(26): p. 11757-62.

83.   Evangelista, M., et al., *Formins direct Arp2/3-independent actin filament assembly to polarize cell growth in yeast.* Nat Cell Biol, 2002. **4**(1): p. 32-41.

84.   Pelham, R.J., Jr. and F. Chang, *Role of actin polymerization and actin cables in actin-patch movement in Schizosaccharomyces pombe.* Nat Cell Biol, 2001. **3**(3): p. 235-44.

85.   DiNubile, M.J., et al., *Actin filament barbed-end capping activity in neutrophil lysates: the role of capping protein-beta 2.* Mol Biol Cell, 1995. **6**(12): p. 1659-71.

86.   Rosenblatt, J., P. Peluso, and T.J. Mitchison, *The bulk of unpolymerized actin in Xenopus egg extracts is ATP-bound.* Mol Biol Cell, 1995. **6**(2): p. 227-36.

87.   Carlsson, L., et al., *Actin polymerizability is influenced by profilin, a low molecular weight protein in non-muscle cells.* J Mol Biol, 1977. **115**(3): p. 465-83.

88.   Mockrin, S.C. and E.D. Korn, *Acanthamoeba profilin interacts with G-actin to increase the rate of exchange of actin-bound adenosine 5'-triphosphate.* Biochemistry, 1980. **19**(23): p. 5359-62.

89.   Goldschmidt-Clermont, P.J. and P.A. Janmey, *Profilin, a weak CAP for actin and RAS.* Cell, 1991. **66**(3): p. 419-21.

90.   Goldschmidt-Clermont, P.J., et al., *Mechanism of the interaction of human platelet profilin with actin.* J Cell Biol, 1991. **113**(5): p. 1081-9.

91.   Goldschmidt-Clermont, P.J., et al., *Regulation of phospholipase C-gamma 1 by profilin and tyrosine phosphorylation.* Science, 1991. **251**(4998): p. 1231-3.

92.   Pantaloni, D. and M.F. Carlier, *How profilin promotes actin filament assembly in the presence of thymosin beta 4.* Cell, 1993. **75**(5): p. 1007-14.

93.   Kang, F., D.L. Purich, and F.S. Southwick, *Profilin promotes barbed-end actin filament assembly without lowering the critical concentration.* J Biol Chem, 1999. **274**(52): p. 36963-72.

94.   Didry, D., M.F. Carlier, and D. Pantaloni, *Synergy between actin depolymerizing factor/cofilin and profilin in increasing actin filament turnover.* J Biol Chem, 1998. **273**(40): p. 25602-11.

95.   Perelroizen, I., et al., *Role of nucleotide exchange and hydrolysis in the function of profilin in action assembly.* J Biol Chem, 1996. **271**(21): p. 12302-9.

96.   Schutt, C.E., et al., *The structure of crystalline profilin-beta-actin.* Nature, 1993. **365**(6449): p. 810-6.

97.   Vinson, V.K., et al., *Interactions of Acanthamoeba profilin with actin and nucleotides bound to actin.* Biochemistry, 1998. **37**(31): p. 10871-80.

98.   Gutsche-Perelroizen, I., et al., *Filament assembly from profilin-actin.* J Biol Chem, 1999. **274**(10): p. 6234-43.

99.   Kaiser, D.A., et al., *Profilin is predominantly associated with monomeric actin in Acanthamoeba.* J Cell Sci, 1999. **112** (**Pt 21**): p. 3779-90.

100. Prehoda, K.E., D.J. Lee, and W.A. Lim, *Structure of the enabled/VASP homology 1 domain-peptide complex: a key component in the spatial control of actin assembly.* Cell, 1999. **97**(4): p. 471-80.

101. Safer, D., T.R. Sosnick, and M. Elzinga, *Thymosin beta 4 binds actin in an extended conformation and contacts both the barbed and pointed ends.* Biochemistry, 1997. **36**(19): p. 5806-16.

102. Carlier, M.F., et al., *Modulation of the interaction between G-actin and thymosin beta 4 by the ATP/ADP ratio: possible implication in the regulation of actin dynamics.* Proc Natl Acad Sci U S A, 1993. **90**(11): p. 5034-8.

103. Nefsky, B. and A. Bretscher, *Yeast actin is relatively well behaved.* Eur J Biochem, 1992. **206**(3): p. 949-55.

104. Mullins, R.D. and T.D. Pollard, *Rho-family GTPases require the Arp2/3 complex to stimulate actin polymerization in Acanthamoeba extracts.* Curr Biol, 1999. **9**(8): p. 405-15.

105. Schafer, D.A. and J.A. Cooper, *Control of actin assembly at filament ends.* Annu Rev Cell Dev Biol, 1995. **11**: p. 497-518.

106. Stradal, T., et al., *CH domains revisited.* FEBS Lett, 1998. **431**(2): p. 134-7.

107. Castresana, J. and M. Saraste, *Does Vav bind to F-actin through a CH domain?* FEBS Lett, 1995. **374**(2): p. 149-51.

108. Lappalainen, P., et al., *The ADF homology (ADF-H) domain: a highly exploited actin-binding module.* Mol Biol Cell, 1998. **9**(8): p. 1951-9.

109. Weeds, A. and S. Maciver, *F-actin capping proteins.* Curr Opin Cell Biol, 1993. **5**(1): p. 63-9.

110. Van Troys, M., J. Vandekerckhove, and C. Ampe, *Structural modules in actin-binding proteins: towards a new classification.* Biochim Biophys Acta, 1999. **1448**(3): p. 323-48.

111. Chereau, D., et al., *Actin-bound structures of Wiskott-Aldrich syndrome protein (WASP)-homology domain 2 and the implications for filament assembly.* Proc Natl Acad Sci U S A, 2005. **102**(46): p. 16644-9.

112. Husson, C., et al., *Multifunctionality of the beta-thymosin/WH2 module: G-actin sequestration, actin filament growth, nucleation, and severing.* Ann N Y Acad Sci, 2010. **1194**: p. 44-52.

113. Paunola, E., P.K. Mattila, and P. Lappalainen, *WH2 domain: a small, versatile adapter for actin monomers.* FEBS Lett, 2002. **513**(1): p. 92-7.

114. Lee, S.H., et al., *Structural basis for the actin-binding function of missing-in-metastasis.* Structure, 2007. **15**(2): p. 145-55.

115. Didry, D., et al., *How a single residue in individual beta-thymosin/WH2 domains controls their functions in actin assembly.* EMBO J, 2012. **31**(4): p. 1000-13.

116. Carlier, M.F., et al., *Structure, function, and evolution of the beta-thymosin/WH2 (WASP-Homology2) actin-binding module.* Ann N Y Acad Sci, 2007. **1112**: p. 67-75.

117. Xue, B., A.H. Aguda, and R.C. Robinson, *Models of the actin-bound forms of the beta-thymosins.* Ann N Y Acad Sci, 2007. **1112**: p. 56-66.

118. Hertzog, M., et al., *The beta-thymosin/WH2 domain; structural basis for the switch from inhibition to promotion of actin assembly.* Cell, 2004. **117**(5): p. 611-23.

119. Irobi, E., et al., *Structural basis of actin sequestration by thymosin-beta4: implications for WH2 proteins.* EMBO J, 2004. **23**(18): p. 3599-608.

120. Aguda, A.H., et al., *The structural basis of actin interaction with multiple WH2/beta-thymosin motif-containing proteins.* Structure, 2006. **14**(3): p. 469-76.

121. Rebowski, G., et al., *Structure of a longitudinal actin dimer assembled by tandem w domains: implications for actin filament nucleation.* J Mol Biol, 2010. **403**(1): p. 11-23.

122. Martinez-Quiles, N., et al., *WIP regulates N-WASP-mediated actin polymerization and filopodium formation.* Nat Cell Biol, 2001. **3**(5): p. 484-91.

123. Marchand, J.B., et al., *Interaction of WASP/Scar proteins with actin and vertebrate Arp2/3 complex.* Nat Cell Biol, 2001. **3**(1): p. 76-82.

124.   Mattila, P.K., et al., *Mouse MIM, a tissue-specific regulator of cytoskeletal dynamics, interacts with ATP-actin monomers through its C-terminal WH2 domain.* J Biol Chem, 2003. **278**(10): p. 8452-9.

125.   Thanabalu, T., et al., *Verprolin function in endocytosis and actin organization. Roles of the Las17p (yeast WASP)-binding domain and a novel C-terminal actin-binding domain.* FEBS J, 2007. **274**(16): p. 4103-25.

126.   Meng, L., et al., *Actin binding and proline rich motifs of CR16 play redundant role in growth of vrp1Delta cells.* Biochem Biophys Res Commun, 2007. **357**(1): p. 289-94.

127.   Robertson, A.S., et al., *The WASP homologue Las17 activates the novel actin-regulatory activity of Ysc84 to promote endocytosis in yeast.* Mol Biol Cell, 2009. **20**(6): p. 1618-28.

128.   Feliciano, D. and S.M. Di Pietro, *SLAC, a complex between Sla1 and Las17, regulates actin polymerization during clathrin-mediated endocytosis.* Mol Biol Cell, 2012. **23**(21): p. 4256-72.

129.   Urbanek, A.N., et al., *A novel actin-binding motif in Las17/WASP nucleates actin filaments independently of Arp2/3.* Curr Biol, 2013. **23**(3): p. 196-203.

130.   Welch, M.D., et al., *Interaction of human Arp2/3 complex and the Listeria monocytogenes ActA protein in actin filament nucleation.* Science, 1998. **281**(5373): p. 105-8.

131.   Egile, C., et al., *Activation of the CDC42 effector N-WASP by the Shigella flexneri IcsA protein promotes actin nucleation by Arp2/3 complex and bacterial actin-based motility.* J Cell Biol, 1999. **146**(6): p. 1319-32.

132.   Higgs, H.N., L. Blanchoin, and T.D. Pollard, *Influence of the C terminus of Wiskott-Aldrich syndrome protein (WASp) and the Arp2/3 complex on actin polymerization.* Biochemistry, 1999. **38**(46): p. 15212-22.

133.   Machesky, L.M. and R.H. Insall, *Scar1 and the related Wiskott-Aldrich syndrome protein, WASP, regulate the actin cytoskeleton through the Arp2/3 complex.* Curr Biol, 1998. **8**(25): p. 1347-56.

134.   Kurisu, S. and T. Takenawa, *The WASP and WAVE family proteins.* Genome Biol, 2009. **10**(6): p. 226.

135.   Machesky, L.M., et al., *Scar, a WASp-related protein, activates nucleation of actin filaments by the Arp2/3 complex.* Proc Natl Acad Sci U S A, 1999. **96**(7): p. 3739-44.

136.   Rohatgi, R., et al., *The interaction between N-WASP and the Arp2/3 complex links Cdc42-dependent signals to actin assembly.* Cell, 1999. **97**(2): p. 221-31.

137.   Yarar, D., et al., *The Wiskott-Aldrich syndrome protein directs actin-based motility by stimulating actin nucleation with the Arp2/3 complex.* Curr Biol, 1999. **9**(10): p. 555-8.

138.   Ti, S.C., et al., *Structural and biochemical characterization of two binding sites for nucleation-promoting factor WASp-VCA on Arp2/3 complex.* Proc Natl Acad Sci U S A, 2011. **108**(33): p. E463-71.

139.   Padrick, S.B., et al., *Arp2/3 complex is bound and activated by two WASP proteins.* Proc Natl Acad Sci U S A, 2011. **108**(33): p. E472-9.

140.   Mullins, R.D., J.A. Heuser, and T.D. Pollard, *The interaction of Arp2/3 complex with actin: nucleation, high affinity pointed end capping, and formation of branching networks of filaments.* Proc Natl Acad Sci U S A, 1998. **95**(11): p. 6181-6.

141.   Blanchoin, L., et al., *Direct observation of dendritic actin filament networks nucleated by Arp2/3 complex and WASP/Scar proteins.* Nature, 2000. **404**(6781): p. 1007-11.

142.   Miki, H., S. Suetsugu, and T. Takenawa, *WAVE, a novel WASP-family protein involved in actin reorganization induced by Rac.* EMBO J, 1998. **17**(23): p. 6932-41.

143.   Rodal, A.A., et al., *Negative regulation of yeast WASp by two SH3 domain-containing proteins.* Curr Biol, 2003. **13**(12): p. 1000-8.

144.   Sun, Y., A.C. Martin, and D.G. Drubin, *Endocytic internalization in budding yeast requires coordinated actin nucleation and myosin motor activity.* Dev Cell, 2006. **11**(1): p. 33-46.

145.   Abdul-Manan, N., et al., *Structure of Cdc42 in complex with the GTPase-binding domain of the 'Wiskott-Aldrich syndrome' protein.* Nature, 1999. **399**(6734): p. 379-83.

146. Fedorov, A.A., et al., *Structure of EVH1, a novel proline-rich ligand-binding module involved in cytoskeletal dynamics and neural function.* Nat Struct Biol, 1999. **6**(7): p. 661-5.

147. Kim, A.S., et al., *Autoinhibition and activation mechanisms of the Wiskott-Aldrich syndrome protein.* Nature, 2000. **404**(6774): p. 151-8.

148. Eden, S., et al., *Mechanism of regulation of WAVE1-induced actin nucleation by Rac1 and Nck.* Nature, 2002. **418**(6899): p. 790-3.

149. Derivery, E., et al., *The Wave complex is intrinsically inactive.* Cell Motil Cytoskeleton, 2009. **66**(10): p. 777-90.

150. Naqvi, S.N., et al., *The WASp homologue Las17p functions with the WIP homologue End5p/verprolin and is essential for endocytosis in yeast.* Curr Biol, 1998. **8**(17): p. 959-62.

151. Li, R., *Bee1, a yeast protein with homology to Wiscott-Aldrich syndrome protein, is critical for the assembly of cortical actin cytoskeleton.* J Cell Biol, 1997. **136**(3): p. 649-58.

152. Deeks, M.J., et al., *Arabidopsis NAP1 is essential for Arp2/3-dependent trichome morphogenesis.* Curr Biol, 2004. **14**(15): p. 1410-4.

153. Bear, J.E., J.F. Rawls, and C.L. Saxe, 3rd, *SCAR, a WASP-related protein, isolated as a suppressor of receptor defects in late Dictyostelium development.* J Cell Biol, 1998. **142**(5): p. 1325-35.

154. Sawa, M., et al., *Essential role of the C. elegans Arp2/3 complex in cell migration during ventral enclosure.* J Cell Sci, 2003. **116**(Pt 8): p. 1505-18.

155. Ben-Yaacov, S., et al., *Wasp, the Drosophila Wiskott-Aldrich syndrome gene homologue, is required for cell fate decisions mediated by Notch signaling.* J Cell Biol, 2001. **152**(1): p. 1-13.

156. Kim, K., et al., *Actin-based motility during endocytosis in budding yeast.* Mol Biol Cell, 2006. **17**(3): p. 1354-63.

157. Young, M.E., J.A. Cooper, and P.C. Bridgman, *Yeast actin patches are networks of branched actin filaments.* J Cell Biol, 2004. **166**(5): p. 629-35.

158. Winter, D., et al., *The complex containing actin-related proteins Arp2 and Arp3 is required for the motility and integrity of yeast actin patches.* Curr Biol, 1997. **7**(7): p. 519-29.

159. Lappalainen, P. and D.G. Drubin, *Cofilin promotes rapid actin filament turnover in vivo.* Nature, 1997. **388**(6637): p. 78-82.

160. Gungabissoon, R.A. and J.R. Bamburg, *Regulation of growth cone actin dynamics by ADF/cofilin.* J Histochem Cytochem, 2003. **51**(4): p. 411-20.

161. Aspenstrom, P., *Roles of F-BAR/PCH proteins in the regulation of membrane dynamics and actin reorganization.* Int Rev Cell Mol Biol, 2009. **272**: p. 1-31.

162. Roberts-Galbraith, R.H. and K.L. Gould, *Setting the F-BAR: functions and regulation of the F-BAR protein family.* Cell Cycle, 2010. **9**(20): p. 4091-7.

163. Roberts-Galbraith, R.H., et al., *Dephosphorylation of F-BAR protein Cdc15 modulates its conformation and stimulates its scaffolding activity at the cell division site.* Mol Cell, 2010. **39**(1): p. 86-99.

164. Campellone, K.G. and M.D. Welch, *A nucleator arms race: cellular control of actin assembly.* Nat Rev Mol Cell Biol, 2010. **11**(4): p. 237-51.

165. Weaver, A.M., et al., *Integration of signals to the Arp2/3 complex.* Curr Opin Cell Biol, 2003. **15**(1): p. 23-30.

166. Ono, S., *Mechanism of depolymerization and severing of actin filaments and its significance in cytoskeletal dynamics.* Int Rev Cytol, 2007. **258**: p. 1-82.

167. Kueh, H.Y., et al., *Actin disassembly by cofilin, coronin, and Aip1 occurs in bursts and is inhibited by barbed-end cappers.* J Cell Biol, 2008. **182**(2): p. 341-53.

168. Heil-Chapdelaine, R.A., N.K. Tran, and J.A. Cooper, *The role of Saccharomyces cerevisiae coronin in the actin and microtubule cytoskeletons.* Curr Biol, 1998. **8**(23): p. 1281-4.

169. Gandhi, M., et al., *Coronin switches roles in actin disassembly depending on the nucleotide state of actin.* Mol Cell, 2009. **34**(3): p. 364-74.

170. Lin, M.C., et al., *Overlapping and distinct functions for cofilin, coronin and Aip1 in actin dynamics in vivo.* J Cell Sci, 2010. **123**(Pt 8): p. 1329-42.

171. Okada, K., et al., *Aip1 and cofilin promote rapid turnover of yeast actin patches and cables: a coordinated mechanism for severing and capping filaments.* Mol Biol Cell, 2006. **17**(7): p. 2855-68.

172. Galletta, B.J., D.Y. Chuang, and J.A. Cooper, *Distinct roles for Arp2/3 regulators in actin assembly and endocytosis.* PLoS Biol, 2008. **6**(1): p. e1.

173. Kubler, E. and H. Riezman, *Actin and fimbrin are required for the internalization step of endocytosis in yeast.* EMBO J, 1993. **12**(7): p. 2855-62.

174. Adams, A.E., D. Botstein, and D.G. Drubin, *Requirement of yeast fimbrin for actin organization and morphogenesis in vivo.* Nature, 1991. **354**(6352): p. 404-8.

175. Ayscough, K.R., et al., *High rates of actin filament turnover in budding yeast and roles for actin in establishment and maintenance of cell polarity revealed using the actin inhibitor latrunculin-A.* J Cell Biol, 1997. **137**(2): p. 399-416.

176. Goodman, A., et al., *The Saccharomyces cerevisiae calponin/transgelin homolog Scp1 functions with fimbrin to regulate stability and organization of the actin cytoskeleton.* Mol Biol Cell, 2003. **14**(7): p. 2617-29.

177. Winder, S.J., T. Jess, and K.R. Ayscough, *SCP1 encodes an actin-bundling protein in yeast.* Biochem J, 2003. **375**(Pt 2): p. 287-95.

178. Le Clainche, C., et al., *A Hip1R-cortactin complex negatively regulates actin assembly associated with endocytosis.* EMBO J, 2007. **26**(5): p. 1199-210.

179. Rocca, D.L., et al., *Inhibition of Arp2/3-mediated actin polymerization by PICK1 regulates neuronal morphology and AMPA receptor endocytosis.* Nat Cell Biol, 2008. **10**(3): p. 259-71.

180. Shimada, A., et al., *Mapping of the basic amino-acid residues responsible for tubulation and cellular protrusion by the EFC/F-BAR domain of pacsin2/Syndapin II.* FEBS Lett, 2010. **584**(6): p. 1111-8.

181. Kessels, M.M. and B. Qualmann, *Syndapin oligomers interconnect the machineries for endocytic vesicle formation and actin polymerization.* J Biol Chem, 2006. **281**(19): p. 13285-99.

182. Boettner, D.R., et al., *The F-BAR protein Syp1 negatively regulates WASp-Arp2/3 complex activity during endocytic patch formation.* Curr Biol, 2009. **19**(23): p. 1979-87.

183. Rader, D.J., J. Cohen, and H.H. Hobbs, *Monogenic hypercholesterolemia: new insights in pathogenesis and treatment.* J Clin Invest, 2003. **111**(12): p. 1795-803.

184. Gerrard, J.M., *Platelet aggregation: cellular regulation and physiologic role.* Hosp Pract (Off Ed), 1988. **23**(1): p. 89-98, 103-4, 107-8.

185. McNicol, A. and S.J. Israels, *Platelet dense granules: structure, function and implications for haemostasis.* Thromb Res, 1999. **95**(1): p. 1-18.

186. Rendu, F. and B. Brohard-Bohn, *The platelet release reaction: granules' constituents, secretion and functions.* Platelets, 2001. **12**(5): p. 261-73.

187. King, S.M. and G.L. Reed, *Development of platelet secretory granules.* Semin Cell Dev Biol, 2002. **13**(4): p. 293-302.

188. Notarangelo, L.D., et al., *Missense mutations of the WASP gene cause intermittent X-linked thrombocytopenia.* Blood, 2002. **99**(6): p. 2268-9.

189. Aldrich, R.A., A.G. Steinberg, and D.C. Campbell, *Pedigree demonstrating a sex-linked recessive condition characterized by draining ears, eczematoid dermatitis and bloody diarrhea.* Pediatrics, 1954. **13**(2): p. 133-9.

190. Thrasher, A.J., *New insights into the biology of Wiskott-Aldrich syndrome (WAS).* Hematology Am Soc Hematol Educ Program, 2009: p. 132-8.

191. Sullivan, K.E., et al., *A multiinstitutional survey of the Wiskott-Aldrich syndrome.* J Pediatr, 1994. **125**(6 Pt 1): p. 876-85.

192. Zhu, Q., et al., *Wiskott-Aldrich syndrome/X-linked thrombocytopenia: WASP gene mutations, protein expression, and phenotype.* Blood, 1997. **90**(7): p. 2680-9.

193. Stewart, D.M., et al., *Studies of the expression of the Wiskott-Aldrich syndrome protein.* J Clin Invest, 1996. **97**(11): p. 2627-34.

194. Banin, S., et al., *Wiskott-Aldrich syndrome protein (WASp) is a binding partner for c-Src family protein-tyrosine kinases.* Curr Biol, 1996. **6**(8): p. 981-8.

195. Cory, G.O., et al., *Evidence that the Wiskott-Aldrich syndrome protein may be involved in lymphoid cell signaling pathways.* J Immunol, 1996. **157**(9): p. 3791-5.

196. Kinnon, C., et al., *The identification of Bruton's tyrosine kinase and Wiskott-Aldrich syndrome protein associated proteins and signalling pathways.* Biochem Soc Trans, 1997. **25**(2): p. 648-50.

197. Finan, P.M., et al., *Identification of regions of the Wiskott-Aldrich syndrome protein responsible for association with selected Src homology 3 domains.* J Biol Chem, 1996. **271**(42): p. 26291-5.

198. Hussain, N.K., et al., *Endocytic protein intersectin-l regulates actin assembly via Cdc42 and N-WASP.* Nat Cell Biol, 2001. **3**(10): p. 927-32.

199. McGavin, M.K., et al., *The intersectin 2 adaptor links Wiskott Aldrich Syndrome protein (WASp)-mediated actin polymerization to T cell antigen receptor endocytosis.* J Exp Med, 2001. **194**(12): p. 1777-87.

200. Otsuki, M., T. Itoh, and T. Takenawa, *Neural Wiskott-Aldrich syndrome protein is recruited to rafts and associates with endophilin A in response to epidermal growth factor.* J Biol Chem, 2003. **278**(8): p. 6461-9.

201. Aspenstrom, P., U. Lindberg, and A. Hall, *Two GTPases, Cdc42 and Rac, bind directly to a protein implicated in the immunodeficiency disorder Wiskott-Aldrich syndrome.* Curr Biol, 1996. **6**(1): p. 70-5.

202. Miki, H., et al., *Induction of filopodium formation by a WASP-related actin-depolymerizing protein N-WASP.* Nature, 1998. **391**(6662): p. 93-6.

203. Higgs, H.N. and T.D. Pollard, *Activation by Cdc42 and PIP(2) of Wiskott-Aldrich syndrome protein (WASp) stimulates actin nucleation by Arp2/3 complex.* J Cell Biol, 2000. **150**(6): p. 1311-20.

204. Bu, W., et al., *The Toca-1-N-WASP complex links filopodial formation to endocytosis.* J Biol Chem, 2009. **284**(17): p. 11622-36.

205. Baba, Y., et al., *Involvement of wiskott-aldrich syndrome protein in B-cell cytoplasmic tyrosine kinase pathway.* Blood, 1999. **93**(6): p. 2003-12.

206. Ochs, H.D., et al., *The Wiskott-Aldrich syndrome: studies of lymphocytes, granulocytes, and platelets.* Blood, 1980. **55**(2): p. 243-52.

207. White, J.G. and J.M. Gerrard, *Ultrastructural features of abnormal blood platelets. A review.* Am J Pathol, 1976. **83**(3): p. 589-632.

208. Bellucci, S., *Megakaryocytes and inherited thrombocytopenias.* Baillieres Clin Haematol, 1997. **10**(1): p. 149-62.

209. Volkman, B.F., et al., *Structure of the N-WASP EVH1 domain-WIP complex: insight into the molecular basis of Wiskott-Aldrich Syndrome.* Cell, 2002. **111**(4): p. 565-76.

210. Rajmohan, R., et al., *Characterization of Wiskott-Aldrich syndrome (WAS) mutants using Saccharomyces cerevisiae.* FEMS Yeast Res, 2009. **9**(8): p. 1226-35.

CHAPTER 2

SLAC, A COMPLEX BETWEEN SLA1 AND LAS17, REGULATES ACTIN

POLYMERIZATION DURING CLATHRIN-MEDIATED ENDOCYTOSIS[1]

2.1 Summary

During clathrin-mediated endocytosis, branched actin polymerization nucleated by the Arp2/3 complex provides force needed to drive vesicle internalization. Las17 (yeast WASp) is the strongest activator of the Arp2/3 complex in yeast cells, it is not autoinhibited, and arrives to endocytic sites 20 seconds before actin polymerization begins. It is unclear how Las17 is kept inactive for 20 seconds at endocytic sites thus restricting actin polymerization to late stages of endocytosis. Here we demonstrate that Las17 is part of a large and biochemically stable complex with Sla1, a clathrin adaptor that inhibits Las17 activity. The interaction is direct, multivalent, and strong, and was mapped to novel Las17 polyproline motifs that are simultaneously class I and class II. *In vitro* pyrene-actin polymerization assays established that Sla1 inhibition of Las17 activity depends on the class I/II Las17 polyproline motifs and is based on competition between Sla1 and monomeric actin for binding to Las17. Furthermore, live cell imaging showed the interaction with Sla1 is important for normal Las17 recruitment to endocytic sites, inhibition

[1] Daniel Feliciano, and Santiago M. Di Pietro
Department of Biochemistry and Molecular Biology, Colorado State University,
Fort Collins, Colorado 80523, USA.

during the initial 20 seconds, and efficient endocytosis. These results advance our understanding of the regulation of actin polymerization in endocytosis.

2.2 Introduction

Endocytosis is essential for a variety of cellular activities including nutrient uptake, cell surface remodeling, and regulation of signal transduction. Clathrin-mediated endocytosis (CME) is a fundamental endocytic pathway involving numerous proteins that collect cargo into a coated pit, invaginate a vesicle, pinch it off, and transport the vesicle to endosomes [1, 2]. This process is highly conserved throughout evolution and proceeds through a well defined sequence of events [3-6]. Actin polymerization is a critical component of CME which was first discovered in yeast, where it forms characteristic cortical actin patches. Mutations in actin cytoskeletal genes, including the Arp2/3 complex, or treatment of yeast cells with drugs that inhibit actin polymerization block endocytic vesicle internalization [7]. The key role of actin in CME has also been established in mammalian cells. A burst of actin polymerization provides force needed for internalization during late stages of CME, however, the mechanisms that control the precise timing of actin polymerization are not well understood [4, 8, 9].

Budding yeast has been a very fruitful system to dissect CME through a combination of genetics, live cell fluorescence microscopy, and biochemistry. Several studies have revealed discrete stages for endocytic vesicle generation and a well-choreographed assembly and disassembly pathway of endocytic factors [3, 6]. First, there is an immobile phase where clathrin and other components arrive to a defined region of the plasma membrane, form a coated pit, and begin collecting transmembrane cargo such as receptors. This step is long (1-2 minutes) and includes proteins such as clathrin, AP-2, and Ede1. Second, another wave of components of the

immobile phase, including Las17 and Sla1, assemble about 20 seconds before actin polymerization [10]. Las17 is the yeast Wiskott-Aldrich syndrome protein (WASp) homolog, and the strongest activator of the Arp2/3-mediated actin polymerization both *in vitro* and *in vivo* [10-13]. Sla1 is both a regulator of the actin cytoskeleton and a clathrin adaptor protein for the internalization of transmembrane protein cargo containing the NPFxD endocytic signal [14-17]. Third, a fast mobile stage of endocytosis occurs concomitant with Arp2/3-mediated actin polymerization that is typically observed by following Abp1. Components of the coat such as Sla1 move about 200 nm into the cell together with the incipient vesicle. This mobile stage of endocytosis is brief (about 10-15 seconds) and culminates with vesicle scission, facilitated by the BAR-domain proteins Rvs161/167. Fourth, quickly after the scission step most components of the coat disassemble as the released vesicle moves towards endosomes along actin cables [18]. It was initially thought that Las17 dissipates from the plasma membrane rather than moving with the invagination, suggesting actin assembly takes place with barbed ends oriented towards the cell surface [3, 5]. However, recent studies indicate Las17 likely moves inward along with the nascent vesicle, consistent with actin polymerization with barbed ends oriented towards the invaginating vesicle [4, 11, 19].

The rate-limiting step for de novo actin filament assembly is nucleation [20]. The primary cellular factor involved in actin nucleation in endocytosis is the conserved Arp2/3 complex. While isolated Arp2/3 complex is a poor actin nucleator, upon interaction with nucleation promoting factors (NPFs) Arp2/3 starts nucleating actin assembly with various strengths [10, 21]. Yeast cells express five NPFs: Las17, Myo5, Myo3, Pan1, and Abp1. The strength with which these NPFs stimulate actin polymerization by Arp2/3 ranges greatly with Las17 reported to be the strongest both *in vitro* and *in vivo*, followed by Myo5/3 [10, 11, 22]. Pan1 and Abp1

display a rather modest NPF activity [23, 24]. Little is known about how the activities of these NPFs are regulated spatially or temporally. Two Arp2/3 NPFs, Las17 and Pan1, arrive to endocytic sites with the same timing as other components of the coat module, about 20 seconds before actin assembly is initiated [10]. In order to understand the regulation of the actin cytoskeleton in endocytosis, it is essential to determine the mechanism that restricts actin assembly to late stages of the endocytic internalization pathway. This is particularly critical for Las17 because, as stated above, it is the strongest Arp2/3 activator, arrives early to endocytic sites, and it is not autoinhibited like some members of the WASp/WAVE family [10, 13, 21]. Three components of the yeast endocytic machinery, Sla1, Bbc1, and Syp1 have been described to inhibit the Las17 NPF activity *in vitro* using the well-characterized pyrene-actin assembly reaction [13, 25]. Therefore Sla1, Bbc1, and Syp1 are candidates to keep Las17 inactive during those initial ~20 seconds before actin assembly at endocytic sites. Analysis of the dynamics of these proteins revealed that Las17 and Sla1 arrive at approximately the same time to endocytic sites, Syp1 is recruited much earlier but overlaps partially with Sla1 and Las17, and Bbc1 is recruited ~20 seconds later than Las17 [10, 25-27]. Taken together, these observations indicate that Sla1 and Syp1 are good candidates for maintaining Las17 inactive during the last 20 seconds of the immobile-phase of endocytosis.

Here we show Sla1 and Las17 form a large biochemically stable complex in the cytosol and that they are co-recruited to sites of endocytosis. Sla1 and Las17 display a direct, multivalent, and high affinity interaction mediated by specific polyproline-SH3 recognition. The interaction was mapped to distinct Las17 polyproline motifs that are simultaneously class I and class II. Disruption of the Sla1-Las17 interaction uncouples the recruitment of Sla1 and Las17 to endocytic sites, causes a defect in Las17 recruitment, and abrogates the ability of Sla1 to inhibit

50

Las17 NPF activity both in pyrene-actin polymerization assays and in live cells. The data supports an important role for Sla1 in negatively regulating the Las17 NPF activity during the initial 20 seconds of recruitment to endocytic sites.

2.3 Results

2.3.1 Las17 and Sla1 display similar spatiotemporal distribution at endocytic sites

Las17-RFP and Sla1-GFP display a high level of colocalization in cells carrying a deletion of the *SLA2* gene which causes endocytic site arrest [5]. In addition, live cell fluorescence microscopy data with wild type cells suggest Las17 and Sla1 are recruited to endocytic sites at approximately the same time [10]. However, this was an indirect comparison rather than a determination made with cells simultaneously expressing both tagged Las17 and Sla1. To more directly assess the relative timing of arrival of Las17 and Sla1 at endocytic sites, a strain expressing both Las17-RFP and Sla1-GFP from the corresponding endogenous locus was generated and analyzed by two-color live cell confocal fluorescence microscopy (Figure 2.1A). Kymographs constructed from these movies show Las17 and Sla1 arriving and dissipating at the same time (Figure 2.1A). We recently reported Sla1 directly interacts with clathrin and that cells expressing Sla1 with a mutation in its clathrin binding motif (Sla1[AAA]-GFP) have a significantly longer patch lifetime compared to wild type Sla1-GFP [14]. Interestingly, cells co-expressing the same mutant Sla1 tagged with GFP (Sla1[AAA]-GFP) and Las17-RFP showed an extended patch lifetime of both proteins and tight colocalization over time (Figure 2.1B). End3 is a well-established component of the yeast endocytic machinery whose deletion causes a significant endocytic defect and prolongs the patch lifetime of Sla1 and other coat proteins [3, 28]. Sla1 and
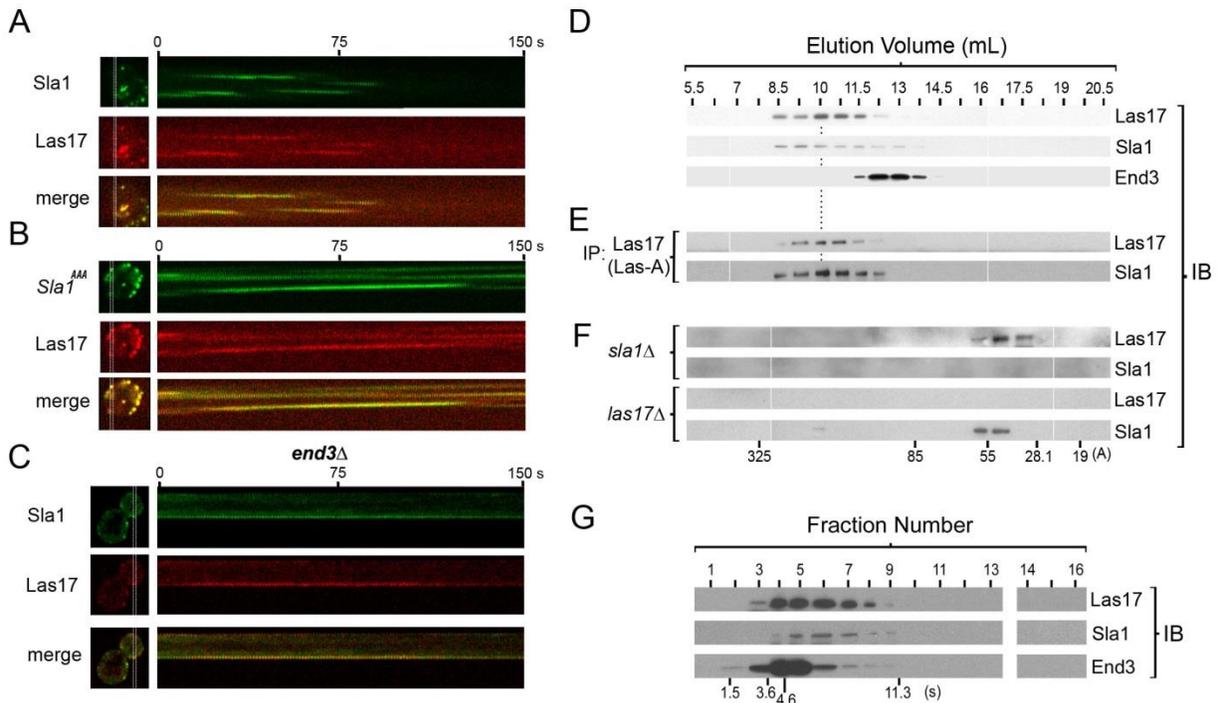
Figure 2. 1

Sla1 and Las17 simultaneously arrive and dissipate at sites of endocytosis and are stably associated in the cytosol. (A) *S.cerevisiae* cells expressing Las17-RFP and Sla1-GFP from endogenous loci (SDY145) were analyzed by live cell fluorescence microscopy using a spinning disk confocal microscope. The areas between white lines on the images (left panels) indicate the region from which kymographs were created (right panels). (B) *S.cerevisiae* cells expressing Las17-RFP and Sla1AAA-GFP (carrying a mutation in the Sla1 clathrin binding motif) from endogenous loci (SDY284) were analyzed by live cell imaging microscopy. (C) *S.cerevisiae* cells expressing Las17-RFP and Sla1-GFP from endogenous loci and carrying a deletion of the END3 gene (*end3Δ*) (SDY474) were analyzed by live cell imaging microscopy. (D) Co-fractionation of Sla1 with Las17 from S. cerevisiae (TVY614) cytosol upon size-exclusion chromatography on a Superose-6 column and immunoblotting analysis (IB) of the fractions, A dotted line is located at the peak (10 ml elution volume) to guide the eye. (E) *S. cerevisiae* (TVY614) cytosol was fractionated by size-exclusion chromatography followed by immunoprecipitation (IP) of each fraction with the Las-A antibody and IB analysis with Las-B or anti-Sla1 antibodies. (F) Size-exclusion chromatography and IB analysis of cytosolic extracts obtained from cells carrying a deletion of the SLA1 gene (*sla1Δ*, GPY3130) or the LAS17 gene (*Las17Δ*, SDY161). Note the shift in Las17 and Sla1 elution profiles compared with cytosolic extracts from wild type cells in (D). (G) S. cerevisiae (TVY614) cytosol was fractionated in a 5-20% sucrose gradient and fractions analyzed by IB as indicated.

52

Las17 colocalized over time in cells carrying a deletion of the *END3* gene (*end3Δ*) (Figure 2.1C). These results fine tune the dynamics of Las17 and Sla1 previously reported and suggest they may be co-recruited from the cytosol to endocytic sites.

2.3.2 Las17 is associated with Sla1 into a stable and large complex

To study endogenous Las17, we raised affinity-purified polyclonal antibodies against recombinant Las17 amino- and carboxi-terminal fragments and named them Las-A and Las-B, respectively. By immunoblotting analysis, both antibodies recognize a band of the expected molecular weight in *S. cerevisiae* cytosolic extracts (Figure 2.2A). Confirmation that the band corresponds to endogenous Las17 protein was obtained by using cytosolic extracts from cells carrying a deletion of the *LAS17* gene (*las17Δ*) in immunoblotting experiments with both the Las-A antibody (Figure 2.2A, third panel) and Las-B antibody (not shown). Both Las-A and Las-B also cross react with other bands considered non-specific because they are also observed in *las17Δ* cell extracts, their apparent molecular weight is far from the Las17 molecular mass (67.7 KDa), and they are not detected by both antibodies (Figure 2.2A). The Las-A antibody works well for immunoprecipitation of endogenous Las17 from yeast cell extracts (Figure 2.2A, fourth panel).

Epitope-tagged Las17 was reported to co-immunoprecipitate with Sla1 from detergent-containing yeast total extracts suggesting they interact physically – directly or indirectly – *in vivo*, presumably at endocytic sites [12]. The newly generated anti-Las17 antibodies were used in immunoprecipitation-immunoblotting experiments to test if endogenous Las17 co-immunoprecipitates with endogenous Sla1 from the yeast cytosolic fraction (Figure 2.2B). For this purpose, a detergent-free extract was prepared and all membrane fractions removed by
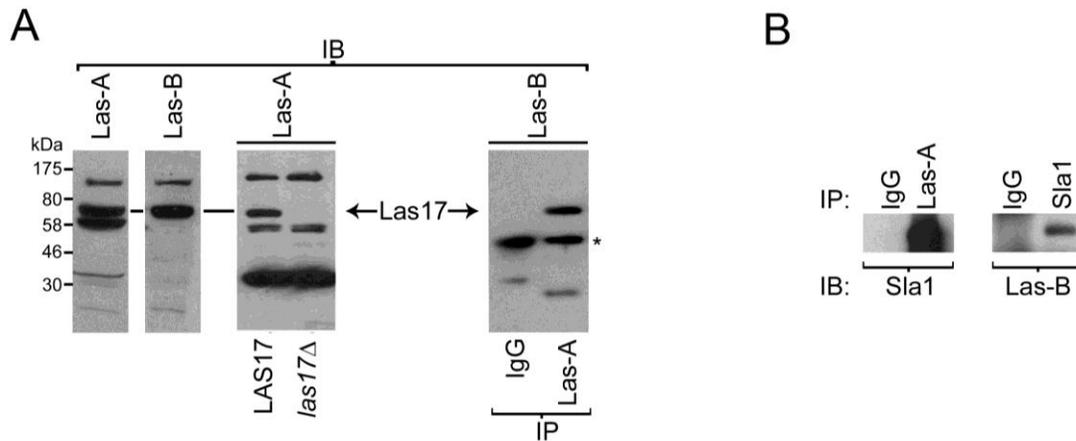
Figure 2. 2
Immunochemical detection of endogenous Las17 and co-immunoprecipitation with endogenous Sla1. (A) Immunoblotting (IB) analysis of *S.cerevisiae* cytosolic extracts illustrating the specificity of affinity purified polyclonal antibodies against Las17 amino- and carboxi-terminal fragments, Las-A and Las-B, respectively. Note the absence of the Las17 band in extracts prepared from cells carrying a deletion of the LAS17 gene (*las17Δ*, SDY161) compared with wild type cells (LAS17, TVY614) (third panel). * non-specific band recognized by the secondary antibody during IB (fourth panel). (B) Co-immunoprecipitation of Sla1 with Las17 (left panel) and of Las17 with Sla1 (right panel) from wild type yeast cytosolic extracts (TVY614).

ultracentrifugation. Sla1 was detected in Las17 but not in control immunoprecipitates and, conversely, Las17 was detected in Sla1 but not in control immunoprecipitates (Figure 2.2B). This result indicates Las17 and Sla1 may interact physically – directly or indirectly – both on the plasma membrane and in the cytosol, suggesting they may be more stably associated than previously appreciated.

To test the possibility of stable association of Las17 with Sla1, yeast cytosolic extracts were fractionated by size exclusion chromatography and each fraction was analyzed by immunoblotting (Figure 2.1D). Las17 co-fractionated with Sla1, but not with End3, another endocytic coat protein (Figure 2.1D). Furthermore, in a separate experiment each size exclusion chromatography fraction was subsequently subjected to immunoprecipitation with the Las-A antibody and immunoblotting analysis with both Las-A and Sla1 antibodies (Figure 2.1E). As expected, Las17 showed the same profile as in Figure 2.1D. Importantly, Sla1 was also present and peaked in the same fractions as Las17, around an elution volume of 10 ml. This result indicates those fractions contain Las17 associated with Sla1 in a stable complex as opposed to a random co-fractionation. To further test the possibility of a stable association between Las17 and Sla1, cytosolic extracts were prepared from yeast strains carrying a deletion of the *SLA1* (*sla1Δ*) or *LAS17* (*las17Δ*) gene and fractionated by size exclusion chromatography (Figure 2.1F). Immunoblotting analysis of the fractions showed that in the absence of Sla1, Las17 elution volume changed dramatically (~10 ml to ~17 ml) displaying a significantly smaller Stokes radius (Figure 2.1F). Conversely, in the absence of Las17, the elution profile of the bulk of Sla1 also changed dramatically (~10 ml to ~16.5 ml) to a considerably smaller Stokes radius (Figure 2.1F). Together these results show Sla1 and Las17 are associated into a stable complex.

From the experiments with wild type cells we estimated the Sla1-Las17 complex has a Stokes radius of 224 ± 6 Å and from sedimentation velocity experiments (Figure 2.1G) we estimated a sedimentation coefficient of 8.1 ± 0.5 S. The native molecular mass of the Sla1-Las17 complex was calculated from the Stokes radius and sedimentation coefficient as 822 ± 28 kDa [29]. A similar analysis for the well-known hetero-tetrameric AP-2 complex revealed a native molecular mass of 212 ± 5 kDa, while its theoretical molecular mass (one copy each of the Apl1, Apl3, Apm4, Aps2 subunits) is 286 kDa (Di Pietro, unpublished). Therefore, this analysis of the Sla1-Las17 complex may have slightly underestimated its native molecular mass. Since the molecular masses of Sla1 and Las17 are 135.8 kDa and 67.6 kDa respectively, the complex must contain multiple copies of Sla1 and Las17, includes additional proteins, or both. The Stokes radius obtained for Las17 with *sla1Δ* cells 40 ± 1 Å or for Sla1 with *las17Δ* cells 47 ± 4 Å (Figure 2.1F) are compatible with monomeric Las17 and Sla1 respectively, suggesting that there may be no additional components to the complex or that they dissociate from the complex if Las17 or Sla1 are not present.

To test the possibility of additional subunits, endogenous Las17 complex was isolated from a strain expressing C-terminus tandem affinity purification (TAP)-tagged Las17 from the *LAS17* locus. Following the TAP purification procedure, proteins associated with Las17 were identified by mass spectrometry. A control experiment was carried out in parallel with an untagged strain subjected to the same TAP purification procedure and mass spectrometry. Proteins detected with the Las17-TAP-tagged strain but not with the untagged strain are presented in Table 2.1. In addition to Sla1, seven proteins were detected. Five of these proteins were found in a previous study using Las17-derived actin networks produced with Las17-functionalized microbeads and yeast extract (Table 2.1) [30]. The two additional proteins found

Table 2.1   Las17 interacting proteins detected by Mass spectrometry

| This study	Michelot *et al.* (2010)
Las17	+
Sla1	+
Vrp1	+
Bbc1	+
Myo3	+
Actin	+
Pil1	+
Pan1	-
Clathrin heavy chain	-

here are clathrin heavy chain and Pan1, both known to interact physically with Sla1 [14, 31]. These seven proteins are likely transient Las17 or Sla1 interactors rather than stable components of the Sla1-Las17 complex. For instance, most of these proteins (Vrp1, Bbc1, Myo3, actin, and clathrin) display dynamics at endocytic patches different from that of Sla1 and Las17 and are therefore incompatible as components of a stable complex. Pan1 does have patch dynamics similar to Sla1 and Las17 (Sun 2006), but it has been shown to form a stable complex with End3 and Sla2 [32] and our gel filtration analysis showed End3 is not a component of the Sla1-Las17 stable complex (Figure 2.1D). Consistently, in similar yeast cytosol gel filtration analysis the bulk of Pan1 and Sla2 peaked in fractions corresponding to Stokes radius smaller than Sla1 and Las17, but similar to End3 (Di Pietro, unpublished). Likewise, gel filtration analysis of the eisosome component Pil1 using a cytosolic fraction from a Pil1-GFP strain showed it does not co-fractionate with the Sla1-Las17 complex (data not shown). These mass spectrometry and gel filtration experiments suggest there may not be additional subunits in the Sla1-Las17 complex. Nevertheless, we cannot rule out putative additional subunits that might have failed mass spectrometry detection for reasons such as poor peptide ionization.

Together, these biochemical studies demonstrate all endogenous Las17 in the cytosol is associated into a large and stable complex with Sla1, consistent with the idea of their co-recruitment to endocytic sites.

2.3.3 Novel Las17 class I/II polyproline motifs mediate direct and high affinity binding to Sla1 SH3 domains

From amino- to carboxi-terminus, Las17 is composed of a WH1 domain, a polyproline region, a WH2 domain, and an acidic tail (Figure 2.3A). While WH2 and the acidic tail (also
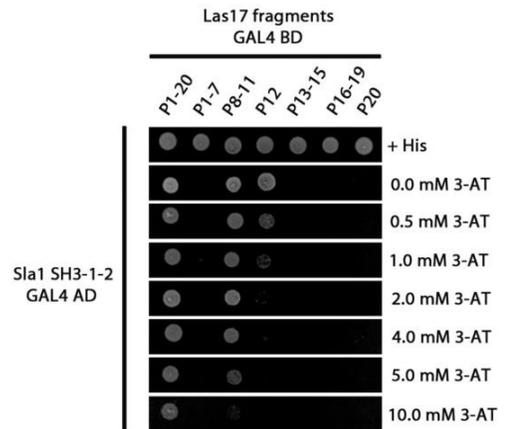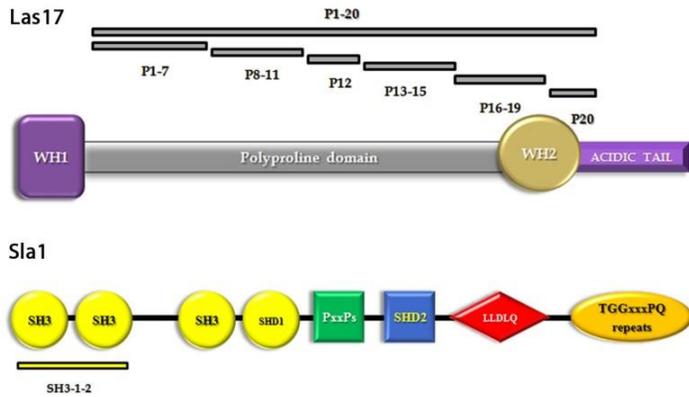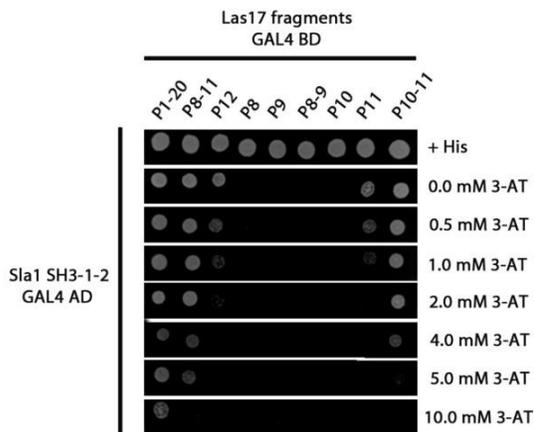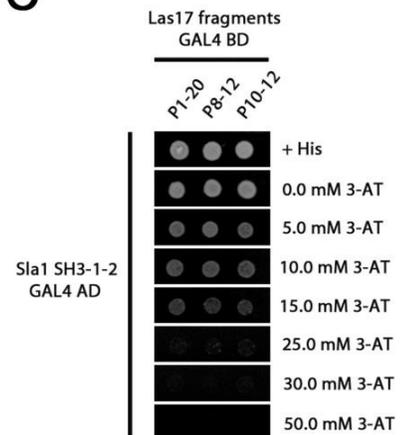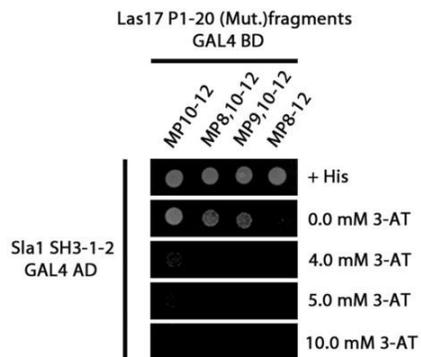
Figure 2. 3
Identification of Las17 polyproline motifs involved in Sla1 binding by yeast two-hybrid analysis. (A) Left, cartoon representation of Las17 and Sla1 domains. Grey bars above Las17 indicate the various fragments containing polyproline motifs (P1 through P20) tested for binding to Sla1 SH3 domains 1 and 2 (yellow bar, SH3-1-2). Right, yeast cells (AH109) were co-transformed with expression plasmids containing GAL4 DNA-binding (GAL4 BD) and activation (GAL4 AD) domains fused in frame to the indicated Las17 fragments and Sla1-SH3-1-2, respectively. Double transformants were first selected on minimal media lacking leucine and tryptophan and containing histidine (+His) and then spotted onto plates containing the same medium (as control) or selective medium lacking histidine and containing various concentrations of 3-AT. (B) Yeast two-hybrid analysis comparing the strength of interaction of single and double polyproline motifs within the P8-P12 fragment. (C) Yeast two-hybrid analysis showing similar strength of interaction between P1-20, P8-12, or P10-12 with Sla1-SH3-1-2. (D) Various point mutations were introduced that selectively inactivated specific polyproline motifs (class I/II) in the context of the P1-20 construct and analyzed using the yeast two-hybrid system. Mutations consisted in two proline-to-alanine changes per polyproline motif in order to disrupt the PxxP core sequence of each target motif.

known as VCA motif) are the actin and Arp2/3 binding regions that mediate its conserved NPF activity, the central polyproline region of Las17 can interact with proteins containing SH3 domains (Figure 2.2A) [33]. Sla1 is composed of three amino-terminal SH3 domains and other domains important for cargo recruitment (SHD1), clathrin binding (LLDLQ), and both Sla1 oligomerization and regulation of binding to clathrin (SHD2) (Figure 2.3A) [14-17]. Importantly, a study by Rodal et al. (2003) showed that the first and second Sla1 SH3 domains, but not the third, can inhibit the Las17 NPF activity in pyrene-actin *in vitro* polymerization assays. Therefore the first and second Sla1 SH3 domains are good candidates to mediate a direct interaction with Las17.

Our analysis of the central polyproline region of Las17 indicates it can be dissected into 20 separate segments each containing sequences conforming to the SH3 binding PxxP motif (P1 through P20, Figure 2.3A). Yeast two hybrid analysis was performed to test for binding of the Las17 polyproline motifs to the first and second Sla1 SH3 domains (Figure 2.3A-D). The full length polyproline region containing all 20 Las17 PxxP motifs (P1-20), and two fragments (P8-11 and P12) interacted with the Sla1 SH3 domains as evidenced by yeast growth in selective plates lacking histidine (Figure 2.3A). A comparison of the relative interaction strength for the different fragments was obtained by using selective plates with increasing concentration of 3-Amino-1,2,4-triazole (3-AT) (Figure 2.3A). P1-20 displayed the strongest interaction followed by P8-11 and P12. Sequence analysis of the polyproline motifs in fragments P8-11 and P12 revealed that all five core PxxP sequences are flanked by arginine residues and match class I (RxxPxxP) or class II (PxxPxR) polyproline motifs consensus. This is consistent with a previous study in which the first and second SH3 domains of Sla1 were predicted to bind class I or class II polyproline motifs [34]. Interestingly, P8, P9, P11 and P12 sequences simultaneously fit the

requirement for both polyproline class I and class II motifs and we refer to these polyproline motifs as class I/II (Figure 2.4). P10 is an imperfect fit to the class I/II motif (Figure 2.4). The discovery of the Las17 class I/II polyproline motifs is important since it implies the binding of Sla1 SH3 domains to Las17 is not restricted to a specific orientation as was described for other SH3 domains and their ligands (Figure 2.4) [35].

To further dissect the contribution of these 5 polyproline motifs to complex formation, additional constructs containing one or two motifs were examined (Figure 2.3B). Analysis of the individual polyproline motifs indicated only P11 and P12 were able to show cell growth in selective plates. In addition, a fragment containing both P10 and P11 displayed cell growth at higher 3-AT concentration than P11 alone. In contrast, P8 and P9 did not show cell growth either individually or together, and only contributed modestly when they were combined with P10 and P11 (P8-11 versus P10-11) (Figure 2.3B). These findings suggest that the core for the Sla1 binding site spans from P10 to P12 (Figure 2.3B). To further test the relevance of P10, P11 and P12 and determine their contribution to binding Sla1 SH3 domains, two additional constructs were tested, one containing a Las17 fragment P8 through P12 (P8-12) and another spanning P10 through P12 (P10-12), and compared to the full central polyproline region (P1-20) (Figure 2.3C). All three constructs showed similar level of interaction with cell growth up to 25 mM 3-AT suggesting that P10, P11, and P12 are the key motifs mediating the Las17-Sla1 interaction (Figure 2.3C). An alignment between P10, P11, and P12 revealed their sequences are more closely related to each other than to other class I/II (P8 and P9) or non-class I/II motifs (P7) (Figure 2.4). Features within the P10, P11, and P12 consensus sequence likely explain the preference of Sla1 SH3-1-2 for these three class I/II polyproline motifs.

A

**Sequence alignment
of PxxPs in P8-12**

```
*P7  FPFPIPEIPSTQS

 P8  QNRPLPQLPNRNN
 P9  NNRPVPPPPPMRT
P10  VRLPAPPPPPRRG
P11  RRGPAPPPPPHRH
P12  RRGPAPPPPPRAS

       Consensus
     .nrP.PppPpr..
```

**Sequence alignment
of PxxPs in P10-12**

```
P10  VRLPAPPPPPRRG
P11  RRGPAPPPPPHRH
P12  RRGPAPPPPPRAS

       Consensus
     rRgPAPPPPPrr.
```

B
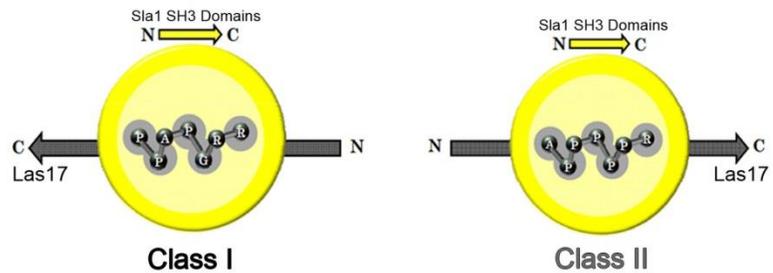
Figure 2. 4
Alignment of Las17 Class I/II polyproline motifs. (**A**) Comparative alignment between all Las17 Class I/II polyproline motifs in P8-12 and P10-12. The asterisk (*) depicts a non-Class I/II polyproline motif in Las17. (**B**) Top panel shows an example of a Las17 Class I/II motif (P12) that conforms to both Class I and Class II consensus motifs. Lower panel depicts a model for the potential Las17-Sla1 binding orientations based on previous SH3 domain studies.

To confirm the specificity of the interaction, we introduced point mutations that selectively destroyed the class I/II motifs in the context of the P1-20 construct, but maintained all other polyproline motifs intact (Figure 2.3D). The mutations consisted in two proline-to-alanine changes per polyproline motif in order to disrupt the PxxP core sequence. Consistently, mutation of P10, P11 and P12 (MP10-12) strongly affected the ability of these cells to growth at higher 3-AT concentration and additional mutations in both P8 and P9 (MP8-12) completely destroyed any residual binding to Sla1 SH3 domains (Figure 2.3D). Together, the yeast two hybrid experiments have mapped the interaction of the Sla1 SH3 domains 1 and 2 to specific Las17 polyproline motifs that belong to a new class I/II, with a subset composed of polyprolines P10, P11, and P12 likely representing the core binding site.

To corroborate a direct association between Las17 and Sla1 specifically mediated by the class I/II polyproline motifs, we carried out GST-fusion binding assays. Four GST-fusion proteins were constructed and purified, which contain Las17 fragments P8-12, P10-12, P8-11, or P12. Binding of these GST-fusion proteins to an hexahistidine-tagged Sla1 fragment spanning the SH3 domains 1 and 2 (His-Sla1-SH3-1-2) was analyzed by Coomassie blue staining and IB (Figure 2.5A). GST-P8-12 and GST-P10-12 showed significant and similar ability to bind His-Sla1-SH3-1-2. GST-P8-11 showed an intermediate level of binding, and GST-P12 displayed a barely detectable binding. The relative level of binding paralleled the data obtained by yeast two hybrid analyses (Figure 2.3) and confirmed a direct interaction between Las17 and Sla1. The results also suggest the presence of multiple polyproline motifs in Las17 may mediate strong binding due to an avidity effect with a divalent Sla1 fragment.

To estimate the affinity of the interaction between Las17 polyproline motifs and Sla1 SH3 domains we followed a quantitative ligand depletion approach [22]. Using a constant

concentration of His-Sla1-SH3-1-2 and increasing concentrations of GST-P8-12 bound to glutathione beads, the free ligand (His-Sla1-SH3-1-2) was determined after incubation. The free His-Sla1-SH3-1-2 fraction present in the supernatant was analyzed by SDS-PAGE and coomassie staining followed by densitometric quantitation (Figure 2.5B). Bound fractions were calculated by substraction from the total amount of ligand available for binding (Figure 2.5B). Binding was saturable and fitting of the data using non-linear regression determined a K_d of 56 ± 8 nM (Figure 2.5B). Binding curves with the same GST-P8-12 protein containing point mutations that substitute alanine for the key proline residues in the P10, P11, and P12 motifs (GST-P8-12 MP10-12) showed minimal residual binding. This high affinity binding between Sla1 SH3 domains 1 and 2 and specific Las17 class I/II polyproline motifs supports the notion of a stable complex between the full length proteins.

2.3.4 Class I/II polyproline motifs are necessary for Sla1 inhibition of Las17 NPF activity in vitro

Purified Las17, like purified WAVE, is not autoinhibited and potently activates Arp2/3 mediated actin polymerization [10, 13]. However, Sla1 SH3 domains 1 and 2 were shown to inhibit Las17 NPF activity using the pyrene-actin polymerization assay [13]. Similar pyrene-actin polymerization experiments were carried out here using recombinant full length Las17 purified from bacteria to ensure that no Sla1 or other Las17 interacting protein co-purified. Las17 triggered rapid actin polymerization that was inhibited by purified His-Sla1-SH3-1-2 in a concentration dependent manner, as evidenced by a decrease in the polymerization rate (slope) and an extended lag phase (Figure 2.6A). Saturating amounts of His-Sla1-SH3-1-2 inhibited

A

GST | GST-P8-12 | GST-P10-12 | GST-P8-11 | GST-P12 | 6% Input

His-Sla1 SH3 1-2

IB: anti-His

Coommassie

B

GST-P8-12 Wt
GST-P8-12 MP10-12

Kd = 56.0 ± 8.0 nM

Sla1 SH3 1-2 Bound fraction

GST-P8-12 (nM)

1280 nM
0
GST-P8-12 Wt

Free
Sla1 SH3 1-2

1280 nM
0
GST-P8-12 MP10-12

Free
Sla1 SH3 1-2
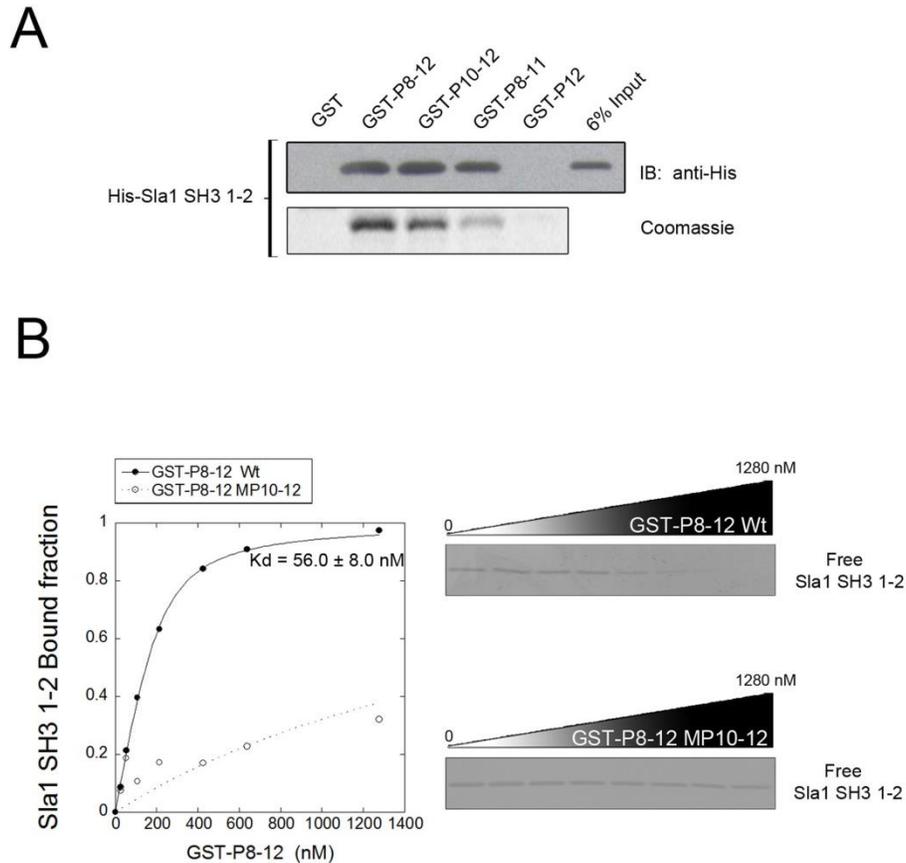
Figure 2. 5

The interaction between Las17 and Sla1 is direct and strong. (**A**) GST fusion affinity assay was carried out with recombinant GST alone as a control, or GST fused to las17 fragments P8-12 (GST-P8-12), P10-12 (GST-P10-12), P8-11 (GST-P8-11), and P12 (GST-P12). Each GST-fusion protein was bound to glutathione beads and incubated with purified polyhistidine-tagged Sla1 fragment SH3-1-2 (His-Sla1-SH3-1-2). The bound His-Sla1-SH3-1-2 fraction was analyzed by coomassie staining and immunobloting with an anti-polyhistidine antibody. (**B**) A constant concentration of His-Sla1-SH3-1-2 (150 nM) was incubated with increasing concentrations of GST-P8-12 or GST-P8-12-MP10-12 (point mutations in P10, P11 and P12) bound to glutathione beads as described in (**A**). The free His-Sla1-SH3-1-2 fraction remaining in the supernatant was determined by densitometry of SDS-PAGE staining. The His-Sla1-SH3-1-2 bound fractions were calculated and fitted to non-linear regression to estimate the K_d for the interaction.

A

B

C

Las17 Wt

D

Las17 MP10-12

E

Las17 MP8-12

F

67
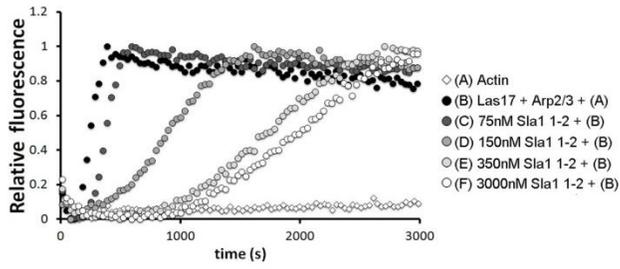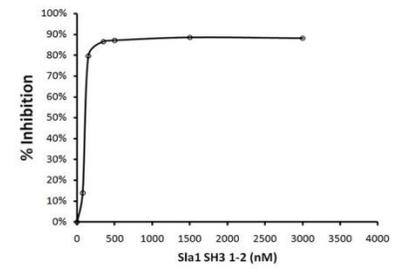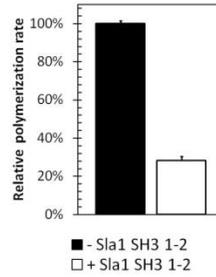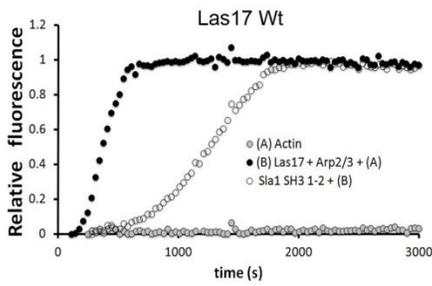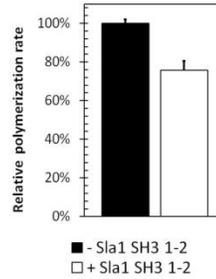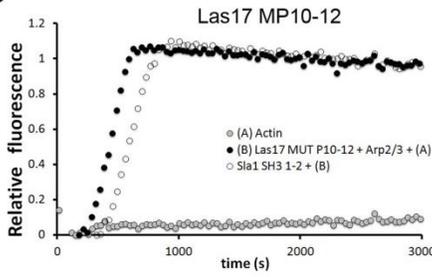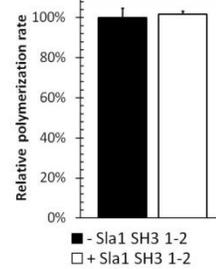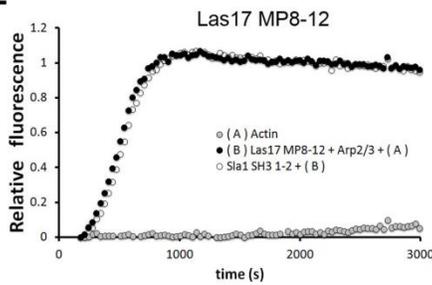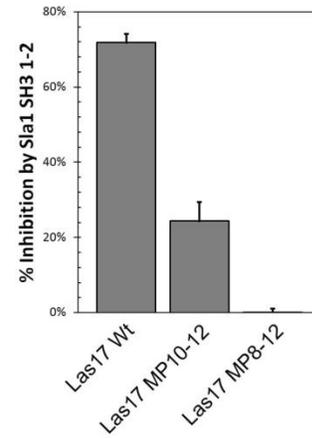
Figure 2. 6

Class I/II polyproline motifs are critical for Sla1-SH3-1-2 fragment inhibition of Las17 NPF activity in pyrene-actin polymerization assays. (A) Actin (1.5 μM, 99% pyrene labeled) was polymerized in the presence of Arp2/3 complex (75 nM), full length wild type Las17 (75 nM), and a range of concentrations of His-Sla1-SH3-1-2 fragment. (B) Concentration-dependent effects of His-Sla1-SH3-1-2 inhibition on Las17-Arp2/3 induced actin polymerization. Percent inhibition was calculated from the reduction in polymerization rate as determined in (A). (C-E) The ability of full length wild type Las17 (75 nM) (C), Las17-MP10-12 (75 nM) (D), and Las17-MP8-12 (75 nM) (E) to activate Arp2/3-mediated actin polymerization was measured as described in (A) in the absence (black circles) or presence of His-Sla1-SH3-1-2 (150 nM) (white circles). The effect of His-Sla1-SH3-1-2 on the Las17 activity is expressed as relative polymerization rate (C-E) or percent inhibition (F). Polymerization rates and inhibition percentages are expressed as the average ± SEM of three independent determinations.

Las17 activity by 86% with a half-maximal concentration (IC_{50}) of 120 nM (Figure 2.6A and 2.6B). These results are consistent with previously reported data [13].

To test the possibility that Sla1 inhibition is dependent on the same Las17 class I/II polyproline motif that mediate the Las17-Sla1 association, we purified from bacteria full length Las17 containing the same polyproline motif point mutations that abrogated binding, Las17 MP10-12 and Las17-MP8-12 (Figure 2.3D and 2.5B). Pyrene-actin polymerization assays showed both Las17-MP10-12 and Las17-MP8-12 retained a strong NPF activity similar to the wild type protein assayed under the same conditions, indicating their ability to bind to actin and the Arp2/3 complex was intact (Figure 2.6C-E). Addition of 150 nM His-Sla1-SH3-1-2 inhibited the activity of Las17 wild type by 75% (25% residual NPF activity) (Figure 2.6C and 2.6F). Importantly, addition of 150 nM His-Sla1-SH3-1-2 inhibited Las17-MP10-12 by only 25% (75% residual NPF activity), and did not inhibit Las17-MP8-12 at all (100% residual NPF activity) (Figure 2.6D-F). These observations indicate that the class I/II polyproline motifs identified here are not only important for Las17-Sla1 strong association but are also key components of Las17 NPF negative regulation by Sla1.

2.3.5 The presence of Sla1 SH3 domains disrupts Las17 interaction with G-actin

A second monomeric actin binding site – additional to the WH2 domain – was recently discovered in Las17 [36] which may in part explain the very strong Las17 activity compared to other NPFs. This new monomeric actin binding site was not fully characterized but was located within residues 300 and 422 of Las17. Interestingly, our Las17-P8-12 fragment spans residues 300-404. Thus, the ability of the Sla1 SH3 domains to inhibit Las17 NPF activity may depend on competition between monomeric actin and the SH3 domains for binding to this region of Las17.

We first tested for the ability of Las17-P8-12 fragment to bind monomeric actin. For this purpose a pyrene-actin polymerization assay was carried out in conditions where polymerization of actin (3 µM) by itself – in the absence of Arp2/3 complex – is readily detected (Figure 2.7). Addition of Las17-P8-12 fragment in excess of the monomeric actin concentration (6 µM) dramatically inhibited actin polymerization, consistent with monomeric actin binding and sequestration (Figure 2.7). Importantly, further addition of Sla1-SH3-1-2 reverted the Las17-P8-12 fragment inhibition, likely by binding to the Las17-P8-12 fragment thus competing off monomeric actin and returning it to the free pool available for polymerization. Subsaturating concentrations of Sla1-SH3-1-2 fragment (2 µM) elicited partial rescue, while saturating concentrations (12 µM) caused full rescue (Figure 2.7). These results indicate that Sla1 inhibits Las17 NPF activity at least in part by disrupting Las17 ability to interact with G-actin through this novel binding site.

2.3.6 Class I/II polyproline motifs are important for normal Las17 recruitment and inhibition at sites of endocytosis

So far our results indicate that Las17 and Sla1 arrive to endocytic sites at the same time because they are associated into a stable complex that likely keeps Las17 in an inactive state by competing off G-actin. Moreover, specific Las17 polyproline motifs involved in both the *in vitro* interaction and inhibition were mapped. We reasoned that disrupting the physical interaction between Las17 and Sla1 in cells may cause a defect in the Las17 recruitment to endocytic sites and/or a lack of inhibition of Las17 NPF activity. To test these possibilities we tagged the Las17 endogenous gene with GFP and subsequently introduced the same polyproline motif point mutations that abolished binding to Sla1 (Figure 2.3D and 2.5B), and disrupted the inhibition in actin polymerization assays (Figure 2.6C-F). We crossed this strain with one expressing
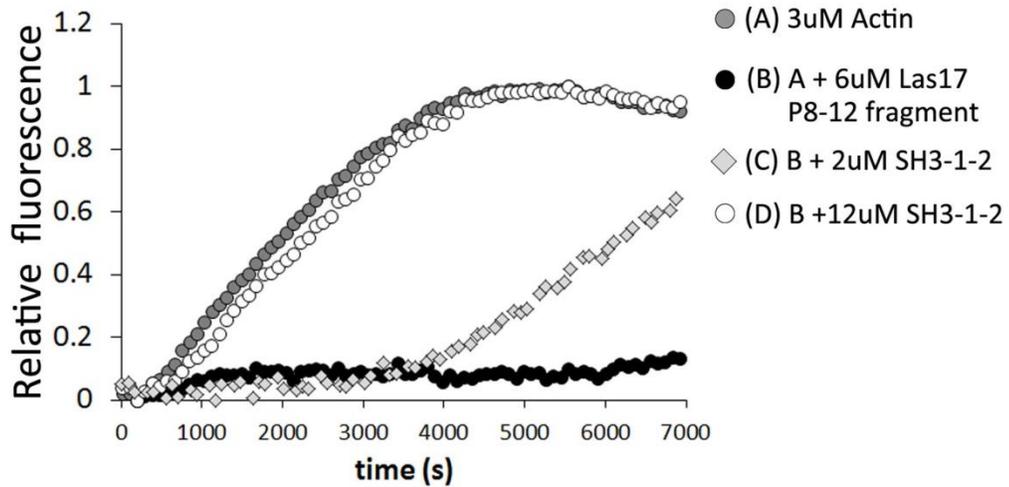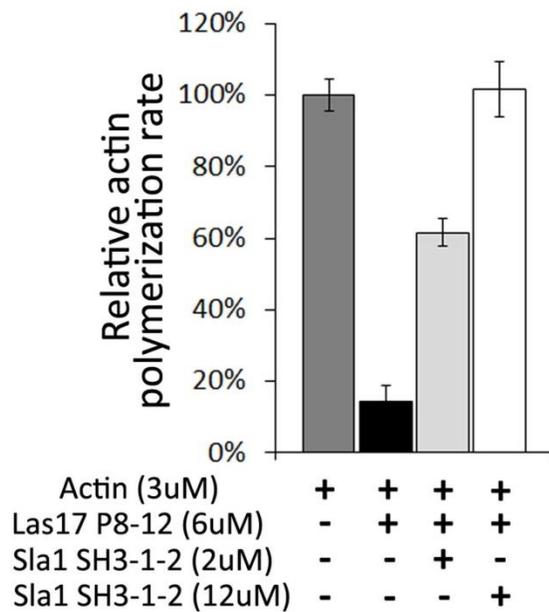
Figure 2. 7
The presence of Sla1 SH3 domains disrupts Las17 interaction with G-actin. (A) Actin (3 μM, 99% pyrene labeled) was allowed to polymerize alone (in the absence of Arp2/3 complex or any other protein) (grey circles), in the presence of Las17-P8-12 fragment (6 μM) (black circles), both Las17-P8-12 fragment (6 μM) and His-Sla1-SH3-1-2 (2 μM) (light grey diamonds), or both Las17-P8-12 fragment (6 μM) and His-Sla1-SH3-1-2 (12 μM) (white circles). (B) Relative actin polymerization rates are expressed as the average ± SEM of three independent determinations.

Sla1-RFP or Abp1-RFP from the corresponding endogenous locus, sporulated the resulting diploids, and obtained haploid cells expressing the mutant Las17-GFP (Las17-MP8-12-GFP) and Sla1-RFP or Abp1-RFP. Similar strains with wild type Las17-GFP and Sla1-RFP or Abp1-RFP were also generated for comparison. By confocal fluorescence microscopy analysis, wild type Las17-GFP and Sla1-RFP displayed an indistinguishable endocytic patch lifetime and they arrived and dissipated simultaneously (Figure 2.8A, Figure 2.9A). Notably, a similar analysis with cells expressing Las17-MP8-12-GFP and Sla1-RFP showed mutant Las17 arrived ~18 seconds after Sla1 (Figure 2.8B, Figure 2.9B). In addition, the patch lifetime of Las17 decreased and that of Sla1 increased (Figure 2.8B). During the course of these investigations it became apparent that while Las17-MP8-12-GFP does localize to endocytic sites, its patch fluorescence intensity was lower and the cytosolic background was higher compared with wild type Las17-GFP. Quantitation of the fluorescence intensity ratio of Las17-MP8-12-GFP at endocytic patches to cytosol confirmed a statistically significant decrease compared with wild type Las17-GFP suggesting less mutant Las17 molecules localize to the patch (Figure 2.10A). This difference is not a result of overall destabilization of mutant Las17 as determined by immunoblotting analysis of total cell extracts (Figure 2.10B). These results are consistent with a defect in Las17 recruitment to endocytic sites when its association with Sla1 is compromised. We also noticed that in a previous study *sla1Δ* cells displayed a higher Las17-GFP background than wild type cells, although the experiment was not focused on the recruitment aspect and this defect was not quantified [3]. Perhaps the known Sla1 interactions with endocytic transmembrane cargo, clathrin, Pan1, and numerous other coat proteins are important for Las17 recruitment in the context of the native complex with Sla1. Las17-MP8-12-GFP residual recruitment to sites of endocytosis may be mediated by some remaining interaction with other Sla1 domains,
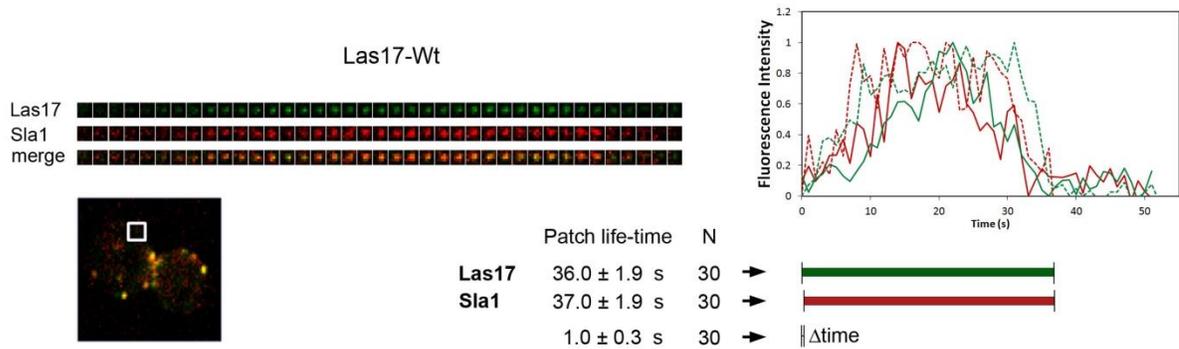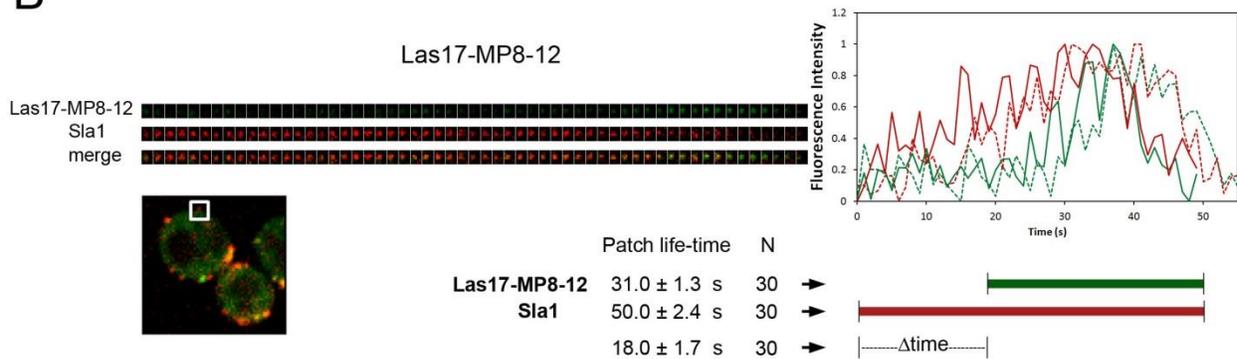
Figure 2. 8
Uncoupling of the Las17 and Sla1 complex in vivo after mutation of class I/II polyproline motifs. Dynamics of (A) Las17-GFP and (B) Las17-MP8-12-GFP with Sla1-RFP at endocytic sites (SDY382 and SDY384, respectively). Time series (left) showing localization of Las17 and Sla1 at an endocytic patch from two-color movies (1 frame/s). Alignment of Las17 (green) and Sla1 (red) patch intensities as function of time (right panel depicts examples of two distinct patches, solid and dashed line, respectively). Patch life times ± SEM, Δtime ± SEM and number of patches analyzed (N) are indicated. Differences in Las17 (P=0.01) and Sla1 (P=0.0001) patch lifetimes and Δtime (P<0.0001) between Las17 and Las17- MP8-12 cells were statistically significant.
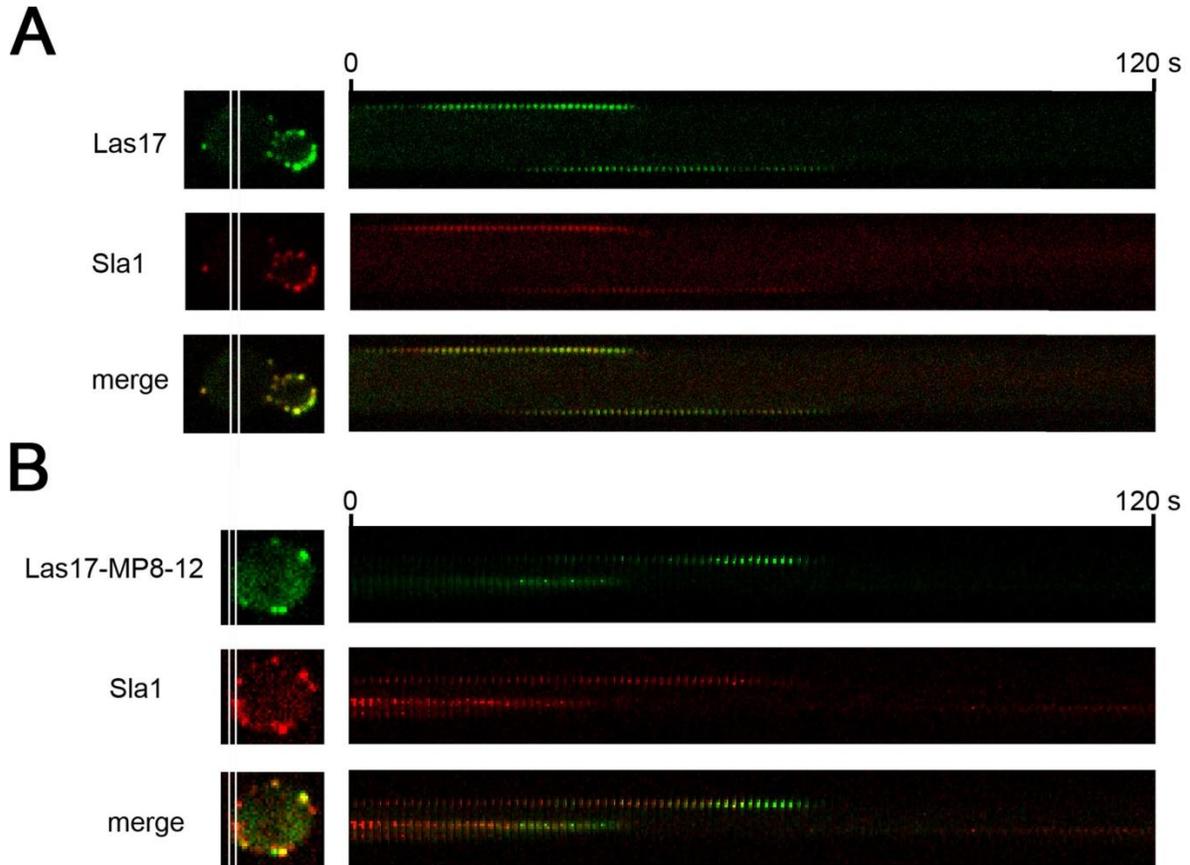
Figure 2. 9
Uncoupling of the Las17 and Sla1 complex *in vivo* after mutation of class I/II polyproline motifs. (**A**) *S.cerevisiae* cells expressing Las17-GFP and Sla1-RFP from endogenous loci (SDY382) were analyzed by live cell fluorescence microscopy using a spinning disk confocal microscope. The areas between white lines on the images (left panels) indicate the region from which kymographs were created (right panels). (**B**) *S.cerevisiae* cells expressing Las17-MP8-12-GFP and Sla1-RFP from endogenous loci (SDY384) were analyzed by live cell imaging microscopy.

A

B
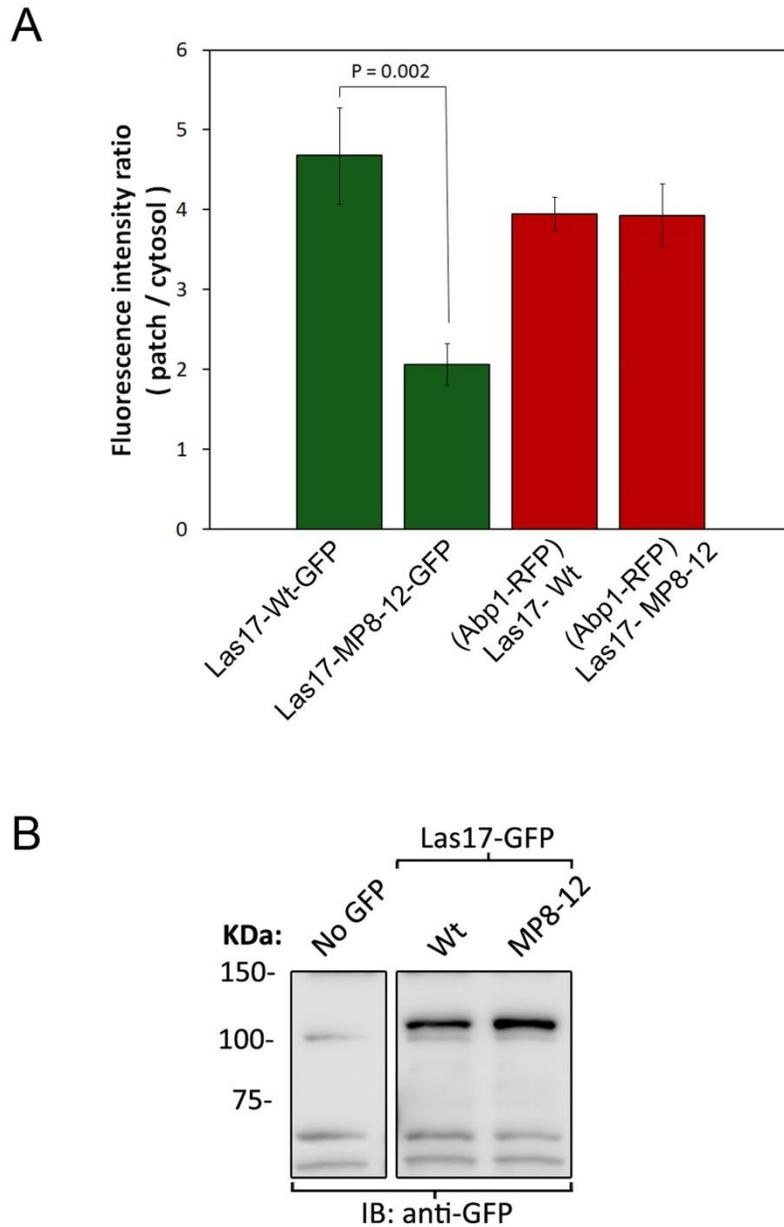
Figure 2. 10
Class I/II polyproline motifs are important for Las17 recruitment to endocytic sites. (A) The patch (membrane) maximal fluorescence intensity and internal (cytosol) fluorescence intensity for Las17-GFP and Abp1-RFP were determined after imaging wild type Las17 (SDY371) and Las17-MP8-12 (SDY372) cells and the membrane/cytosol fluorescence intensity ratio calculated. (B) Immunoblotting (IB) analysis of total extracts from yeast control cells (SDY088) or cells expressing wild type Las17-GFP (SDY367) or Las17-MP8-12-GFP (SDY363).

75

interactions with other endocytic proteins, or a combination of both.

Similar to published studies, in wild type cells Abp1-RFP was detected at endocytic sites 19 seconds after Las17-GFP and their patch lifetime was 14 and 33 seconds, respectively (Figure 2.11A) [10]. In contrast, Abp1-RFP was detected only 9 seconds after Las17-MP8-12-GFP, which can be explained by the lack of inhibition by Sla1 (Figure 2.11B). This is even more remarkable considering that less molecules of mutant Las17 were concentrated at endocytic sites compared with wild type Las17 (Figure 2.10A). In cells expressing Las17-MP8-12-GFP the patch lifetime of Abp1-RFP was increased from 14 to 20 seconds (Figure 2.11), but the maximum Abp1-RFP concentration reached was unchanged (Figure 2.10A). These results indicate that productive endocytosis likely requires a given amount of Arp2/3-mediated actin polymerization that in mutant Las17 takes longer time to be achieved because there are less Las17 molecules.

Overall, live cell fluorescence microscopy analysis suggests that Las17 molecules that are unable to bind Sla1 and therefore not in the native complex are deficiently recruited to sites of endocytosis. However, the Las17 molecules that do get recruited have the NPF activity readily manifested. These results support the idea that in wild type cells Las17 recruitment to sites of endocytosis is facilitated by being in a preformed complex with Sla1 where the NPF activity of Las17 is initially inhibited.

In order to compare the severity of the Las17 inhibition defect caused by the las17-MP8-12 mutation, we determined the time from Las17-GFP arrival to detection of Abp1-RFP (delta time) in cells carrying deletions of other genes involved in Las17 regulation: *SYP1*, *BBC1*, and *BZZ1* (Figure 2.12A). *bbc1Δ* and *bzz1Δ* cells did not show a change in early Las17 inhibition, consistent with their later arrival to endocytic patches (Figure 2.12A). However, *syp1Δ* cells
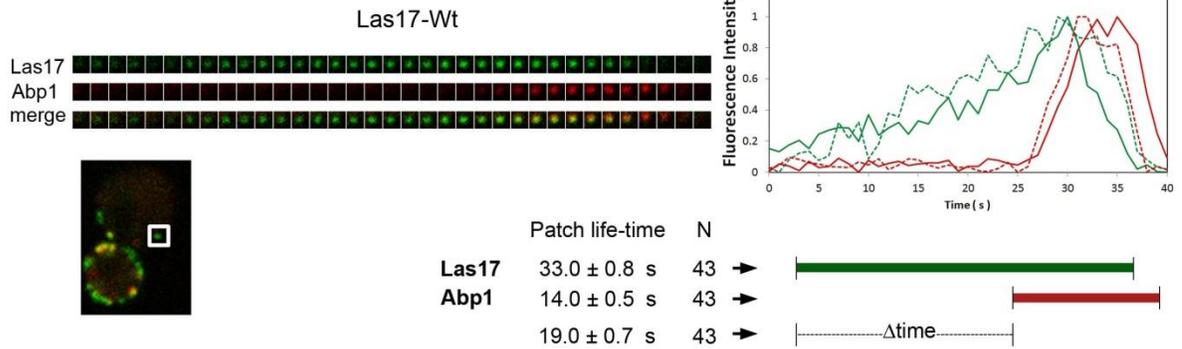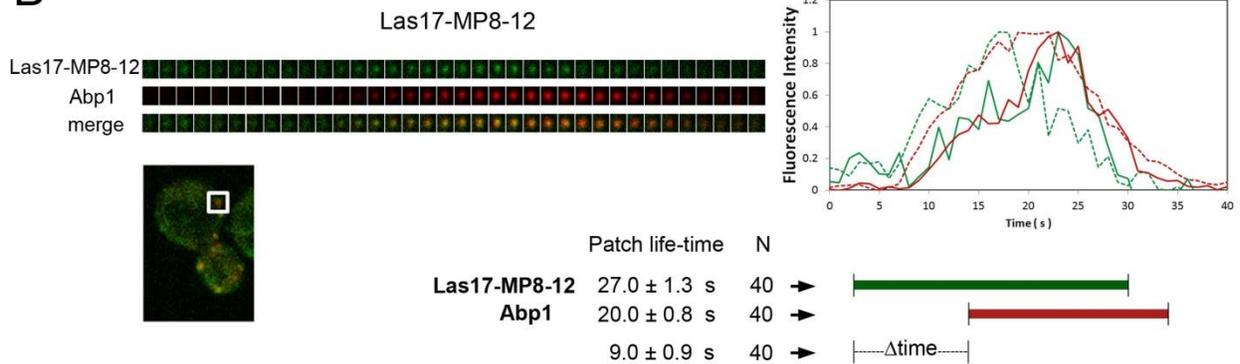
Figure 2. 11

Class I/II polyproline motifs are critical for Sla1 inhibition of Las17 NPF activity in vivo. Dynamics of (A) wild type Las17-GFP and (B) Las17-MP8-12-GFP with Abp1-RFP at endocytic sites (SDY371 and SDY372, respectively). Time series (left) showing localization of Las17 and Abp1 from two-color movies (1 frame/s). Alignment of Las17 (green) and Abp1 (red) patch intensities as function of time (right panel depicts examples of two distinct patches, solid and dashed line, respectively). Patch life times ± SEM, Δtime ± SEM and number of patches analyzed (N) are indicated. Differences in Las17 (P=0.0002) and Abp1 (P<0.0001) patch lifetimes and Δtime (P<0.0001) between wild type Las17 and Las17- MP8-12 cells were statistically significant.
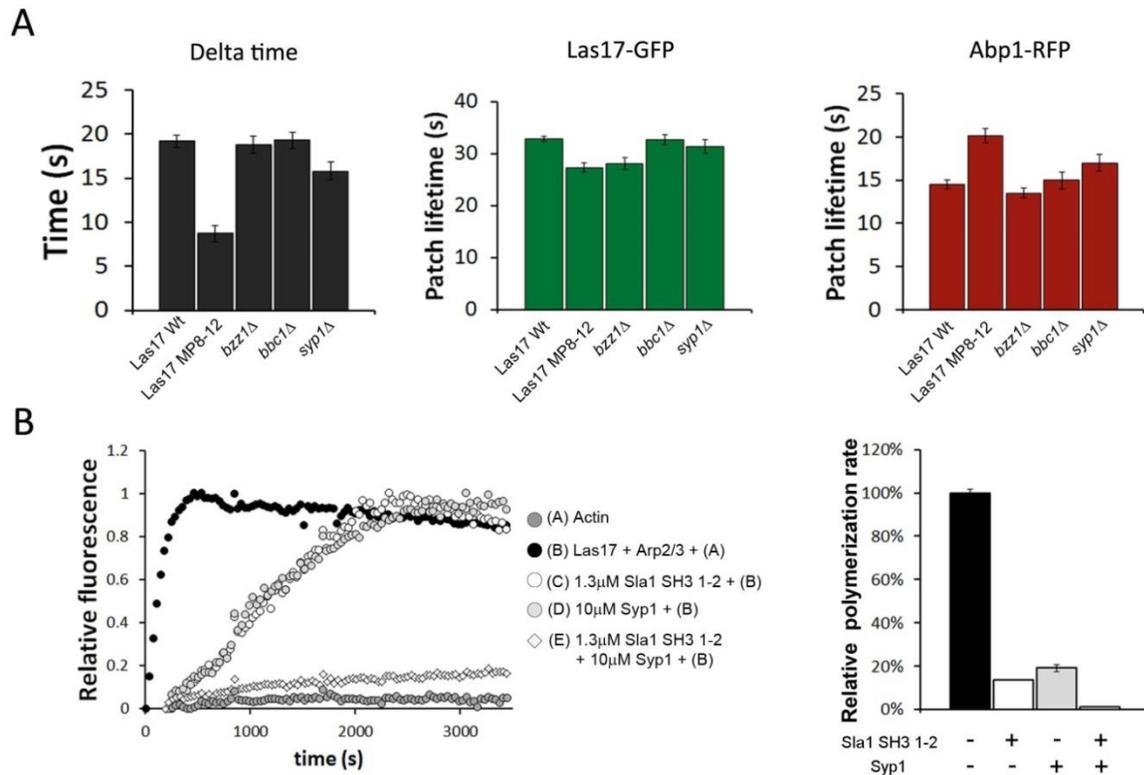
Figure 2.12

Syp1 deletion has a subtle in vivo effect on the delta time between Las17 and Abp1 recruitment and cooperates with Sla1 to inhibit Las17 in vitro. (A) The time from Las17-GFP arrival to detection of Abp1-RFP (delta time) was determined in cells carrying deletions of genes involved in Las17 regulation, SYP1 (syp1Δ, SDY471), BBC1 (bbc1Δ, SDY472), or BZZ1 (bzz1Δ, SDY473). A strain carrying the Las17 mutation, Las17-MP8-12-GFP (SDY372), was also included to facilitate comparison. Differences in delta time between wild type cells and syp1Δ cells were statistically significant (P<0.01) (number of patches analyzed = 20 to 45). (B) His-Sla1-SH3-1-2 and His-Syp1 have additive inhibitory effects on Las17. Actin (1.5 μM, 99% pyrene labeled) was polymerized in the presence of Arp2/3 complex (75 nM), full length Las17 (75 nM), and the indicated concentrations of His-Sla1-SH3-1-2 fragment and/or full length His-Syp1. Relative polymerization rates are expressed as the average ± SEM of three independent determinations.

showed a small but statistically significant defect compared to wild type cells (15 s versus 19 s) (Figure 2.12A). This defect is consistent with the known Syp1 ability to inhibit Las17 *in vitro* and its presence at endocytic sites at the time of Las17 arrival [25-27]. While this defect is less severe than the one elicited by the Las17-MP8-12 mutation, it suggests Sla1 and Syp1 may cooperate to inhibit las17 during the initial 20 seconds. Pyrene-actin polymerization assays were used to test the possibility of Sla1 and Syp1 cooperation to inhibit Las17 (Figure 2.12B). The single presence of the Sla1-SH3-1-2 fragment (1.3 µM) or full length Syp1 (10 µM) at saturating concentrations inhibited the actin polymerization rate by 87% and 81% respectively (Figure 2.12B). Simultaneous addition of Sla1-SH3-1-2 and Syp1, however, caused significantly more – virtually complete – inhibition of Las17 (99% inhibition) (Figure 2.12B). This additive effect between Sla1 and Syp1 inhibition suggest a scenario where Sla1 and Syp1 cooperate to inhibit Las17 early after its recruitment to endocytic sites.

2.3.7 Class I/II polyproline motifs are important for normal overall endocytic patch dynamics and for fluid phase and clathrin-mediated endocytosis

The defects in Las17, Sla1, and Abp1 dynamics described above in live cells expressing Las17-MP8-12 suggest that overall endocytic patch dynamics may be abnormal and endocytosis may be less efficient in these mutant cells. To investigate these possibilities we first examined the patch lifetime of early (Syp1), intermediate (Pan1), and late (Myo5) coat components in cells expressing Las17-MP8-12 or wild type Las17 from the endogenous *LAS17* locus (Figure 2.13). Early (Syp1) and intermediate (Pan1) proteins showed a statistically significant increase in their patch lifetime in mutant Las17 cells compared to wild type Las17 cells (Figure 2.13A-B). Interestingly, the number of patches counted at steady state was also increased in these mutant
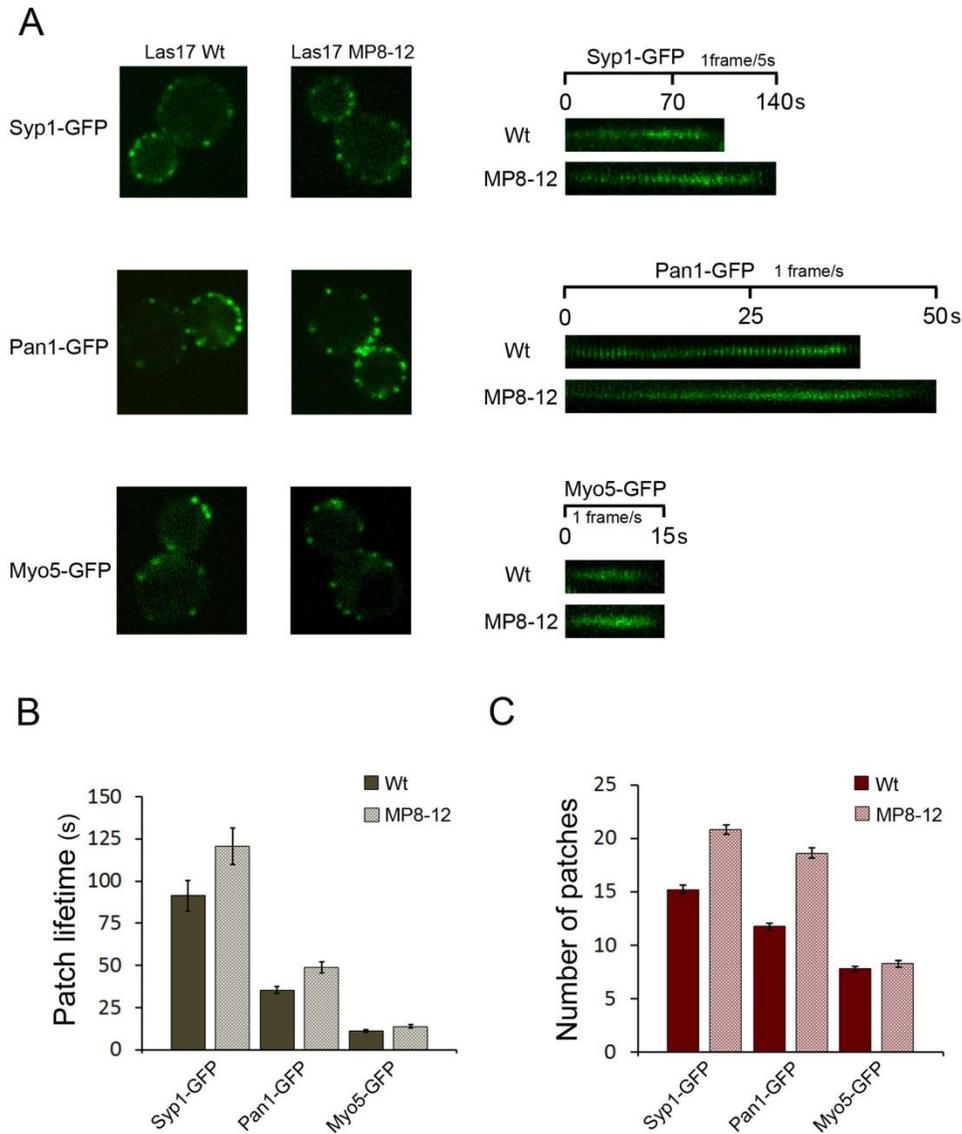
Figure 2. 13

Class I/II polyproline motifs are important for normal overall endocytic patch dynamics. Patch lifetime and number of patches was analyzed for endocytic patch components Syp1-GFP, Pan1-GFP, and Myo5-GFP in cells expressing wild type Las17 (SDY465, SDY466, and SDY467, respectively) or Las17-MP8-12 (SDY468, SDY469, and SDY470, respectively) from the corresponding endogenous loci. (A) Kymographs (right) were constructed from time- lapse movies of Syp1-GFP (1 frame/5s), Pan1-GFP (1 frame/s) and Myo5-GFP (1 frame/s). A frame from each movie is shown (left). (B) Patch lifetimes are expressed as the average ± SEM (n=25). Patch lifetimes differences between Syp1-GFP (P=0.04) and Pan1-GFP (P=0.008) in wild type Las17 and Las17-MP8-12 cells were statistically significant. (C) Number of patches is expressed as the average ± SEM (n=25). The differences in patch number of Syp1-GFP (P<0.0001) and Pan1-GFP (P<0.0001) between wild type Las17 and Las17-MP8-12 cells was statistically significant.

cells (Figure 2.13C). The simplest explanation for these results is that initial formation of the endocytic site is not affected, but that the endocytic event takes longer time to complete, thus the number of patches counted at any given time is higher. The difference in patch lifetime and number of patches appeared to be more marked in early and intermediate markers (Syp1, Pan1) than in late markers (Myo5).

To evaluate the effect of the Las17-MP8-12 mutation on cell physiology (Figure 2.14A), we examined growth at 30 ºC and did not observe a significant defect compared to wild type cells .However, growth at 40 ºC was severely impaired in Las17-MP8-12 cells compared to wild type cells (Figure 2.14A). As previously reported [12], cells carrying a deletion of the *LAS17* gene (*las17Δ*) did show a significant growth defect at all temperatures (Figure 2.14A). Bulk endocytosis, assayed by Lucifer yellow uptake, was less efficient in Las17-MP8-12 cells than in wild type cells, although it was not as severely affected as in *las17Δ* cells (Figure 2.14B). The impact of the Las17-MP8-12 mutation in clathrin-mediated endocytosis was addressed by examining localization of Wsc1, a native clathrin-dependent endocytic cargo [14]. Wsc1 is a cell wall stress sensor that normally displays a polarized localization with high concentration at sites of new cell surface growth through clathrin- and Sla1-mediated endocytosis and recycling from endosomes [14, 37]. In wild type cells, polarized localization of Wsc1 is manifested as an enrichment in the plasma membrane of the bud compared to the mother cell, which can be detected in living cells expressing Wsc1-GFP. Endocytosis defects lead to uniform distribution of Wsc1-GFP in both the mother cell and the bud. Consequently, polarized localization provides a sensitive measure of Wsc1-GFP endocytosis [15, 37]. Accordingly, we determined Wsc1-GFP localization in wild-type cells, Las17-MP8-12 cells, and *las17Δ* cells (Figure 2.14C). In wild-type cells, Wsc1-GFP was primarily located at the cell surface of buds. In both Las17-MP8-12
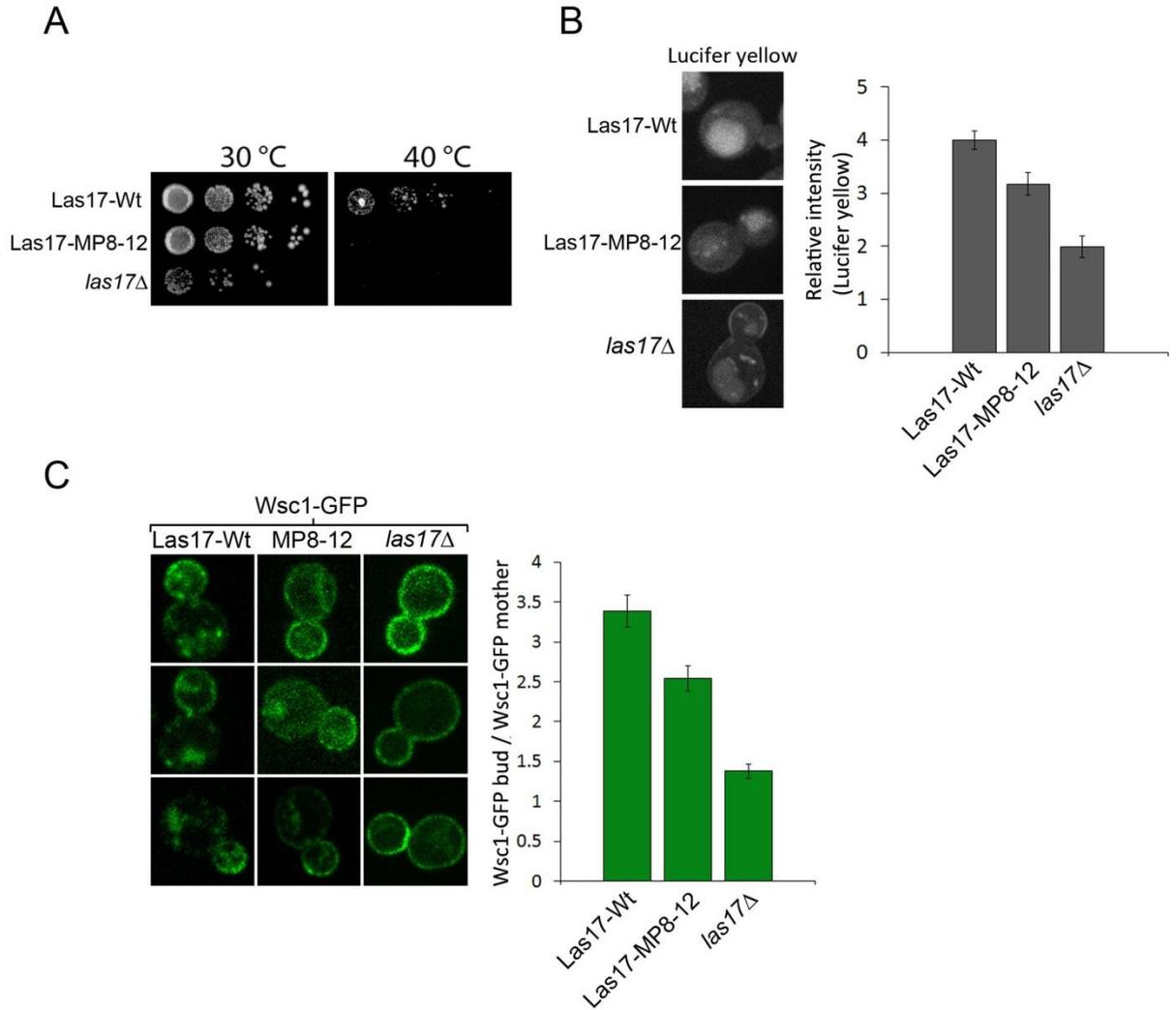
Figure 2. 14

(A) Wild type, Las17MP8-12 and las17Δ (SDY367, SDY363 and SDY161) cells were grown to early log phase (OD600= 0.2), platted in ten-fold serial dilutions on YPD plates, and incubated for 72 hr at 30oC or 40oC. (B) Wild type, Las17MP8-12 and las17Δ cells were grown to early log phase, incubated for 2 hr at 24oC with Lucifer yellow, and imaged by confocal fluorescence microscopy. The fluorescence intensity of the vacuole was measured, normalized by the intensity of the background, and expressed as the average ± SEM (n=15). Differences between wild type and Las17MP8-12 (P=0.007) or las17Δ (P=0.0006) cells, and between Las17MP8-12 and las17Δ (P=0.02) cells were statistically significant. An example of each cell type is presented on the left panels. (C) A pRS313-WSC1-GFP plasmid was introduced in wild type, Las17MP8-12 and las17Δ cells to generate strains SDP478, SDP479, and SDP480, respectively. The Wsc1-GFP fluorescence intensities in the cortex of the bud and mother cells was determined and the intensity ratio between the bud and mother was calculated for each bud-mother pair. The bud to mother Wsc1-GFP intensity ratios were expressed as the average ± SEM for wild type (n=40), Las17MP8-12 (n=30) and las17Δ (n=25). Both Las17MP8-12 and las17Δ cells displayed differences with wild type cells that were statistically significant (P=0.002 and P<0.0001, respectively). las17Δ was also significantly different from Las17MP8-12 (P<0.0001). Three examples of each cell type are presented on the left panels.

cells and *las17Δ* cells there was a significantly higher level of Wsc1-GFP at the surface of mother cells, indicative of a partial defect in endocytosis (Figure 2.14C). Fluorescence intensities of bud and mother cell surfaces were determined and a ratio calculated in order to quantify the defect (Figure 2.14C). The analysis indicates a statistically significant defect in Wsc1 endocytosis in Las17-MP8-12 cells and more so in *las17Δ* cells (Figure 2.14C). Overall, characterization of the Las17-MP8-12 mutant cells indicates that this region of interaction with Sla1 is important for normal progression of the endocytic patch and efficient endocytosis.

2.4 Discussion

Arp2/3-mediated actin assembly plays a central role in clathrin-mediated endocytosis providing force needed for the internalization step [4, 7]. Importantly, Arp2/3 activity must be tightly regulated to enable the endocytic patch to properly mature before the burst of actin polymerization that initiates coated vesicle invagination. Las17, the most potent yeast Arp2/3 nucleation promoting factor, is recruited to endocytic sites well before actin polymerization is initiated and in purified form is constitutively active and therefore predicted to be inhibited by direct binding partners, similar to WAVE family proteins [10, 13, 25]. Thus, an important outstanding question has been how Las17 is inhibited during the initial ~20 seconds after its arrival to sites of endocytosis. Sla1 is encoded by a gene that is <u>S</u>ynthetic <u>l</u>ethal with <u>A</u>BP1, and has long been recognized as a central factor for regulation of the actin cytoskeleton in endocytosis. Moreover, the two most amino-terminal SH3 domains of Sla1 were shown to inhibit Las17 NPF activity *in vitro* [13]. The findings here that Las17 exists in a stable complex with Sla1 and that they are co-recruited from the cytosol to sites of endocytosis provide an excellent

explanation to this long standing problem. In addition to Sla1, two other components of the endocytic machinery, Bbc1 and Syp1, reduce the Las17 NPF activity *in vitro*. Because Bbc1 arrives to endocytic sites about 20 seconds after Las17 it cannot be the inhibitor during the initial ~20 seconds of Las17 recruitment, although it may modulate its activity during late stages of endocytosis [10]. Cooperation between Bbc1 and Sla1 to modulate actin polymerization in later stages of endocytosis is consistent with their additive inhibitory effect in pyrene-actin polymerization assays and the exaggerated endocytic actin structures found in live cells carrying deletion of both genes [3, 13]. Syp1 arrives to endoytic sites much earlier than Las17 and could therefore be an inhibitor *in vivo* during the initial ~20 seconds of Las17 recruitment [25-27]. Previous studies found *syp1Δ* cells, much like *bbc1Δ* cells, display relatively mild defect in growth or endocytic dynamics [3, 25-27]. Results in Figure 2.12A indicate that *syp1Δ* cells display a small but statistically significant reduction in the time from Las17 arrival to detection of actin polymerization suggesting a role in early Las17 inhibition. It is therefore possible that Sla1 and Syp1 cooperate to inhibit Las17 during its initial recruitment. This possibility is supported by the pyrene-actin polymerization assays showing additive effect between Sla1-SH3-1-2 fragment and Syp1 to inhibit Las17 (Figure 2.12B). Importantly, the mechanism mediating the Syp1 inhibitory effect is not fully understood, but since it does not contain SH3 domains it is not expected to involve the Las17 polyproline motifs bound by Sla1. Therefore, the fact that the time from Las17 recruitment to actin polymerization is significantly shorter in Las17-MP8-12 (9 seconds) than in wild type Las17 (19 seconds) strains is best explained by the lack of Las17 inhibition by Sla1 (Figure 2.11). The emerging picture is one in which Sla1 is an important inhibitor of Las17 NPF activity *in vivo* during initial recruitment to the endocytic patch, likely in cooperation with Syp1. In the future it will be important to better delineate the molecular

84

mechanism of Syp1 inhibition of Las17 NPF activity and cooperation with Sla1. The physical interaction reported between Sla1 and Syp1 argues for a potentially more intertwined relationship between these two Las17 inhibitors [34].

The complex between Las17 and Sla1 serves other roles in addition to negatively regulate Las17 NPF activity:

First, mutant Las17 impaired for Sla1 binding displayed a significant recruitment defect, both in terms of timing and total amount of protein localized to sites of endocytosis (Figure 2.8, 2.9 and 2.10). The multiple interactions Sla1 makes with transmembrane protein cargo and coat components such as clathrin, Pan1, Sla2, End3, and Syp1 are likely important for proper Las17 recruitment in the context of the complex with Sla1 [14-16, 31, 34, 38-40]. Therefore *in vivo* Sla1 has both positive effects (recruitment to endocytic sites) and negative effects (inhibition of actin polymerization) on Las17 NPF functions. Mutant Las17 impaired for Sla1 binding displayed defects in overall coat dynamics (Figure 2.13), growth at high temperature (Figure 2.14A), and both fluid phase and clathrin-mediated endocytosis (Figure 2.14B and C). These defects may be the result of both defective recruitment of mutant Las17 to endocytic sites (less molecules and delayed arrival) (Figure 2.8, 2.9, and 2.10) and misregulation of actin polymerization (Figure 2.11 and 2.12).

Second, given that Sla1 is a clathrin adaptor for cargo containing the NPFxD endocytic signal, it is possible that Sla1 senses the maturation state of the coated pit and transmits that information to Las17 in order to initiate actin polymerization when the incipient vesicle is ready for internalization. Therefore this complex has the potential to be a key regulator of the transition from early to late stages of the endocytic pathway.

Third, the Sla1-Las17 complex is large and likely consists of several copies of both Sla1 and Las17 (Figure 2.1). Supporting this possibility, mass spectrometry analysis of the complex purified under conditions mild enough to detect transient interactors failed to uncover additional subunits of the stable Sla1-Las17 complex (Table 2.1). This is also consistent with a multivalent interaction between Las17 and Sla1: three polyproline motifs (P10, P11, and P12) are the core binding site for the Sla1 first and second SH3 domains (Figure 2.3 and 2.5). This raises the possibility of several Sla1 molecules bridging two or more Las17 molecules within the complex. Additionally, we have recently shown that Sla1 can self oligomerize through SHD2-SHD2 interactions and that homo-oligomerization occurs *in vivo* and appears to be mechanistically linked to clathrin binding at the membrane [14]. Such Sla1 oligomers may represent the small residual peak around 10 ml elution volume in gel filtration analysis of cytosol from the *las17Δ* strain (Figure 2.1F). Therefore, Sla1 has the ability to bring multiple Las17 molecules together at endocytic sites and, at least in part, link multimerization to association with the clathrin latice. This is important in light of the new finding that the activity of NPFs increases about 100 times when they are in dimeric form compared to monomeric molecules [21, 41]. This has been elegantly explained at the mechanistic level by the very recent discovery that the Arp2/3 complex has two different binding sites for the VCA motif [42, 43]. Consequently a dimer or multimer of Las17 within the complex with Sla1, when activated (see below), would have significant more potency towards the Arp2/3 complex due to a cooperativity effect. In fact, it has been predicted that binding of two or more WASp molecules to an SH3 protein scaffold/adaptor could bring them together in cells to mediate such stronger activation [21, 41]. The Las17-Sla1 complex uncovered here is likely a very good example of such proposed mechanism.

This work constitutes an important step forward in understanding the mechanism of actin polymerization regulation in endocytosis, but also raises several important questions. For instance, how is Las17 inhibition accomplished at the molecular level by the Sla1 SH3 domains? There are at least two conceivable scenarios to explain these results. One possibility is that the carboxi-terminal WH2 and acidic tail (or VCA motif) may fold back and interact with a surface of the Sla1 SH3 domains 1 and/or 2 that is not involved in binding to Las17 polyproline motifs P10, P11, and/or P12. In this way the WH2/acidic tail would not be available to bind monomeric actin and/or the Arp2/3 complex and would therefore be inhibited. Another possibility involves a second monomeric actin binding site – additional to the WH2 domain – recently described in Las17 and that may in part explain the very strong Las17 activity compared to other yeast NPFs [36]. This new monomeric actin binding site was not fully mapped but is located within residues 300 and 422 of Las17. This region includes the Sla1 binding site, P10-12 (Figure 2.3 and 2.5), thus opening the possibility of mutually exclusive binding between one or both Sla1 SH3 domains and monomeric actin. Results presented here indicate monomeric actin and the Sla1 SH3 domains indeed compete for binding to a region of Las17 spanning residues 300 to 404 (P8-12) (Figure 2.7). Although it is unlikely that monomeric actin binds a PxxP motif like the Sla1 SH3 domains do, it could bind partially overlapping regions of Las17. To better delineate this mechanism, it will be important to define what residues within the 300-404 fragment are involved in monomeric actin binding. These two possible mechanisms for Sla1 inhibition of Las17 NPF activity are not mutually exclusive and there may be additional regulatory contacts with full length Sla1 in the context of the native complex. This result also raises the interesting possibility that other Las17 inhibitors – such as Syp1 – could engage the WH2-acidic tail motif while Sla1 operates on this new actin binding site in order to produce more complete inhibition.

The fact that Syp1 and Sla1 have an additive inhibitory effect on Las17 to produce nearly complete inhibition, at least *in vitro*, support this possibility (Figure 2.12B).

Results presented here demonstrate Las17 arrives together with Sla1 in a complex that keeps its NPF activity inhibited during initial ~20 seconds. However, Las17 NPF activity must be later released to allow internalization to proceed. This could be achieved in two possible ways, by disassembly of the complex or by rearrangement without disassembly such that the newly discovered actin binding site and the WH2-acidic tail are free to exert their NPF activity. The first possibility indicates Las17 would cycle between Sla1-bound and free states. Our gel filtration analysis of endogenous (untagged) Las17 in wild type cells found only the large species that is in complex with Sla1, but not even a small population of free Las17 (Figure 2.1). The most likely explanation for this result is that Las17 is always in complex with Sla1. In this respect Las17 would be similar to mammalian and *Drosophila* WAVE that is part of a constitutive WAVE regulatory complex (WRC) that keeps it inhibited and, upon activation by Rac1 releases its VCA motif without complex dissociation [44]. We cannot however exclude the possibility that activation of Las17 involves complex dissociation, but re-association is so quick that at steady state the free Las17 fraction is too small to be detected.

One unresolved aspect of Las17 function has been its localization during the motile phase of endocytosis. Does it stay at the plasma membrane or does it move with the invaginating coat? This detail is of fundamental importance because the former possibility indicates Las17 mediates actin polymerization with barbed ends oriented towards the plasma membrane, but the later implies polymerization with barbed ends pointing to the invaginating vesicle [4, 45]. In early studies GFP-tagged Las17 appeared to stay at the plasma membrane [3, 5]. More recent studies found that GFP-tagged Las17 does indeed move inwards and internalizes with the incipient

vesicle [4, 11]. Immunoelectron microscopy data of epitope-tagged Las17 was also interpreted as indicating Las17 moves from the plasma membrane although not quite at the tip of the invagination [19]. The emerging picture from these later studies supports an Arp2/3-actin meshwork with barbed ends oriented towards the vesicle. Such an arrangement of actin filaments around clathrin-coated endocytic structures was recently observed in mouse cells by platinum replica electron microscopy in combination with electron tomography [46]. Given the high similarity of the endocytic machinery among eukaryotes, this orientation is expected to be conserved in yeast cells. Because Sla1 is a coat component that internalizes with the invagination, our data of a biochemically stable Sla1-Las17 complex is more in line with the idea that Las17 internalizes along with the incipient vesicle. However, as described above we cannot exclude a very rapid dissociation and re-association between Las17 and Sla1 that would be compatible with Las17 remaining at the plasma membrane.

In summary, this work demonstrates Las17 is associated in a large and biochemically stable complex with Sla1 that is important for normal Las17 recruitment and regulation of endocytosis. Because this complex between Sla1 and Las17 regulates actin polymerization during clathrin-mediated endocytosis, we propose to name it SLAC. Specific SH3-polyproline interactions hold SLAC together and are responsible for inhibition of Las17 NPF activity during initial recruitment to sites of endocytosis. Las17 inhibition is caused, at least in part, by Sla1 SH3 domains masking a novel actin binding site in Las17. A new type of polyproline motif within Las17 simultaneously conforming to class I and class II was uncovered and mapped. The multivalent, direct, and high affinity binding supports both a stable and large SLAC complex where multiple copies of Las17 and Sla1 are likely present. Activation is not expected to involve complex dissociation and thus likely maintains multiple Las17 molecules together providing

strong Arp2/3 activation through cooperative binding. Release of Las17 NPF activity is essential

for endocytosis to proceed and the data presented here suggests activation occurs through SLAC

rearrangement rather than dissociation. In the future it will be interesting to investigate if SH3

proteins arriving later to the patch, such as Bzz1, are responsible for the release of Sla1 inhibition

in vivo as it was observed in *in vitro* experiments [10].

2.5 Experimental Procedures

Plasmids and yeast strains

To generate recombinant GST- or polyhistidine-tagged (His) fusion proteins, the

corresponding DNA sequence fragments of *LAS17*, *SLA1,* or *SYP1* were amplified by PCR and

cloned into pGEX-5X-1 (Amersham Biosciences, Piscataway, NJ, USA) or pET-30a$^+$ (Novagen,

Madison, WI, USA) bacterial expression vectors, respectively. For yeast two hybrid experiments

the corresponding *LAS17* and *SLA1* DNA fragments were amplified by PCR and cloned into

pGBT9 or pGAD424 vector, respectively (Clontech–BD Biosciences, San Jose, CA, USA). A

DNA fragment containing 200 bp of the *LAS17* 5' untranslated region followed by full length

LAS17 ORF was amplified by PCR and cloned into *Not*I/*Sal*I sites of pRS-315 [47] (pSDP320,

Table 2.2). pSDP320 was used as template for various proline-to-alanine site directed

mutagenesis using the Quickchange system (Stratagene, La Jolla, CA, USA). For actin

polymerization assays full length wild type LAS17 was amplified from pSDP320 by PCR and

cloned into pGEX-5X-1 and a sequence encoding amino acids AAAHHHHHH was added to the

reverse primer used in the PCR so that the protein contained a carboxi-terminal His tag for

purification purposes (pSDP438). Similar full length LAS17 constructs were generated

Table 2.2   **Plasmids generated in this study**

Plasmids	Description
pSDP257	pGAD424 - Sla1 SH3 1-2(aa. 1-138)
pSDP261	pGBT9 - Las17 P1-20(aa. 165-623)
pSDP262	pGBT9 - Las17 P1-7(aa. 165-295)
pSDP263	pGBT9 - Las17 P8-11(aa. 300-367)
pSDP264	pGBT9 - Las17 P12(aa. 378-404)
pSDP265	pGBT9 - Las17 P13-15(aa. 419-484)
pSDP266	pGBT9 - Las17 P16-19(aa. 481-544)
pSDP267	pGBT9 - Las17 P20(aa. 591-623)
pSDP274	pGBT9 - Las17 P8(aa. 300-322)
pSDP275	pGBT9 - Las17 P9(aa. 318-341)
pSDP276	pGBT9 - Las17 P8-9(aa. 300-341)
pSDP277	pGBT9 - Las17 P10(aa. 330-351)
pSDP278	pGBT9 - Las17 P11(aa. 349-367)
pSDP279	pGBT9 - Las17 P10-11(aa. 330-367)
pSDP280	pGBT9 - Las17 P8-12(aa. 300-404)
pSDP281	pGBT9 - Las17 P10-12(aa. 330-404)
pSDP282	pET-30- a(+) - Sla1 SH3 1-2 (aa. 1-138)
pSDP287	pGEX-5X-1 - Las17 P8-11(aa. 300-367)
pSDP291	pGEX-5X-1 - Las17 P12(aa. 378-404)
pSDP292	pGEX-5X-1 - Las17 P10-12(aa. 330-404)
pSDP293	pGEX-5X-1 - Las17 P8-12(aa. 300-404)
pSDP315	pSDP293 with PAPPPPP to PAAAPPP mutation in P10,P11 and P12 (MP10-12)
pSDP320	pRS 315 - 200bP 5' UTR - LAS17 ORF
pSDP370	pSDP261 with PLPQLP to PLAQLP in P8 and MP10-12
pSDP371	pSDP261 with PVPPPPP to PAPPPPP in P9 and MP10-12
pSDP372	pSDP261 with MP8-12 mutation
pSDP375	pSDP320 with PLPQLP to PLAQLP in P8, PVPPPPP to PAPPPPP in P9 and MP10-12 (MP8-12)
pSDP438	pGEX-5X-1 - Las17-6xHIs
pSDP439	pSDP438 with MP10-12 mutation
pSDP440	pSDP438 with MP8-12 mutation
pSDP492	pET-30-a(+)-Syp1

containing mutations in polyproline motifs 10, 11, and 12 (MP10-12-LAS17) (pSDP439) and polyproline motifs 8, 9, 10, 11, and 12 (MP8-12-LAS17) (pSDP440).

AH109 cells (Clontech–BD Biosciences, San Jose, CA, USA) were co-transformed with the respective pGBT9 and pGAD424 construct combinations and were analyzed as described [15, 48]. SDY088 (*MAT*a *ura3-52 leu2-3112 his3-Δ200 trp1-Δ901 lys2-801 suc2-Δ9*) was crossed with SDY169 (*MATα ura3-52 leu2-3112 his3-Δ200 trp1-Δ901 lys2-801 suc2-Δ9 LAS17-GFP::HIS3*) and the resulting heterozygous diploid Las17-GFP strain, SDY392 (*MAT*a/*MATα ura3-52 leu2-3112 his3-Δ200 trp1-Δ901 lys2-801 suc2-Δ9 LAS17-GFP::HIS3*) was used to introduce mutations in the *LAS17-GFP* gene while maintaining an intact *LAS17* gene. A two-step approach similar to the one described previously was followed [14, 49]. For the first step, a sequence upstream of the central Las17 polyproline stretch (-200 to + 570) was amplified by PCR (the reverse primer contained XbaI and BamHI restriction sites in series) and cloned into the NotI/BamHI sites of pRS-315. Subsequently, a PCR fragment containing *URA3* was amplified using a reverse primer containing BglII and BamHI restriction sites in series and was subcloned into the XbaI/BamHI sites. An additional fragment containing the *LAS17* sequence downstream the central polyproline stretch (nucleotides 1441-1899) followed by the GFP sequence was amplified by PCR using genomic DNA from SDY169 and subcloned into BglII/SalI sites of the above construct. The resulting construct was cleaved with NotI/SalI and the *URA3* fragment was introduced by lithium acetate transformation [50] into SDY392 to generate SDY362 in which the central Las17 polyproline stretch was replaced by *URA3* in the *LAS17-GFP* gene, but leaving the rest of the *LAS17* gene intact. In the second step, NotI/SalI fragments from pSDP320 and pSDP375 were cotransformed with pRS-314 (*TRP1*) [47] into SDY362. Colonies that grew in plates lacking tryptophan were replica-plated onto agar medium

92

containing 5-fluorotic acid to identify cells in which the wild type or mutant sequences replaced *URA3*. These diploid cells were then subjected to sporulation and tetrad dissection, thus generating strains SDY367 (*LAS17-GFP*) and SDY363 (*Las17^{MP8-12}-GFP*), respectively.

SDY367 and SDY363 cells were crossed with SDY341 (*MAT*a ura3-52 leu2-3112 his3-Δ200 trp1-Δ901 lys2-801 suc2-Δ9 *SLA1-RFP::KAN*) and SDY360 (*MAT*a ura3-52 leu2-3112 his3-Δ200 trp1-Δ901 lys2-801 suc2-Δ9 *ABP1-RFP::TRP1*). These cells were then subjected to sporulation and tetrad dissection, thus generating strains SDY382 (*MAT*a ura3-52 leu2-3112 his3-Δ200 trp1-Δ901 lys2-801 suc2-Δ9 *LAS17-GFP::HIS3 SLA1-RFP::KAN*), SDY384 (*MAT*α ura3-52 leu2-3112 his3-Δ200 trp1-Δ901, lys2-801, suc2-Δ9 *Las17^{MP8-12}-GFP::HIS3 SLA1-RFP::KAN*), SDY371 (*MAT*a ura3-52 leu2-3112 his3-Δ200 trp1-Δ901, lys2-801, suc2-Δ9 *LAS17-GFP::HIS3 ABP1-RFP::TRP1*) and SDY372 (*MAT*a ura3-52 leu2-3112 his3-Δ200 trp1-Δ901, lys2-801, suc2-Δ9 *Las17^{MP8-12}-GFP::HIS3 ABP1-RFP::TRP1*).

SDY159 (*MAT*a *his3-Δ1 leu2-Δ0 ura3-Δ0*), and SDY161 (*MAT*a *his3-Δ1 leu2-Δ0 ura3-Δ0 Las17Δ::KanMX4*) were generated by sporulation and tetrad dissection of the corresponding heterozygous diploid knock-out collection strain (BY4743 clone ID 22437, Open Biosystems).

SDY108 (*MAT*a *ura3-52 leu2-3112 his3-Δ200 trp1-Δ901 lys2-801 suc2-Δ9 LAS17-RFP::KANMX6*) was crossed with SDY063 (*MAT*a *ura3-52 leu2-3112 his3-Δ200 trp1-Δ901 lys2-801 suc2-Δ9 SLA1-GFP::TRP1*) and SDY210 (*MAT*a *ura3-52 leu2-3112 his3-Δ200 trp1-Δ901 lys2-801 suc2-Δ9 Sla1^{AAA}-GFP::TRP1*). These cells were then subjected to sporulation and tetrad dissection, thus generating strains SDY145 (*MAT*a *ura3-52 leu2-3112 his3-Δ200 trp1-Δ901 lys2-801, suc2-Δ9 LAS17-RFP::KanMX6, SLA1-GFP::TRP1*) and SDY284 (*MAT*a *ura3-52 leu2-3112 his3-Δ200 trp1-Δ901 lys2-801 suc2-Δ9, LAS17-RFP::KanMX6, Sla1^{AAA}-GFP::TRP1*). SDY149 (*MAT*α *ura3-52 leu2-3112 his3-Δ200 trp1-Δ901 lys2-801, suc2-Δ9*

93

LAS17-RFP::HIS3, SLA1-GFP::TRP1) was mated with cells lacking the *END3* gene (*MAT*a *his3-Δ1 leu2-Δ0 ura3-Δ0 endΔ::KanMX4*, Open Biosystems) followed by sporulation and tetrad dissection to generate SDY474 (*MAT*a *LAS17-RFP::KanMX6, SLA1-GFP::TRP1, end3Δ::HIS*).

SDY139 (*MAT*α *ura3-52 leu2-3112 his3-Δ200 trp1-Δ901 lys2-801 suc2-Δ9 LAS17-RFP::KANMX6*) and SDY463 (*MAT*α ura3-52 leu2-3112 his3-Δ200 trp1-Δ901, lys2-801, suc2-Δ9 *Las17^{MP8-12}-RFP::TRP1*) were crossed with the GFP library collection strains (*MAT*a *his3Δ1 leu2Δ0 met15Δ0 ura3Δ0 SYP1-GFP::HIS*), (*MAT*a *his3Δ1 leu2Δ0 met15Δ0 ura3Δ0 PAN1-GFP::HIS*) and (*MAT*a *his3Δ1 leu2Δ0 met15Δ0 ura3Δ0 MYO5-GFP::HIS*), followed by sporulation and tetrad dissection to obtain SDY465 (*MAT*a *SYP1-GFP::HIS LAS17-RFP::KANMX6*), SDY466 (*MAT*a *PAN1-GFP::HIS LAS17-RFP::KANMX6*), SDY467 (*MAT*a *MYO5-GFP::HIS LAS17-RFP::KANMX6*), SDP468 (*MAT*a *SYP1-GFP::HIS Las17^{MP8-12}-RFP::TRP1*), SDP469 (*MAT PAN1-GFP::HIS Las17^{MP8-12}-RFP::TRP1*) and SDP470 (*MAT*a *MYO5-GFP::HIS Las17^{MP8-12}-RFP::TRP1*).

SDY371 (*MAT*a ura3-52 leu2-3112 his3-Δ200 trp1-Δ901, lys2-801, suc2-Δ9 *LAS17-GFP::HIS3 ABP1-RFP::TRP1*) was crossed with the knockout library collection strains (*MAT*a *his3Δ1 leu2Δ0 met15Δ0 ura3Δ0 syp1Δ::KanMX4*), (*MAT*a *his3Δ1 leu2Δ0 met15Δ0 ura3Δ0 bbc1Δ::KanMX4*) and (*MAT*a *his3Δ1 leu2Δ0 met15Δ0 ura3Δ0 bzz1Δ::KanMX4*) (Open Biosystems), followed by sporulation and tetrad dissection to generate SDY471 (*MAT*a *LAS17-GFP::HIS3 ABP1-RFP::TRP1 syp1Δ::KanMX4*), SDY472 (*MAT*a *LAS17-GFP::HIS3 ABP1-RFP::TRP1 bbc1Δ::KanMX4*), SDY473 (*MAT*a *LAS17-GFP::HIS3 ABP1-RFP::TRP1 bzz1Δ::KanMX4*).

SDY088, SDY463, and SDY161 were transformed with a pRS313-WSC1-GFP plasmid to generate strains SDY478 (*MAT*a *ura3-52 leu2-3112 his3-Δ200 trp1-Δ901 lys2-801 suc2-Δ9;*

pRS-313-WSC1-GFP), SDY479 (*MATα* ura3-52 leu2-3112 his3-Δ200 trp1-Δ901, lys2-801, suc2-Δ9 *Las17^{MP8-12}-RFP::TRP1; pRS-313-WSC1-GFP*), and SDY480(*MAT*a *his3-Δ1 leu2-Δ0 ura3-Δ0 Las17Δ::KanMX4; pRS-313-WSC1-GFP*).

Antibodies

The generation and characterization of antibodies against Las17 was carried out as described previously [51]. The polyclonal antibody Las-A was raised in rabbit by immunizing with recombinant GST-Las17 (433-633) protein, and the polyclonal antibody Las-B was raised in rat by immunizing with recombinant GST-Las17 (1-151) protein. Subsequently, these antibodies were affinity-purified using as a ligand recombinant His-Las17 (433-633) (Las-A) and GST-Las17 (1-151) (Las-B) that had been covalently coupled to Affi-Gel 15 beads (Bio-Rad, Hercules, CA, USA). Las-B was adsorbed using immobilized GST protein.

Biochemical methods

To obtain cytosolic extracts, liquid nitrogen frozen yeast pellets were ground in a blender, resuspended in PBS (12 mM phosphate, 147 mM NaCl, 3 mM KCl, pH 7.35) or buffer A (20 mM HEPES, 150 mM NaCl, 1 mM EGTA, 1 mM dithiothreitol, pH 7.4) supplemented with protease inhibitor cocktail (Sigma Aldrich, St Louis, MO, USA), and subjected to ultracentrifugation at 4°C for 15 min at 400,000 x *g* as previously described [49]. The following yeast strains were used: TVY614 (*MAT*a *ura3-52 leu2-3112 his3-Δ200 trp1-Δ901 lys2-801 suc2-Δ9 pep4::LEU2 prb1::HISG prc1::HIS3*) [52], GPY3130 (*MAT*a *ura3-52 leu2-3112 his3-Δ200 trp1-Δ901 suc2-Δ9 sla1Δ::URA3*) [14], SDY159 (*MAT*a *his3-Δ1 leu2-Δ0 ura3-Δ0*), and SDY161 (*MAT*a *his3-Δ1 leu2-Δ0 ura3-Δ0 Las17Δ::KanMX4*).

Co-immunoprecipitation analysis was performed as previously described using cytosolic extracts prepared in PBS [14, 49]. GST-fusion protein affinity assays were performed in PBS containing 0.5% TX100 as previously described [14, 15, 49]. Quantitative GST-fusion protein affinity assays were performed as described [22]. Briefly, recombinant His-Sla1-SH3-1-2 (150nM) was incubated with increasing concentrations of wild type GST-Las17-P8-12 or GST-Las17-P8-12-MP10-12 bound to glutathione-sepharose beads for 1 hour at 4 °C. Unbound His-Sla1-SH3-1-2 was recovered in the supernatant and protein concentration determined by gel densitometry.

Size exclusion chromatography fractionation of cytosolic extracts was carried out with a Superose 6 column (10 x 300 mm, Amersham Biosciences) connected to a FPLC system (Amersham Biosciences) and equilibrated with buffer A. Elution was performed at a flow rate of 0.4 ml/min, at 4 °C. Fractions (0.750 ml) were collected and analyzed by immunoblotting or immunoprecipitation-immunoblotting using antibodies to Las17, Sla1, and End3. The column was calibrated using blue dextran and the following standard proteins of known Stokes radii: bovine thyroglobulin (85 Å), γ-globulin (55 Å), Ovalbumin (28 Å), Myoglobin (19 Å), vitamin B12 (Å) (Bio-Rad Laboratories). Sedimentation velocity analysis of cytolosolic extracts (0.2 ml) was performed using linear 5–20% (w/v) sucrose gradients prepared in a Gradient Master® (Biocomp instruments, Fredericton, NB, Canada) in buffer A (total volume: 12 ml). The samples were layered on top of the gradients and centrifuged in a SW41 rotor (Beckman Coulter, Fullerton, CA) at 39,000 rpm (261,000 x g) for 18 h at 4 °C. Fractions (0.75 ml) were collected from the top of the tube using a density gradient fractionator and analyzed by immunoblotting. The following protein standards of known sedimentation coefficient were analyzed in parallel:

bovine catalase (11.3 S), BSA (4.6 S), ovalbumin (3.6 S) and Cytoctome C (1.5 S) (Sigma Aldrich).

Protein Purification

GST- and His-fusion proteins were expressed in *Escherichia coli* (BL21) and affinity purified using glutathione–Sepharose-4B or the TALON cobalt affinity resin (Clontech–BD Biosciences, San Jose, CA, USA) as described [53]. Full length wild type-Las17, Las17-MP10-12 and Las17-MP8-12 were expressed in *Escherichia coli* (BL21) and subjected to a sequential affinity purification using glutathione–Sepharose-4B (GST-tag at amino-terminus) followed by TALON cobalt affinity resin (His-tag at carboxi-terminus).

Actin Polymerization assay

Actin polymerization experiments were performed with 1.5 μM rabbit actin (99% pyrene labeled) and 75 nM bovine Arp2/3 complex (Cytoskeleton, Denver, CO, USA). Pyrene-actin (0.4 mg/ml) was incubated in G-Buffer (10 mM Tris, pH 8.0, 0.2 mM $CaCl_2$, 0.2 mM ATP) on ice for 1.5 hours to promote depolymerization and subsequently centrifuged at 100,000 rpm in a TLA100.3 rotor (Beckman Coulter, Fullerton, CA) at 4 °C for 1.5 hours. Pyrene-actin was incubated in exchange buffer (1 mM EGTA, 0.1 mM $MgCl_2$) for 10 minutes and added to a 96 well plate already containing the proteins of interest (75 nM wild type or mutant Las17, and variable concentrations of His-Sla1-SH3-1-2 in Figure 2.6A or 150 nM in Figure 2.6C-E). In Figure 2.12B His-Sla1-SH3-1-2 was used at 1.3 μM and His-Syp1 at was used at 10 μM. For G-actin sequestering studies (Figure 2.7), 3 μM rabbit actin (99% pyrene labeled) was used in all experiments along with 6 μM Las17-P8-12 fragment, 2 or 12 μM Sla1 SH3-1-2, and no Arp2/3

complex was added to the reactions. Polymerization buffer (50 mM KCl, 2 mM MgCl2, 1 mM ATP) was added to the reaction (t=0) and actin polymerization was measured over time using a Victor[3] V microplate reader (PerkinElmer, Waltham, MA, USA) with excitation and emission wavelengths of 365 nm and 406 nm, respectively. Actin polymerization rates were calculated from the slope of the linear portion of assembly curves (25-50% polymerization).

Fluorescence microscopy

Fluorescence microscopy was performed as described [49] using an Olympus IX81 spinning disc confocal microscope with Photometrics Cascade II camera and a 100x/1.40NA objective. Time-lapse movies were generated by collecting 120 or 150 images at 1 frame/s at room temperature using cells grown until early log phase. To quantitate number of patches, patch lifetimes and patch intensities, Slidebook 5 software (Intelligent Imaging Innovations, Denver, CO, USA) was used to generate a mask, covering endocytic spots or regions inside the cell. Kaleidagraph (Synergy Sofware) was used for photobleaching corrections and patch-lifetime determination for each GFP- and RFP-tagged protein by integrating the intensities of each consecutive time point and establishing the minimum and maximum value of the integral. Delta times (time that takes for Abp1-RFP to appear after Las17-GFP detection) were calculated by subtraction of Abp1-RFP first recruitment time point (minimum value of the Abp1-RFP integral) to Las17-GFP first recruitment time point (minimum value of the Las17-GFP integral) within the same time lapse. Lucifer yellow uptake experiments were performed as described [23]. Cells were incubated for 2 hr at 24°C with Lucifer yellow (Invitrogen™ L682), and endocytic uptake was analyzed by fluorescence microscopy. The fluorescence intensity of the vacuole was measured and normalized by the intensity of the background. Quantification of Wsc1-GFP

localization was done as described [14]. Student's t-test was used to determine statistical significance.

Mass Spectrometry Analysis

Tandem affinity purification (TAP) of Las17 was performed using cells expressing C-terminally TAP-tagged Las17 (Open Biosystems) and untagged control cells as described [54]. The samples were concentrated in a preparative polyacrylamide gel and digested in-gel with trypsin. Mass spectrometry was performed at the Colorado State University Proteomics and Metabolomics facility. Peptides were purified and concentrated using an on-line enrichment column (Agilent Zorbax C18, 5μm, 5 x 0.3mm). Subsequent chromatographic separation was performed on a reverse phase nanospray column (Agilent 1100 nanoHPLC, Zorbax C18, 5μm, 75 μm ID x 150mm column) using a 42 minute linear gradient from 25%-55% buffer B (90% ACN, 0.1% formic acid) at a flow rate of 300 nanoliters/min. Peptides were eluted directly into the mass spectrometer (Thermo Scientific LTQ linear ion trap) and spectra were collected over a m/z range of 200-2000 Da using a dynamic exclusion limit of 2 MS/MS spectra of a given peptide mass for 30 s (exclusion duration of 90 s). Compound lists of the resulting spectra were generated using Bioworks 3.0 software (Thermo Scientific) with an intensity threshold of 5,000 and 1 scan/group. MS/MS spectra were searched against the appropriate protein database (NCBI baker's yeast) using the Mascot database search engine (version 2.3). Peptides were validated using Scaffold 3 file (version 3.3.1) with minimum 99% protein, 95% peptide and minimum 2 peptide threshold.

REFERENCES

1.   Doherty, G.J. and H.T. McMahon, *Mechanisms of endocytosis.* Annu Rev Biochem, 2009. **78**: p. 857-902.
2.   Traub, L.M., *Tickets to ride: selecting cargo for clathrin-regulated internalization.* Nat Rev Mol Cell Biol, 2009. **10**(9): p. 583-96.
3.   Kaksonen, M., C.P. Toret, and D.G. Drubin, *A modular design for the clathrin- and actin-mediated endocytosis machinery.* Cell, 2005. **123**(2): p. 305-20.
4.   Galletta, B.J. and J.A. Cooper, *Actin and endocytosis: mechanisms and phylogeny.* Curr Opin Cell Biol, 2009. **21**(1): p. 20-7.
5.   Kaksonen, M., Y. Sun, and D.G. Drubin, *A pathway for association of receptors, adaptors, and actin during endocytic internalization.* Cell, 2003. **115**(4): p. 475-87.
6.   Weinberg, J. and D.G. Drubin, *Clathrin-mediated endocytosis in budding yeast.* Trends Cell Biol, 2012. **22**(1): p. 1-13.
7.   Engqvist-Goldstein, A.E. and D.G. Drubin, *Actin assembly and endocytosis: from yeast to mammals.* Annu Rev Cell Dev Biol, 2003. **19**: p. 287-332.
8.   Boulant, S., et al., *Actin dynamics counteract membrane tension during clathrin-mediated endocytosis.* Nat Cell Biol, 2011. **13**(9): p. 1124-31.
9.   Taylor, M.J., D. Perrais, and C.J. Merrifield, *A high precision survey of the molecular dynamics of mammalian clathrin-mediated endocytosis.* PLoS Biol, 2011. **9**(3): p. e1000604.
10.   Sun, Y., A.C. Martin, and D.G. Drubin, *Endocytic internalization in budding yeast requires coordinated actin nucleation and myosin motor activity.* Dev Cell, 2006. **11**(1): p. 33-46.
11.   Galletta, B.J., D.Y. Chuang, and J.A. Cooper, *Distinct roles for Arp2/3 regulators in actin assembly and endocytosis.* PLoS Biol, 2008. **6**(1): p. e1.
12.   Li, R., *Bee1, a yeast protein with homology to Wiscott-Aldrich syndrome protein, is critical for the assembly of cortical actin cytoskeleton.* J Cell Biol, 1997. **136**(3): p. 649-58.
13.   Rodal, A.A., et al., *Negative regulation of yeast WASp by two SH3 domain-containing proteins.* Curr Biol, 2003. **13**(12): p. 1000-8.
14.   Di Pietro, S.M., et al., *Regulation of clathrin adaptor function in endocytosis: novel role for the SAM domain.* EMBO J, 2010. **29**(6): p. 1033-44.
15.   Mahadev, R.K., et al., *Structure of Sla1p homology domain 1 and interaction with the NPFxD endocytic internalization motif.* EMBO J, 2007. **26**(7): p. 1963-71.
16.   Howard, J.P., et al., *Sla1p serves as the targeting signal recognition factor for NPFX(1,2)D-mediated endocytosis.* J Cell Biol, 2002. **157**(2): p. 315-26.
17.   Holtzman, D.A., S. Yang, and D.G. Drubin, *Synthetic-lethal interactions identify two novel genes, SLA1 and SLA2, that control membrane cytoskeleton assembly in Saccharomyces cerevisiae.* J Cell Biol, 1993. **122**(3): p. 635-44.
18.   Toshima, J.Y., et al., *Spatial dynamics of receptor-mediated endocytic trafficking in budding yeast revealed by using fluorescent alpha-factor derivatives.* Proc Natl Acad Sci U S A, 2006. **103**(15): p. 5793-8.
19.   Idrissi, F.Z., et al., *Distinct acto/myosin-I structures associate with endocytic profiles at the plasma membrane.* J Cell Biol, 2008. **180**(6): p. 1219-32.
20.   Pollard, T.D., L. Blanchoin, and R.D. Mullins, *Molecular mechanisms controlling actin filament dynamics in nonmuscle cells.* Annu Rev Biophys Biomol Struct, 2000. **29**: p. 545-76.
21.   Padrick, S.B. and M.K. Rosen, *Physical mechanisms of signal integration by WASP family proteins.* Annu Rev Biochem, 2010. **79**: p. 707-35.
22.   Sirotkin, V., et al., *Interactions of WASp, myosin-I, and verprolin with Arp2/3 complex during actin patch assembly in fission yeast.* J Cell Biol, 2005. **170**(4): p. 637-48.

23. Duncan, M.C., et al., *Yeast Eps15-like endocytic protein, Pan1p, activates the Arp2/3 complex.* Nat Cell Biol, 2001. **3**(7): p. 687-90.

24. Goode, B.L., et al., *Activation of the Arp2/3 complex by the actin filament binding protein Abp1p.* J Cell Biol, 2001. **153**(3): p. 627-34.

25. Boettner, D.R., et al., *The F-BAR protein Syp1 negatively regulates WASp-Arp2/3 complex activity during endocytic patch formation.* Curr Biol, 2009. **19**(23): p. 1979-87.

26. Reider, A., et al., *Syp1 is a conserved endocytic adaptor that contains domains involved in cargo selection and membrane tubulation.* EMBO J, 2009. **28**(20): p. 3103-16.

27. Stimpson, H.E., et al., *Early-arriving Syp1p and Ede1p function in endocytic site placement and formation in budding yeast.* Mol Biol Cell, 2009. **20**(22): p. 4640-51.

28. Raths, S., et al., *end3 and end4: two mutants defective in receptor-mediated and fluid-phase endocytosis in Saccharomyces cerevisiae.* J Cell Biol, 1993. **120**(1): p. 55-65.

29. Siegel, L.M. and K.J. Monty, *Determination of Molecular Weights and Frictional Ratios of Macromolecules in Impure Systems: Aggregation of Urease.* Biochem Biophys Res Commun, 1965. **19**: p. 494-9.

30. Michelot, A., et al., *Reconstitution and protein composition analysis of endocytic actin patches.* Curr Biol, 2010. **20**(21): p. 1890-9.

31. Tang, H.Y., J. Xu, and M. Cai, *Pan1p, End3p, and S1a1p, three yeast proteins required for normal cortical actin cytoskeleton organization, associate with each other and play essential roles in cell wall morphogenesis.* Mol Cell Biol, 2000. **20**(1): p. 12-25.

32. Toshima, J., et al., *Negative regulation of yeast Eps15-like Arp2/3 complex activator, Pan1p, by the Hip1R-related protein, Sla2p, during endocytosis.* Mol Biol Cell, 2007. **18**(2): p. 658-68.

33. Tong, A.H., et al., *A combined experimental and computational strategy to define protein interaction networks for peptide recognition modules.* Science, 2002. **295**(5553): p. 321-4.

34. Tonikian, R., et al., *Bayesian modeling of the yeast SH3 domain interactome predicts spatiotemporal dynamics of endocytosis proteins.* PLoS Biol, 2009. **7**(10): p. e1000218.

35. Mayer, B.J., *SH3 domains: complexity in moderation.* J Cell Sci, 2001. **114**(Pt 7): p. 1253-63.

36. Robertson, A.S., et al., *The WASP homologue Las17 activates the novel actin-regulatory activity of Ysc84 to promote endocytosis in yeast.* Mol Biol Cell, 2009. **20**(6): p. 1618-28.

37. Piao, H.L., I.M. Machado, and G.S. Payne, *NPFXD-mediated endocytosis is required for polarity and function of a yeast cell wall stress sensor.* Mol Biol Cell, 2007. **18**(1): p. 57-65.

38. Costa, R. and K.R. Ayscough, *Interactions between Sla1p, Lsb5p and Arf3p in yeast endocytosis.* Biochem Soc Trans, 2005. **33**(Pt 6): p. 1273-5.

39. Ayscough, K.R., et al., *Sla1p is a functionally modular component of the yeast cortical actin cytoskeleton required for correct localization of both Rho1p-GTPase and Sla2p, a protein with talin homology.* Mol Biol Cell, 1999. **10**(4): p. 1061-75.

40. Warren, D.T., et al., *Sla1p couples the yeast endocytic machinery to proteins regulating actin dynamics.* J Cell Sci, 2002. **115**(Pt 8): p. 1703-15.

41. Padrick, S.B., et al., *Hierarchical regulation of WASP/WAVE proteins.* Mol Cell, 2008. **32**(3): p. 426-38.

42. Padrick, S.B., et al., *Arp2/3 complex is bound and activated by two WASP proteins.* Proc Natl Acad Sci U S A, 2011. **108**(33): p. E472-9.

43. Ti, S.C., et al., *Structural and biochemical characterization of two binding sites for nucleation-promoting factor WASp-VCA on Arp2/3 complex.* Proc Natl Acad Sci U S A, 2011. **108**(33): p. E463-71.

44. Ismail, A.M., et al., *The WAVE regulatory complex is inhibited.* Nat Struct Mol Biol, 2009. **16**(5): p. 561-3.

45. Takenawa, T. and S. Suetsugu, *The WASP-WAVE protein network: connecting the membrane to the cytoskeleton.* Nat Rev Mol Cell Biol, 2007. **8**(1): p. 37-48.

46. Collins, A., et al., *Structural organization of the actin cytoskeleton at sites of clathrin-mediated endocytosis.* Curr Biol, 2011. **21**(14): p. 1167-75.

47.   Sikorski, R.S. and P. Hieter, *A system of shuttle vectors and yeast host strains designed for efficient manipulation of DNA in Saccharomyces cerevisiae.* Genetics, 1989. **122**(1): p. 19-27.

48.   Starcevic, M. and E.C. Dell'Angelica, *Identification of snapin and three novel proteins (BLOS1, BLOS2, and BLOS3/reduced pigmentation) as subunits of biogenesis of lysosome-related organelles complex-1 (BLOC-1).* J Biol Chem, 2004. **279**(27): p. 28393-401.

49.   Feliciano, D., et al., *In vivo andin vitro studies of adaptor-clathrin interaction.* J Vis Exp, 2011(47).

50.   Ito, H., et al., *Transformation of intact yeast cells treated with alkali cations.* J Bacteriol, 1983. **153**(1): p. 163-8.

51.   Di Pietro, S.M., J.M. Falcon-Perez, and E.C. Dell'Angelica, *Characterization of BLOC-2, a complex containing the Hermansky-Pudlak syndrome proteins HPS3, HPS5 and HPS6.* Traffic, 2004. **5**(4): p. 276-83.

52.   Vida, T.A. and S.D. Emr, *A new vital stain for visualizing vacuolar membrane dynamics and endocytosis in yeast.* J Cell Biol, 1995. **128**(5): p. 779-92.

53.   Falcon-Perez, J.M., et al., *BLOC-1, a novel complex containing the pallidin and muted proteins involved in the biogenesis of melanosomes and platelet-dense granules.* J Biol Chem, 2002. **277**(31): p. 28191-9.

54.   Rigaut, G., et al., *A generic protein purification method for protein complex characterization and proteome exploration.* Nat Biotechnol, 1999. **17**(10): p. 1030-2.

CHAPTER 3

NEW INSIGHTS ON THE REGULATION OF THE SLAC COMPLEX AND THE

CHARACTERIZATION OF A NOVEL G-ACTIN BINDING MOTIF[2]

3.1 Summary

During endocytosis, remodeling of the plasma membrane requires a repertoire of endocytic regulatory proteins working in concert to achieve cargo accumulation and vesicular internalization. Clathrin-mediated endocytosis is a fundamental pathway conserved from yeast to humans that proceeds by forming a clathrin coat at the plasma membrane followed by the recruitment of proteins that promote membrane curvature, actin polymerization, and scission. In budding yeast, cortical actin assembly is a critical event necessary for proper endocytosis and is regulated by the Arp2/3 complex and its activators, such as Las17 (WASp). Las17 forms a large biochemically stable complex with the clathrin adaptor Sla1 (intersectin), where Las17 is inhibited (SLAC). Sla1 binds to sequences overlapping a newly identified G-actin binding site in Las17, thus blocking G-actin binding. Bzz1 (syndapin), a membrane tubulation protein, can bind to the plasma membrane and stimulate Las17 activity *in vitro.* Here we present new findings for SLAC regulation by Bzz1 and will describe the *in vitro* and *in vivo* characterization of the Las17 novel G-actin binding motif.

[2]Daniel Feliciano, Michael Hughes, and Santiago M. Di Pietro
Department of Biochemistry and Molecular Biology, Colorado State University,
Fort Collins, Colorado 80523, USA.

3.2 Introduction

Membrane remodeling occurs during various cellular activities including cytokinesis, cell motility, and endocytic processes, such as clathrin-mediated endocytosis (CME) [1-3]. CME is the major route for somatic nutrient uptake, vesicular recycling in neuronal synapses, and receptor internalization [3] . Formation of a clathrin coated vesicle (CCV) can be summarized in three steps [1, 3, 4] . First, clathrin triskelia and adaptor proteins are recruited to a flat part of the plasma membrane where the clathrin coat is assembled. During coat assembly, cargo recognition and accumulation supports the formation of a clathrin-coated pit (CCP) that gradually invaginates. Second, actin regulatory proteins are recruited to CCPs and actin polymerization is initiated. Third, scission proteins are recruited to the neck of the CCP, and together with actin polymerization events cooperate to complete the scission of the CCV from the plasma membrane. In this stage, proteins mediating membrane curvature and regulating the organization of the actin cytoskeleton have essential roles in generating tubular invaginations of the plasma membrane at endocytic sites [5]. Some endocytic proteins that arrive at early or intermediate stages, such as Sla2 (HipR), Pan1 (Eps15), and _Bin1/Amphiphysin/Rvs167_ (BAR) superfamily proteins including Syp1 (FCHO1) and Bzz1 (syndapin), associate with both membrane lipids and components of the actin cytoskeleton [6-9]. Tubulation and membrane curvature is mainly attributed to the intrinsic banana-shape of the BAR-domain homodimer [10]. BAR domain superfamily proteins are involved in multiple steps during CME, but their role regulating the actin cytoskeleton is less well- understood [11, 12].

Most members of the _F_es/CIP4 homology-_B_in/_A_mphiphysin/_R_vsp (F-BAR) subfamily proteins contain Src homology 3 (SH3) domains at the C- terminus [13, 14]. SH3 domains can

bind to various targets, including dynamins and members of the Wiskott-Aldrich syndrome protein (WASp) superfamily that are involved in actin polymerization processes [8, 15-19]. Proteins that regulate actin assembly at sites of endocytosis include cofilin, profilin, capping proteins and the Arp2/3 complex. Activators of the Arp2/3 complex, such as the WASp superfamily proteins, are also recruited to endocytic sites promoting actin polymerization.

WASp and its homologues play a main role in activation of the Arp2/3 complex and actin nucleation in several cytoskeletal processes, such as the scission step in CME [3, 20, 21]. These proteins contain a C-terminal <u>W</u>ASp homology 2 (WH2) /<u>C</u>entral/<u>A</u>cidic domain (WCA domain), also known as VCA, that can bind to Arp2/3 and G-actin to stimulate actin assembly. The WH2 has a well conserved basic sequence (LKKT/V) that influences its ability to bind G-actin [22, 23]. Several WH2 or WH2-like sequences have been identified among different organisms, including virus, bacteria, yeast and humans [24]. Recently, studies in yeast have described novel G-actin binding sequences with important roles in cell polarity and regulation of the actin cytoskeleton during CME [25, 26]. Further identification and characterization of new actin binding sequences could shed light on the mechanisms involved in actin polymerization during membrane internalization processes.

One such mechanism is the inhibition of the only WASp homologue in yeast, Las17, by the clathrin adaptor protein Sla1. Las17 is associated in a large and biochemically stable complex with Sla1 that we have termed SLAC. The complex is held together by association of the first two SH3 domains in Sla1 and a series of polyproline motifs in Las17 P8-12 region that belongs to a new type (classI/II) (Figure 2.3, 2.4). This high affinity SH3-polyproline interaction (Kd = 56 ± 8 nM) is responsible -at least in part- for inhibition of Las17 nucleation promoting factor (NPF) activity during initial recruitment to sites of endocytosis. A recent study has identified a

new actin binding site within the central polyproline stretch in Las17, but the relevance of this site in CME was not further characterized [25]. We have shown that Sla1 SH3 domains block G-actin binding to Las17 approximately in the same region of this uncharacterized novel actin binding site, thus inhibiting Las17 NPF activity. However, this new G-actin binding site, within the P8-12 region, has not been mapped. The SLAC complex is important for normal regulation of actin polymerization and, together with membrane tubulation proteins, fine-tunes the temporal control of vesicular internalization in yeast. Two F-BAR-domain containing proteins, Syp1 and Bzz1, are recruited to endocytic sites with different timing, suggesting both have distinct roles during membrane remodeling (Figure 3.1) [5, 27-29]. Syp1 can bind Las17 and cooperate with Sla1 to inhibit Las17 NPF activity in *vitro* and *in vivo* (Figure 2.12). However, Syp1 does not have an SH3 domain implying that the mechanism of Las17 inhibition is likely different from that of Sla1 [28, 29].

As with most F-BAR domain containing proteins, Bzz1 comprises two SH3 domains at its C-terminus [13]. Bzz1 is recruited to Las17 patches right before actin polymerization is detected, suggesting it has an actin regulatory function for releasing Sla1 inhibition and stimulating Las17 NPF activity [27]. In *Schizosaccharomyces pombe*, SH3 domains in Bzz1 are essential for its recruitment to actin patches and mutations to these domains reduces actin accumulation at endocytic sites up to 80% [30]. Binding affinity assays showed that both SH3 domains in Bzz1 bind to the S. *pombe* WASp homologue (Wsp1) with low micromolar affinity (Kd ~0.1 μM). In addition, actin polymerization assays showed that dimers of Bzz1-SH3 domains further stimulate the ability of Wsp1 to activate the Arp2/3 complex [30]. Together, these data supports the idea that Bzz1, in *Saccharomyces cerevisiae,* also has important roles in actin regulatory processes mediated in part by its SH3 domains.
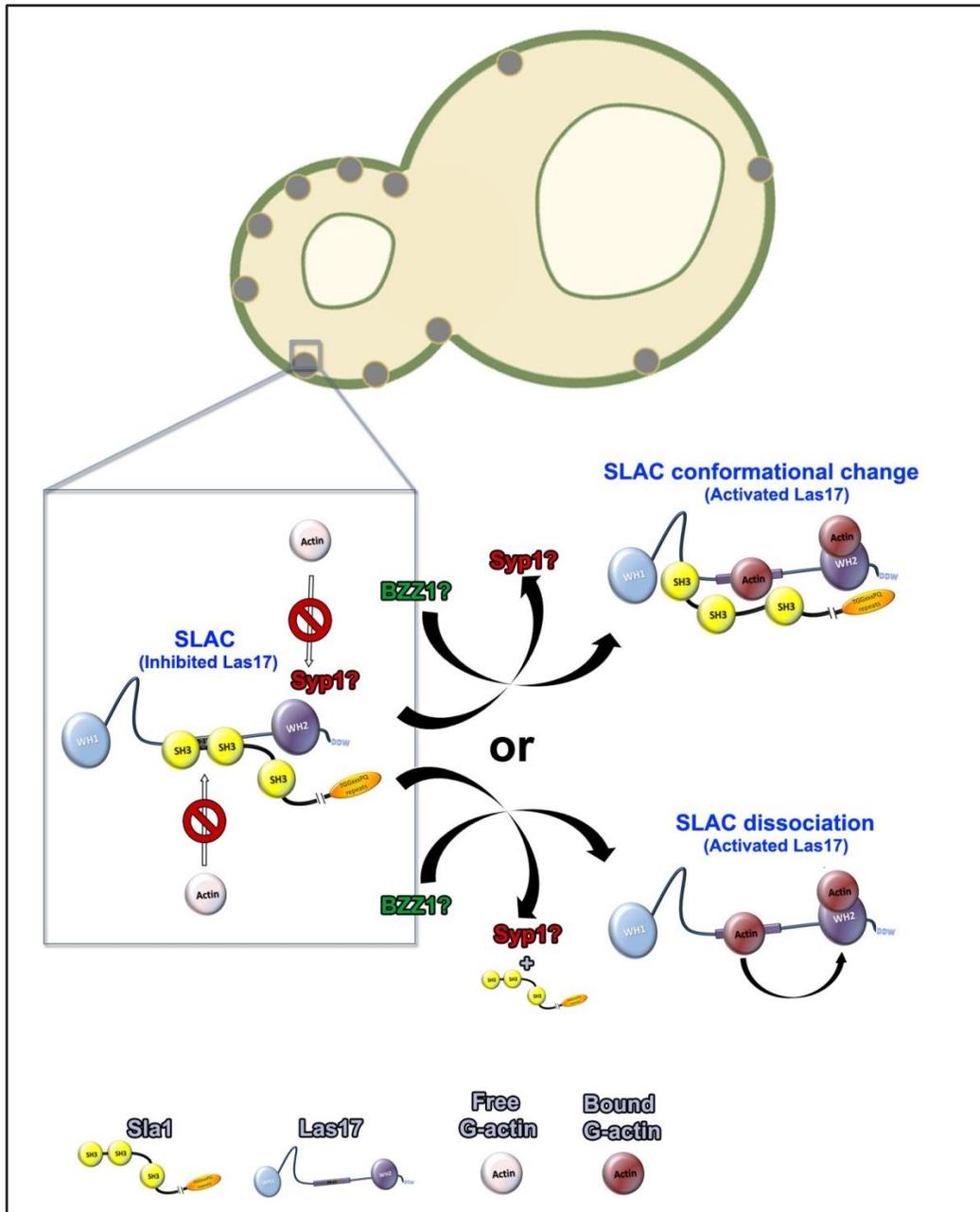
Figure 3. 1

Preliminary mechanistic model for SLAC inhibition and activation in *Saccharomyces cerevisiae*. Las17 is recruited to sites of endocytosis as part of a preformed complex with Sla1, known as SLAC. Within the SLAC complex Sla1 binds and blocks a novel G-actin binding motif in Las17 inhibiting its NPF activity. Syp1 cooperates with Sla1 to achieve additional Las17 inhibition at endocytic sites. During the transition from coat formation to the actin polymerization stage, Bzz1 is recruited and Syp1 dissociates from the endocytic site. Bzz1 can potentially activate the SLAC complex by two mechanisms including conformational change or complex dissociation.

107

Here we present new insights on SLAC complex regulation by Bzz1 and describe the *in vitro* and *in vivo* characterization of Las17 novel actin binding motif and its dependence on a group of arginine residues. Release of Las17 NPF activity is essential for endocytosis to proceed, and the data presented here suggest activation occurs through a mechanism independent of SLAC dissociation.

3.3 Results and Discussion

3.3.1 Arginines within the novel G-actin binding site are important for actin binding and Las17 NPF activity in vitro and in vivo.

A recent study identified a new actin binding site located within residues 300-422 of the Las17 central polyproline stretch [25]. We demonstrated that this region interacts with Sla1 SH3 domains and affects Las17 NPF activity both *in vitro* and *in vivo* (Figure 2.6, 2.11). Pyrene- actin sequestration experiments showed that binding of Sla1 SH3 domains to this site blocks G-actin binding to Las17 (Figure 2.7). To better establish the relevance of this new monomeric actin binding motif for the activity and regulation of the SLAC complex, additional analyses are needed.

To further characterize of this novel G-actin binding site, a combination of biochemical and fluorescence microscopy experiments were performed. First, a series of yeast two hybrid assays were carried out to examine the ability of several Las17 fragments to bind actin (Act1). The full length Las17 fragment (P1-20) and four other fragments (P8-11, P8-12, P10-12 and VCA) were able to bind actin with different strengths. Fragment P1-20 exhibited the strongest interaction, followed by P8-12 and VCA with similar binding capabilities. Based on the cell

growth observed in yeast two hybrid experiments, P8-11 displayed the weakest interaction while P10-12 is the smallest fragment that associates with actin with an affinity close to that of P8-12 or VCA (Figure 3.2A). These results show that sequences in P8-12 can bind to actin with a binding strength comparable to that observed for VCA.

Sequence inspection of Las17 P8-12 fragment failed to identify the basic motif (LKKT/V) conserved in known G-actin binding domains [22, 23]. However, searching for sequences with similar hydropathic amino acid patterns, as those observed in Las17 WH2 basic sequence (LRKV), we identified two sites (PRRG and GRRG) that could be important for G-actin binding (Figure 3.2B). To test the significance of these sequences for actin binding, pyrene-actin polymerization assays, in the absence of Sla1, were conducted with recombinant wild type full length Las17 (Las17-Wt) and full length Las17 with arginine to glycine substitutions to both sites (Las17-RR-Mut) (Figure 3.2C). Wild type Las17 promoted rapid actin polymerization as previously presented (Figure 2.6). However, pyrene-actin assays with mutant Las17 displayed a weaker actin assembly activity, as evidenced by a decrease in the polymerization rate and an extended lag phase (Figure 3.2C). Quantification of relative actin polymerization rates shows the mutations in Las17 arginine-rich sites decreased the NPF activity by 73 % (27% residual activity) when compared to wild type Las17(Figure 3.2C right panel). These results are similar to those observed in pyrene-actin assays where Sla1 SH3 domains are added to the reaction, thus leading to blockage of G-actin binding (25% residual activity, Figure 2.6, Figure 2.7). These results suggest that the arginines mutated in these two sites are key components of a site required for NPF activity in Las17. To determine the contribution of these arginine-rich sites to G-actin binding, additional yeast two hybrid assays were conducted. In this experiment the same point mutations were introduced to the arginine-rich sequence flanking P11 (M11 RR) or the sequence
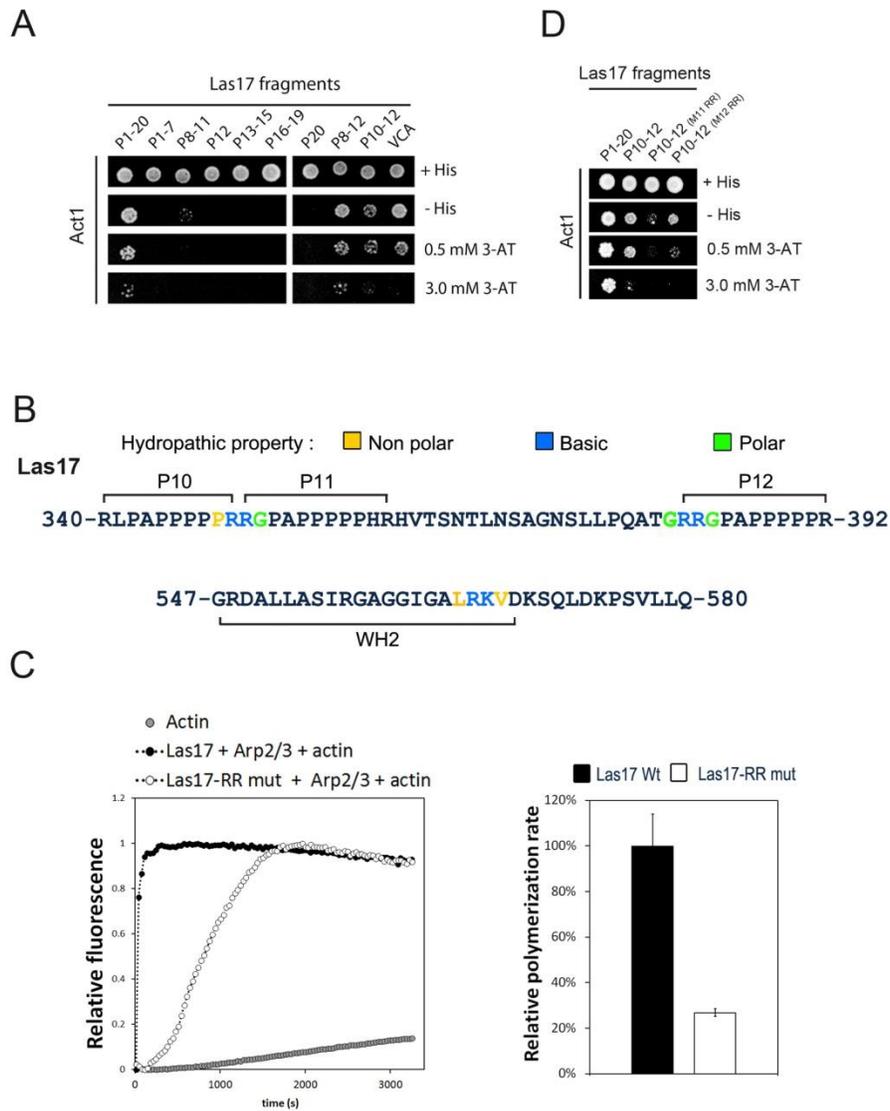
Figure 3.2

Arginines within the novel G-actin binding motif are important for actin binding and Las17 NPF activity. (A) AH109 yeast cells that were cotransformed with expression plasmids containing GAL4 DNA-binding and activation domains fused to Las17 fragments and G-actin (Act1), respectively, were analyzed by yeast two hybrid as described before. (B) Comparison of hydropathic properties of Las17 amino acids that comprise potential G-actin binding sequences (PRRG, GRRG) and the WH2 domain (LRKV). (C) Pyrene-actin (1.5 μM) was polymerized in the presence of Arp2/3 complex (75 nM) and purified full length Las17 wild-type (Las17 Wt) or mutant (Las17-RR-Mut) (75nM). The mutations were substitutions from R to G in potential G-actin binding sequences (PRRG, GRRG). Relative polymerization rates are expressed as the average ± SEM of two independent determinations. (D)Yeast two-hybrid analysis comparing the effect of single arginine cluster mutants (M11 RR or M12RR), within the P10-12, for interaction with G-actin (Act1).

at P12 (M12 RR). The effect of these mutations was analyzed in the context of the P10-12 fragment by yeast two hybrid assays (Figure 3.2D). This assay revealed that both the site flanking P11 and the site at P12 contribute to actin binding but the former is more important, consistent with the differences in the amino acid hydropathic properties observed between these sites and the WH2 domain. (Figure 3.2B, D).

So far these results indicate that two unique sets of arginines within P8-12 are part of a new G-actin binding module potentially comprised of two G-actin binding motifs, and when these sequences are mutated defects in actin binding and a decrease in Las17 NPF activity *in vitro* result. To test if these arginines are significant for Las17 function *in vivo*, the same mutations were introduced into cells endogenously expressing Las17-GFP and this new strain was then crossed with cells endogenously expressing Abp1-RFP. After sporulation of diploids, haploid cells expressing the mutant Las17-GFP (Las17-RR-Mut) and Abp1-RFP were obtained. A strain with wild-type Las17-GFP and Abp1-RFP was used for comparison. Confocal fluorescence microscopy was used to analyze the patch lifetimes of Las17-GFP and Abp1-RFP. As previously described in wild type cells (Figure 2.11A) Las17-GFP and Abp1-RFP patch lifetimes were 30s and 16s, respectively (Figure 3.3). In contrast, analysis of Las17 mutant cells revealed an increment in patch lifetimes for both Las17-GFP (41s) and Abp1-RFP (21s) (Figure 3.3). The increase in Abp1-RFP patch lifetime is consistent with a defect in Las17 NPF activity that leads to a reduction in the rate of actin filament formation at endocytic sites. A decrease in the rate of actin filaments accumulation would likely slowdown the internalization step of endocytosis thus explaining the extended Las17-GFP patch lifetime (Figure 3.3).

111
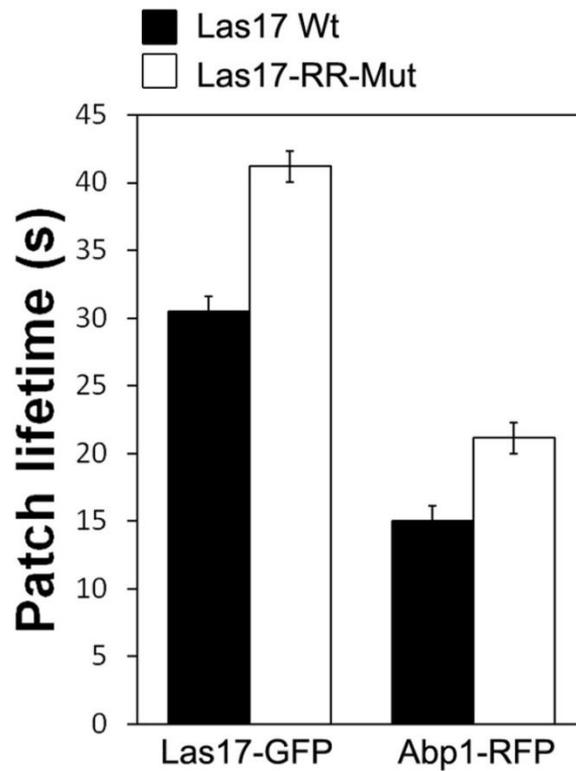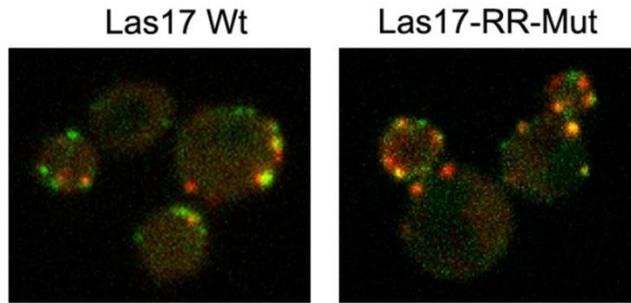
Figure 3.3
Requirement of two arginine-rich clusters in Las17 novel G-actin binding site for normal progression of endocytosis. Dynamics of wild-type (Las17 Wt) and mutant (Las17-RR-Mut) Las17-GFP with Abp1-RFP at endocytic sites were studied by confocal fluorescence microscopy. An example of each strain is presented in the top panel. Time-lapse movies from wild type and mutant Las17 cells were obtained in both green and red channels at 1frame/2s. Las17-GFP and Abp1-RFP patch lifetimes ± SEM were determined for wild type (Las17 Wt) and mutant (Las17-RR-Mut) cells. Differences in Las17 ($p < 0.0001$) and Abp1 ($p = 0.01$) patch lifetimes between wild type and mutant strains are statistically significant.

Together, these results are consistent with a role for Las17 novel G-actin binding site in actin polymerization, and have identified two sets of arginines in this motif as important components for Las17 NPF activity in live cells. Since the significance of this motif has been established both *in vitro* and *in vivo* (Figure 3.2C, 3.3), we propose to name it Las17 novel G-actin binding module 1 (LGM1).

LGM1 is an arginine-polyproline-rich motif in Las17 with an important role for positive and negative regulation of the SLAC complex. Within the complex, Sla1 binds sequences overlapping LGM1, thus inhibiting Las17 by blocking G-actin binding. Actin nucleation is the rate limiting step during actin polymerization events. This is why it is conceivable that the very strong activity of Las17 compared with other NPFs is attributed at least in part to LGM1. During Las17 mediated Arp2/3 activation, actin monomers could bind to both LGM1 and the WH2 domain. Upon binding of Arp2/3 to Las17 acidic tail at the VCA, two G-actin molecules are brought to close proximity with Arp2/3 allowing the formation of a pseudo-actin-tetramer (Arp2, Arp3 and two G-actin molecules), thus increasing the rate of actin nucleation.

In the future, additional mutations to other arginines within LGM1 should be analyzed to determine if these are also involved in G-actin binding. Yeast two hybrid experiments showed similar binding strengths between LGM1, in the P8-12 fragment, and the WH2 in VCA (Figure 3.2A). Determination of dissociation constants for both WH2 and LGM1 can provide some insight on how these two G-actin binding sequences work together within Las17, stimulating actin polymerization. Furthermore, determining the 3D structure of a G-actin-LGM1 complex would identify the entire binding surface that mediates the interaction between actin and the Las17 LGM1 sequence. This would allow the design of models that could explain the mechanisms governing the regulation of the SLAC complex.

3.3.2 Determination of Bzz1 binding site in Las17

Las17, the only WASp homolog in yeast, is kept inactive in the cell as part of the SLAC complex. This complex, which is comprised of the clathrin adaptor Sla1 and Las17, is recruited to endocytic sites where it is inhibited for around 20s before it can activate Arp2/3 to promote actin polymerization. Sla1 can inhibit Las17 by the binding its first and second SH3 domains to specific polyproline sequences in Las17. The inhibition of Las17 by Sla1 in the context of the SLAC complex, potentially in cooperation with other proteins such as Syp1, has been studied. However, the mechanism of Las17 activation to promote assembly of actin filaments is unknown. Pyrene-actin polymerization assays performed in the laboratory of David Drubin have described the F-BAR-domain containing protein Bzz1 (syndapin) as a potential candidate for stimulating Las17 NPF activity (Figure 3.1) [27]. One possibility is that activation of Las17 is driven by binding of Bzz1 C-terminal SH3 domains to the central polyproline stretch in Las17. To test if Bzz1 SH3 domains bind to the polyproline region of Las17, a series of yeast two hybrid assays were performed. First, the Las17 polyproline-rich-domain, containing 20 polyproline motifs (PxxP), was dissected into several fragments which were tested for binding to the Bzz1 SH3 domains (Figure 3.4 A-B). Two Las17 fragments, P1-7 and P8-11, in addition to the full length polyproline construct (P1-20), showed binding to Bzz1 SH3 domains (Figure 3.4B). The relative strength of these interactions were assessed by using selective plates lacking histidine with increasing concentrations of 3-amino-1, 2, 4-triazole (3-AT). These assays showed comparable interaction between Las17 fragments P1-20 and P1-7, while P8-11 was barely detectable and only in plates with no 3-AT (Figure 3.4B).
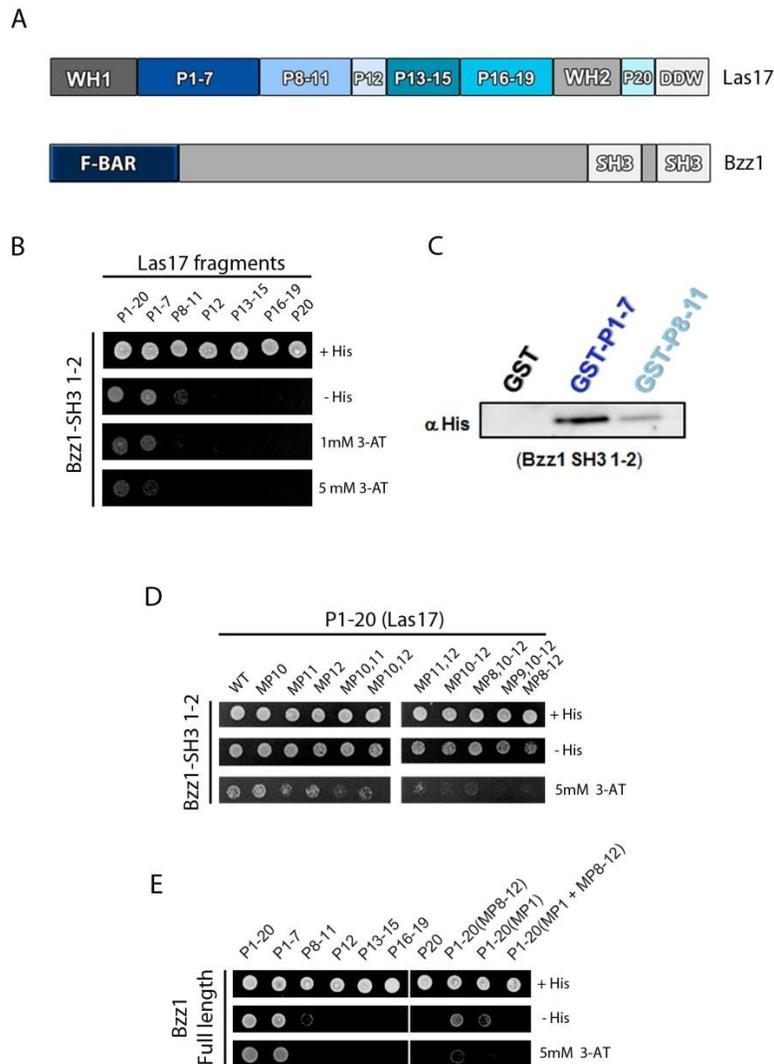
Figure 3.4

Identification of Las17 polyproline motifs involved in Bzz1 binding. (A) Diagram depicting Las17 and Bzz1domains. (B) AH109 yeast cells were cotransformed with expression plasmids containing GAL4 DNA-binding and activation domains fused to the indicated Las17 fragments and Bzz1 SH3-1-2, respectively. Transformants were first selected on minimal media lacking leucine and tryptophan and containing histidine (+His) and then spotted onto plates containing the same medium (as control) or selective medium lacking histidine and containing various concentrations of 3-AT. (C) GST fusion affinity assay was carried out with recombinant GST alone as a control, or GST fused to Las17 fragments P1-7 (GST-P1-7), and P8-11 (GST-P8-11). Each GST-fusion protein was bound to glutathione beads and incubated with purified polyhistidine-tagged Bzz1 SH3-1-2 fragment (Bzz1 SH3-1-2). The bound Bzz1 SH3-1-2 fraction was analyzed by immunoblotting with an anti-polyhistidine antibody. (D)Yeast two-hybrid studies comparing the strength of interaction of single and double polyproline motifs mutants within polyprolines P8 through P12 analyzed in the context of the P1-20 fragment. (E) Yeast two-hybrid analysis showing strength of interaction between several Las17 fragments and full length Bzz1. Various proline-to-alanine point mutations were introduced that selectively inactivated specific polyproline motifs (MP8-12, MP1, and MP1 + MP8-12) in the context of the P1-20 construct.

115

To confirm direct association between Las17 and Bzz1 mediated by SH3-polyproline interactions, glutathione S-transferase (GST)-fusion binding assays were performed. Two GST-fusion proteins, containing Las17 fragment P1-7 and P8-11 were purified and incubated withHis-tagged Bzz1 SH3 domains 1 and 2 (Bzz1 SH3 1-2). Binding between Las17 fragments and Bzz1 SH3 domains was analyzed by immunoblotting (IB) (Figure 3.4C). In these experiments, GST-P1-7 showed significant more binding to Bzz1 SH3 1-2 than GST-P8-11. This result resembles the data acquired from yeast two hybrid assays (Figure 3.4B) and confirms a direct association between Las17 and Bzz1.

Sequence inspection of the PxxPs in P1-7 reveals that among the seven polyproline motifs, P1 (KAPPPPP) was the only sequence with a class I consensus. This is consistent with recent studies where Bzz1 SH3 domains 1 and 2 were predicted to bind class I polyproline motifs preferably containing a lysine residue flanking the N-terminus side of the sequence (KxxPxxP)[31]. As previously reported, P8-11 has four polyproline motifs that simultaneously conform to class I and classII consensus sequences (classI/II), although these are flanked by arginine residues. Variations in positively charged amino acids in these polyprolines motifs could explain the differences in binding strength to Bzz1 SH3 domains between Las17 P1-7 and P8-11 fragments. This result may also suggest that not all four PxxP in P8-11 participate in the interaction with Bzz1. To assess the contribution of the four polyproline motifs in Las17 P8-11 fragment, and identify which of these are involved in Bzz1 binding, site-directed-mutagenesis experiments were performed. Single or double PxxP mutations were introduced to polyprolines within P8 to P12, in the context of the Las17 P1-20 fragment. Analysis of these mutants by yeast two hybrid system demonstrated that polyprolines P10 and P11 are the main contributors for the binding of Las17 P8-11 fragment to Bzz1 SH3 domains (Figure 3.4D).

Bzz1 contains an unstructured central region flanked by an N-terminal F-BAR domain and two C-terminal SH3 domains (Figure 3.4A). To determine if other parts of Bzz1 besides the SH3 domains influence its binding to Las17, experiments with full length Bzz1 were carried out (Figure 3.4 E). Yeast two hybrid assays with full length Bzz1 showed a slight increase in the ability of these cells to growth at 5mM 3-AT compared to when only Bzz1 SH3 domains were analyzed (Figure 3.4B, E). This suggest that there may be additional sequences at the N-terminus or central region of Bzz1 participating in binding of Las17 (Figure 3.4A, B, E). As expected, additional analysis of P1-20 fragment with mutations in the polyprolines spanning from P8 to P12 showed a decrease in full length Bzz1 binding. However, a similar experiment but with a single mutation in P1 strongly affected cell growth in plates with no 3-AT and destroyed the capacity of these cells to grow   at 5mM 3-AT (Figure 3.4E). Combination of P1 and P8-12 mutations completely abrogates the ability of Las17 to bind Bzz1 inhibiting cell growth at both low and high 3-AT concentrations (Figure 3.4E).

Together, these experiments mapped the specific polyproline sequences in Las17 that mediate the interaction with Bzz1 SH3 domains, and revealed a potential contribution of Bzz1 N-terminal sequences for Las17 binding and/or regulation. The polyproline sequences mediating the interaction between Las17 and Bzz1 can be divided in two types of Bzz1 binding sites, a strong (P1) and a weak (P10-11) binding site. Bzz1 could use these sites one at a time or simultaneously to bind and regulate Las17 at different stages in endocytosis. The weak Bzz1 P10-11 site in Las17 overlaps with the Sla1 SH3 domains 1 and 2 binding site (P8-12) and this may result in competition between Sla1 and Bzz1 for the same site. If this is the case, one possibility is that Bzz1 binds to the strongest site (P1) first for its initial recruitment to Las17 patches where its local concentration is high enough to compete out Sla1 from the Las17 P10-11

site. However, binding of Bzz1 to P10-11, which would lead to dissociation of Sla1 from the SLAC complex, could also block binding of G-actin to LGM1. Nevertheless, if the affinity of G-actin for LGM1 at endocytic sites is higher than that of Bzz1 for P10-11, G-actin might displace Bzz1 SH3 domains from the weak P10-11 binding site allowing the stimulation of Las17 NPF activity. To elucidate the mechanism of Las17 activation by Bzz1 binding more extensive analyses are required.

3.3.3 Activation of SLAC requires sequences at the N-terminus of Bzz1 SH3 domains and is independent of complex dissociation.

We have shown that a large part of SLAC inhibition is achieved by obstruction of G-actin binding to a monomeric actin binding module (LGM1) within polyproline sequences mediating the interaction between Sla1 and Las17. However, the molecular mechanism for SLAC activation has yet to be elucidated. In this work we have proposed two mechanisms for activation of SLAC at sites of clathrin-mediated endocytosis (Figure 3.1). One of these mechanisms requires a conformational change or rearrangement of the complex where Sla1 is kept bound to Las17. This would allow binding of monomeric actin to LGM1 in Las17, and concomitant activation of the Arp2/3 complex. The second proposed mode of activation is through dissociation of the SLAC complex, which can also lead to G-actin binding and Arp2/3 activation. Bzz1 is the main candidate to mediate the activation of the SLAC complex through the mechanisms proposed here. In this scenario: 1) Las17 would exist simultaneously bound to Sla1 and Bzz1 and a conformational change in the SLAC complex could be induced or 2) binding of Bzz1 to Las17 could promote complex dissociation by Sla1 release.

118

To distinguish between these two mechanisms, a competition assay was carried out. Purified GST-fusion protein containing Las17 P1-12 fragment was bound to glutathione beads and incubated with saturating amounts of purified His-tagged Sla1 SH3 domains 1 and 2 to reconstitute a truncated version of the SLAC complex (mini-SLAC). A constant amount of reconstituted mini-SLAC bound to glutathione beads was incubated with increasing concentration of purified His-tagged full length Bzz1, and proteins that remained bound to the beads were analyzed by SDS-PAGE (Figure 3.5A). Increasing binding of Bzz1 to P1-12 was detected with increasing Bzz1 concentrations but no dissociation of Sla1 SH3 domains was observed (Figure 3.5A). Similarly, experiments using the GST-P1-12 recombinant protein containing a mutation in P1 (MP1) show no significant dissociation of Sla1 SH3 domains when incubated with Bzz1 (Figure 3.5A, right panel). However, this construct displayed a remarkable binding defect at all Bzz1 concentrations as was observed for constructs with the same P1 mutation analyzed by yeast two hybrid assays (Figure 3.4E, 3.5A). These results confirm the importance of P1 as the main Bzz1 binding site, and strongly suggest that activation of the SLAC complex might be achieved without requiring complex dissociation (Figure 3.5C). This is consistent with previous gel filtration experiments where the monomeric form of Las17 was not detected in cytosolic fractions from wild type cells (Figure 2.1D, E, F).

To estimate the affinity of the interaction between Bzz1 SH3 domains and Las17 polyproline motifs a quantitative ligand-depletion assay was performed. Using a constant amount of full length Bzz1 and increasing concentrations of GST-P1-12 bound to glutathione beads, the unbound Bzz1 fraction was determined after incubation. The free Bzz1 fraction in the su-pernatant was analyzed by SDS–PAGE and Coomassie staining followed by gel densitometry quantification (Figure 3.5B). The bound Bzz1 fraction was calculated by subtraction from the
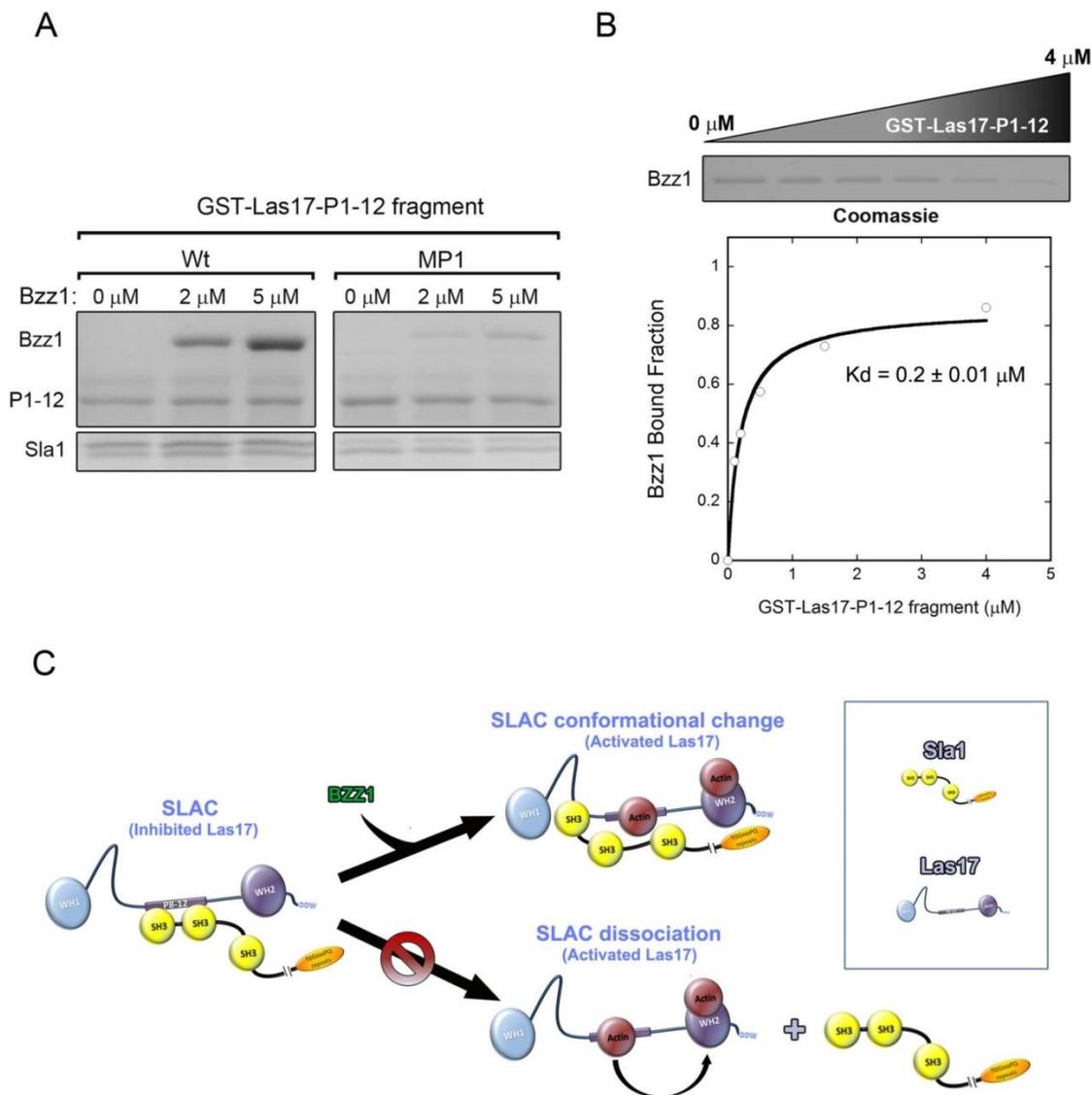
Figure 3.5

Activation of SLAC does not require complex dissociation. (A) Bzz1 titration assays were performed using a recombinant GST-fusion protein of a Las17 fragment containing both Bzz1 and Sla1 binding sites (P1-12) or the same GST-fusion fragment with a mutation in P1 (P1-12 MP1). First, each GST-fusion protein (0.8 μM) was bound to glutathione beads and incubated with saturating amounts (4μM) of Sla1 SH3 1-2 for 1hr. After washing out the excess, unbound Sla1, each reaction was incubated with 0, 2 or 5 μM purified polyhistidine-tagged full length Bzz1. The amount of GST-P1-12 fragments, Bzz1, and Sla1 SH3 1-2 bound to the beads were assessed by SDS-PAGE and Coomassie staining. (B) A constant concentration of full length Bzz1 (600 nM) was incubated with various concentrations of GST-P1-12 bound to glutathione beads. The free Bzz1 fraction in the supernatant was determined by densitometry of SDS–PAGE staining. Bzz1 bound fractions were calculated and fitted by nonlinear regression to estimate the K_d for the interaction. (C) Current model for the Bzz1 mediated activation of SLAC independent from complex dissociation. Bzz1 bound to the active complex was not included in the model for simplicity.

total amount available for binding (Figure 3.5B). Fitting of the data using nonlinear regression provided an estimated $K_d = 0.2 \pm 0.01$ µM (Figure 3.5B). The affinity we have determined here is in the low micromolar range similar to that reported for Bzz1 and Wsp1 interaction in *S. Pombe* (Kd = 0.1µM) [30]. This result suggests that the interaction between Las17 and Bzz1 has close to 4 fold less binding affinity when compared to the interaction between Las17 and Sla1(Kd = 56 ± 8 nM). This is consistent with the notion of a mechanism for SLAC activation mediated by a change in conformation rather than competition between Bzz1 and Sla1 for the same binding site which would lead to complex dissociation.

Yeast two hybrid experiments presented in Figure 3.4 indicate that full length Bzz1 associates with Las17 P1-20 fragment more strongly than Bzz1 SH3 domains alone, as reflected by an increased ability of the cells to grow in 5uM 3-AT. This observation suggests that sequences in the N-terminus of Bzz1 contribute to Las17 binding, in addition to the SH3 domains, and may therefore be important for SLAC activation. To test this idea, pyrene-actin polymerization assays using recombinant full length Las17 and Sla1 SH3 domains 1 and 2 were performed. To determine the relevance of sequences at the N-terminus of Bzz1 for SLAC activation, different concentrations of purified full length Bzz1 or purified Bzz1 SH3 domains were added to these reactions. As previously reported, full length Bzz1 was capable of relieving the inhibitory effect of Sla1 and activated Las17 in a concentration dependent manner (Figure 3.6A) [27]. Surprisingly, addition of Bzz1 SH3 domains caused a concentration-dependent inhibitory effect on Las17 activity that can only be explained by the absence of Bzz1 N-terminus (Figure 3.6B).

Besides an unstructured central region, Bzz1 contains an N-terminal F-BAR domain that can dimerize allowing its binding to the plasma membrane (Figure 3.4A)[13, 14, 32]. It is
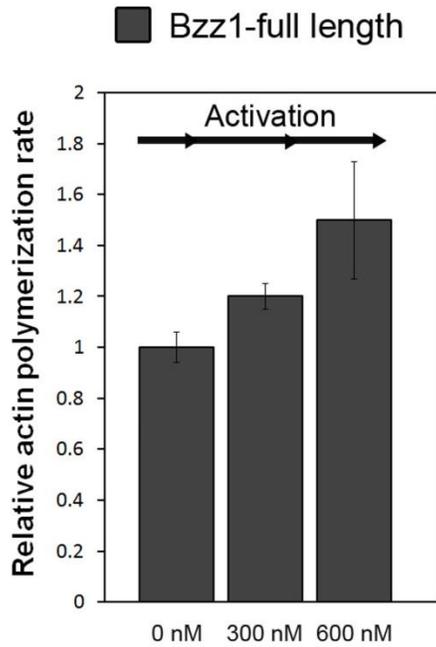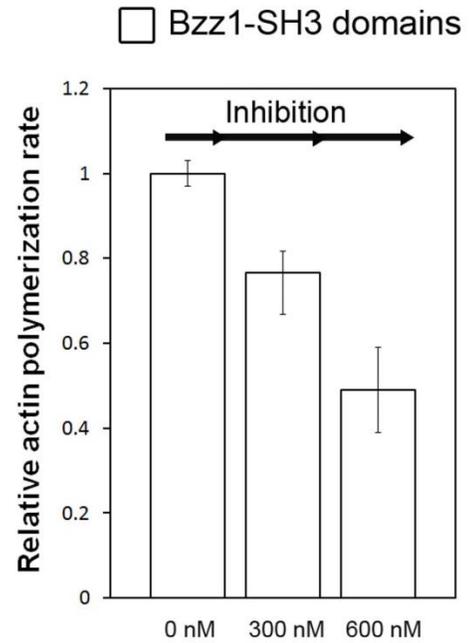
Figure 3.6
SLAC activation requires full length Bzz1 rather than its SH3 domains alone. Pyrene-Actin (1.5 μM) was polymerized in the presence of Arp2/3 complex (75 nM), full-length, wild-type Las17 (75 nM), a sub-saturating concentration of Sla1 (150nM), and a range of concentrations of full length His-Bzz1 or His-Bzz1 SH3 1-2 fragment (A-B). (A) Full length Bzz1 increased the relative Las17-Arp2/3 induced actin polymerization rate, while (B) Bzz1 SH3 domains, lacking the Bzz1 N-terminus, had an inhibitory effect in a concentration-dependent manner. Relative polymerization rates are expressed as the average ± SEM of two independent determinations.

possible that dimerization of Bzz1 F-BAR domains may regulate activation of Las17 by controlling binding of its SH3 domains to Las17. A Bzz1 dimer would have four SH3 domains that could preferably bind to P1. After binding to Las17 P1 motif, one possibility is that two SH3 domains from a Bzz1 dimer could promote Sla1 relocation to Las17 P8 and P9, or it might serve as a platform where Sla1 can bind to Bzz1, thus exposing the LGM1 in Las17. The latter explanation is conceivable since a class I- like polyproline motif is present in a 25 amino acid linker between Bzz1 SH3 domains where Sla1 SH3 domains can bind. The two proposed modes of activation would allow reorganization of the SLAC complex where Sla1 and Bzz1 simultaneously exist associated to Las17, and both are in agreement with a mechanism independent of dissociation of the SLAC complex (Figure 3.5).

Full length Bzz1 activates Las17 in a concentration dependent manner (Figure 3.6A); however, Bzz1 SH3 domains alone caused an inhibitory effect in the presence of sub-saturating amounts of Sla1 SH3 domains (Figure 3.6B). A possible explanation for the differences observed in Figure 3.6 could be the absence of the N-terminal sequence which impedes dimerization of Bzz1 through its F-BAR domain. This would allow the Bzz1 SH3 domains to move freely and associate to any site available for binding. In this scenario, Bzz1 SH3 domains can first bind and saturate P1, while the unbound excess fraction can associate to P10-11 further blocking G-actin binding to LGM1 (Figure 3.6B). This idea suggests a possible role for the F-BAR domain modulating the binding of Bzz1 SH3 domains to Las17.

SLAC has a molecular weight of 822 kDa and possibly contains multiple subunits of Sla1 and Las17. Dimerization of Bzz1 through the F-BAR domain might allow binding to two SLAC complexes, concentrating Las17 molecules locally. This is consistent with new findings showing that dimerization of NPFs increase their activity a 100 times more than when they are in their

monomeric form [33]. In addition, dimerization of Bzz1 might increase its ability to bind Las17, and could explain the stronger interaction between full length Bzz1 and Las17 fragments observed in yeast two hybrid assays (Figure 3.4E).

Overall, inhibition of Las17 NPF activity during the initial 20s of its recruitment is achieved by formation of the SLAC complex. Within the complex, the first and second SH3 domains in Sla1 bind sequences in Las17 overlapping those for LGM1, thus blocking G-actin from binding to Las17. The data presented here suggest full length Bzz1 binds to specific Las17 polyproline motifs through its SH3 domains activating the SLAC complex likely by exposing LGM1 but without disassembly of the complex. This would allow for actin monomers to bind to Las17 stimulating Arp2/3-mediated actin polymerization at sites of endocytosis. Additional work is required to elucidate the role of the F-BAR domains and the central region of Bzz1 during the activation of the SLAC complex.

3.4 Methods

Plasmids and yeast strains

To generate recombinant GST- or polyhistidine-tagged (His) fusion proteins, the corresponding DNA sequence fragments of *LAS17*, *BZZ1,* were amplified by PCR and cloned into pGEX-5X-1 (Amersham Biosciences, Piscataway, NJ, USA) or pET-30a$^+$ (Novagen, Madison, WI, USA) bacterial expression vectors, respectively. For yeast two hybrid experiments the corresponding *LAS17,BZZ1* and *ACT1* DNA fragments were amplified by PCR and cloned into pGBT9 or pGAD424 vector, respectively (Clontech–BD Biosciences, San Jose, CA, USA). Additional cloning and site-directed mutagenesis experiments where done as described in section 2.5 of **Chapter 2**.

AH109 cells (Clontech–BD Biosciences, San Jose, CA, USA) were co-transformed with the respective pGBT9 and pGAD424 construct combinations and were analyzed as described in section 2.5 of **Chapter 2**. SDY362 cells were used to reconstitute the Las17 gene with mutations in the two arginine-rich to generate Las17-RR-Mut-GFP cells (*MAT* α ura3-52 leu2-3112 his3-Δ200 trp1-Δ901, lys2-801, suc2-Δ9 *Las17^{RR-Mut}-GFP::HIS3*) as described in section 2.5 of **Chapter 2**. The Las17-RR-Mut-GFP strain was crossed with SDY360 cells (*MAT*a ura3-52 leu2-3112 his3-Δ200 trp1-Δ901 lys2-801 suc2-Δ9 *ABP1-RFP::TRP1*). These cells were then subjected to sporulation and tetrad dissection, thus generating Las17-RR-GFP/Abp1-RFP cells (*MAT*a ura3-52 leu2-3112 his3-Δ200 trp1-Δ901, lys2-801, suc2-Δ9 *Las17^{RR-Mut}-GFP::HIS3 ABP1-RFP::TRP1*).

Biochemical methods

Bzz1 titration assays were performed using a recombinant GST-fusion protein of a Las17 fragment containing both Bzz1 and Sla1 binding sites (P1-12) or the same GST-fusion fragment with a mutation in P1 (P1-12 MP1). Briefly, wild type and mutant GST-fusion protein (0.8 μM) were bound to glutathione beads and incubated with saturating amounts (4μM) of Sla1 SH3 1-2 for 1hr. After washing out the excess, unbound Sla1, each reaction was incubated with 0, 2 or 5 μM purified polyhistidine-tagged full length Bzz1. The amount of GST-P1-12 fragments, Bzz1, and Sla1 SH3 1-2 bound to the beads were assessed by SDS-PAGE and coomassie staining.

GST-fusion protein affinity assays were performed in PBS containing 0.5% TX100 as described in section 2.5 of **Chapter 2**. Quantitative GST-fusion protein affinity assays were performed as described in section 2.5 of **Chapter 2**. Briefly, recombinant His-Full length Bzz1 (600 nM) was incubated with increasing concentrations of wild type GST-Las17-P1-12 bound to glutathione-sepharose beads for 1 hour at 4 °C. Unbound His-Sla1-SH3-1-2 was recovered in the supernatant and protein concentration determined by gel densitometry.

Protein Purification

GST- and His-fusion proteins were expressed in *Escherichia coli* (BL21) and affinity purified using glutathione–Sepharose-4B or the TALON cobalt affinity resin (Clontech–BD Biosciences, San Jose, CA, USA) as described in section 2.5 of **Chapter 2**. Full length wild type-Las17 was expressed in *Escherichia coli* (BL21) and subjected to a sequential affinity purification using glutathione–Sepharose-4B (GST-tag at amino-terminus) followed by TALON cobalt affinity resin (His-tag at carboxi-terminus).

Actin Polymerization assay

Actin polymerization experiments were performed with 1.5 μM rabbit actin (99% pyrene labeled) and 75 nM bovine Arp2/3 complex (Cytoskeleton, Denver, CO, USA). Pyrene-actin (0.4 mg/ml) was incubated in G-Buffer (10 mM Tris, pH 8.0, 0.2 mM $CaCl_2$, 0.2 mM ATP) on ice for 1.5 hours to promote depolymerization and subsequently centrifuged at 100,000 rpm in a TLA100.3 rotor (Beckman Coulter, Fullerton, CA) at 4 °C for 1.5 hours. Pyrene-actin was incubated in exchange buffer (1 mM EGTA, 0.1 mM $MgCl_2$) for 10 minutes and added to a 96 well plate already containing the proteins of interest (75 nM wild type or mutant Las17 in Figure 3.2C). Variable concentrations of His-Bzz1 SH3-1-2 or His-Bzz1 full length were also added in in Figure 3.6). Polymerization buffer (50 mM KCl, 2 mM $MgCl_2$, 1 mM ATP) was added to the reaction (t=0) and actin polymerization was measured over time using a Victor^3 V microplate reader (PerkinElmer, Waltham, MA, USA) with excitation and emission wavelengths of 365 nm and 406 nm, respectively. Actin polymerization rates were calculated from the slope of the linear portion of assembly curves (25-50% polymerization).

Fluorescence microscopy

Fluorescence microscopy was performed as described in **Appendix** using an Olympus IX81 spinning disc confocal microscope working under the Slidebook 5 software (Intelligent Imaging Innovations, Denver, CO, USA) with Photometrics Cascade II camera and a 100x/1.40NA objective. Time-lapse movies were generated by collecting 120 or 150 images at 1 frame/2s at room temperature using cells grown until early log phase. Quantitation of patch lifetimes were performed by counting the number of frames a patch was observed in the time-lapses and the number obtained was multiplied by two

REFERENCES

1.   Doherty, G.J. and H.T. McMahon, *Mechanisms of endocytosis.* Annu Rev Biochem, 2009. **78**: p. 857-902.
2.   Di Paolo, G. and P. De Camilli, *Does clathrin pull the fission trigger?* Proc Natl Acad Sci U S A, 2003. **100**(9): p. 4981-3.
3.   Merrifield, C.J., D. Perrais, and D. Zenisek, *Coupling between clathrin-coated-pit invagination, cortactin recruitment, and membrane scission observed in live cells.* Cell, 2005. **121**(4): p. 593-606.
4.   Kaksonen, M., C.P. Toret, and D.G. Drubin, *A modular design for the clathrin- and actin-mediated endocytosis machinery.* Cell, 2005. **123**(2): p. 305-20.
5.   Idrissi, F.Z., et al., *Distinct acto/myosin-I structures associate with endocytic profiles at the plasma membrane.* J Cell Biol, 2008. **180**(6): p. 1219-32.
6.   Itoh, T., et al., *Dynamin and the actin cytoskeleton cooperatively regulate plasma membrane invagination by BAR and F-BAR proteins.* Dev Cell, 2005. **9**(6): p. 791-804.
7.   Engqvist-Goldstein, A.E., et al., *An actin-binding protein of the Sla2/Huntingtin interacting protein 1 family is a novel component of clathrin-coated pits and vesicles.* J Cell Biol, 1999. **147**(7): p. 1503-18.
8.   Tsujita, K., et al., *Coordination between the actin cytoskeleton and membrane deformation by a novel membrane tubulation domain of PCH proteins is involved in endocytosis.* J Cell Biol, 2006. **172**(2): p. 269-79.
9.   Yarar, D., C.M. Waterman-Storer, and S.L. Schmid, *SNX9 couples actin assembly to phosphoinositide signals and is required for membrane remodeling during endocytosis.* Dev Cell, 2007. **13**(1): p. 43-56.
10. Peter, B.J., et al., *BAR domains as sensors of membrane curvature: the amphiphysin BAR structure.* Science, 2004. **303**(5657): p. 495-9.
11. McMahon, H.T. and J.L. Gallop, *Membrane curvature and mechanisms of dynamic cell membrane remodelling.* Nature, 2005. **438**(7068): p. 590-6.
12. Gallop, J.L. and H.T. McMahon, *BAR domains and membrane curvature: bringing your curves to the BAR.* Biochem Soc Symp, 2005(72): p. 223-31.
13. Roberts-Galbraith, R.H. and K.L. Gould, *Setting the F-BAR: functions and regulation of the F-BAR protein family.* Cell Cycle, 2010. **9**(20): p. 4091-7.
14. Roberts-Galbraith, R.H., et al., *Dephosphorylation of F-BAR protein Cdc15 modulates its conformation and stimulates its scaffolding activity at the cell division site.* Mol Cell, 2010. **39**(1): p. 86-99.
15. Lippincott, J. and R. Li, *Involvement of PCH family proteins in cytokinesis and actin distribution.* Microsc Res Tech, 2000. **49**(2): p. 168-72.
16. Kessels, M.M. and B. Qualmann, *The syndapin protein family: linking membrane trafficking with the cytoskeleton.* J Cell Sci, 2004. **117**(Pt 15): p. 3077-86.
17. Itoh, T. and P. De Camilli, *BAR, F-BAR (EFC) and ENTH/ANTH domains in the regulation of membrane-cytosol interfaces and membrane curvature.* Biochim Biophys Acta, 2006. **1761**(8): p. 897-912.
18. Takenawa, T. and S. Suetsugu, *The WASP-WAVE protein network: connecting the membrane to the cytoskeleton.* Nat Rev Mol Cell Biol, 2007. **8**(1): p. 37-48.
19. Dawson, J.C., J.A. Legg, and L.M. Machesky, *Bar domain proteins: a role in tubulation, scission and actin assembly in clathrin-mediated endocytosis.* Trends Cell Biol, 2006. **16**(10): p. 493-8.
20. Miki, H. and T. Takenawa, *Regulation of actin dynamics by WASP family proteins.* J Biochem, 2003. **134**(3): p. 309-13.

21.   Kaksonen, M., C.P. Toret, and D.G. Drubin, *Harnessing actin dynamics for clathrin-mediated endocytosis.* Nat Rev Mol Cell Biol, 2006. **7**(6): p. 404-14.

22.   Chereau, D. and R. Dominguez, *Understanding the role of the G-actin-binding domain of Ena/VASP in actin assembly.* J Struct Biol, 2006. **155**(2): p. 195-201.

23.   Chereau, D., et al., *Actin-bound structures of Wiskott-Aldrich syndrome protein (WASP)-homology domain 2 and the implications for filament assembly.* Proc Natl Acad Sci U S A, 2005. **102**(46): p. 16644-9.

24.   Paunola, E., P.K. Mattila, and P. Lappalainen, *WH2 domain: a small, versatile adapter for actin monomers.* FEBS Lett, 2002. **513**(1): p. 92-7.

25.   Robertson, A.S., et al., *The WASP homologue Las17 activates the novel actin-regulatory activity of Ysc84 to promote endocytosis in yeast.* Mol Biol Cell, 2009. **20**(6): p. 1618-28.

26.   Thanabalu, T., et al., *Verprolin function in endocytosis and actin organization. Roles of the Las17p (yeast WASP)-binding domain and a novel C-terminal actin-binding domain.* FEBS J, 2007. **274**(16): p. 4103-25.

27.   Sun, Y., A.C. Martin, and D.G. Drubin, *Endocytic internalization in budding yeast requires coordinated actin nucleation and myosin motor activity.* Dev Cell, 2006. **11**(1): p. 33-46.

28.   Boettner, D.R., et al., *The F-BAR protein Syp1 negatively regulates WASp-Arp2/3 complex activity during endocytic patch formation.* Curr Biol, 2009. **19**(23): p. 1979-87.

29.   Reider, A., et al., *Syp1 is a conserved endocytic adaptor that contains domains involved in cargo selection and membrane tubulation.* EMBO J, 2009. **28**(20): p. 3103-16.

30.   Arasada, R. and T.D. Pollard, *Distinct roles for F-BAR proteins Cdc15p and Bzz1p in actin polymerization at sites of endocytosis in fission yeast.* Curr Biol, 2011. **21**(17): p. 1450-9.

31.   Tonikian, R., et al., *Bayesian modeling of the yeast SH3 domain interactome predicts spatiotemporal dynamics of endocytosis proteins.* PLoS Biol, 2009. **7**(10): p. e1000218.

32.   Shimada, A., et al., *Curved EFC/F-BAR-domain dimers are joined end to end into a filament for membrane invagination in endocytosis.* Cell, 2007. **129**(4): p. 761-72.

33.   Padrick, S.B. and M.K. Rosen, *Physical mechanisms of signal integration by WASP family proteins.* Annu Rev Biochem, 2010. **79**: p. 707-35.

CHAPTER 4

CONCLUSIONS AND IMPLICATIONS FROM THE DISCOVERY AND

CHARACTERIZATION OF THE SLAC COMPEX

4.1 Summary

The discovery and characterization of the SLAC complex presented in this dissertation helped to answer one of the most outstanding questions in the field of endocytic trafficking pertaining to the regulation of Las17 NPF activity. Our results also establish an important role in actin regulation for the G-actin binding module LGM1 in live cells, and have allowed the development of a mechanistic model of SLAC activation by Bzz1. Below these findings and their implication are discussed detail.

4.2 Sla1 and Las17 form a large and stable complex

The study of actin polymerization during membrane remodeling events is of great importance due to the key role of the actin cytoskeleton in multiple cellular processes including cytokinesis, cell motility and endocytosis. Clathrin-mediated endocytosis (CME) is fundamental pathway conserved from yeast to mammals where the actin cytoskeleton plays an important part in vesicle internalization. Cortical actin assembly at CME sites is carried out by the actin nucleator Arp2/3 complex which is activated by nucleation promoting factors (NPFs) such as WASp and its homologues. Importantly, Arp2/3 complex activity must be tightly regulated to

enable the endocytic patch to properly mature before the burst of actin polymerization initiates the vesicle invagination process.

Yeast cells have five NPFs including the only yeast WASp homologue Las17. Las17 is the most potent yeast NPF recruited to endocytic sites well before (~20 seconds) actin polymerization is initiated. Purified Las17 is constitutively active and therefore predicted to be inhibited by direct binding partners [1-3]. *One of the unanswered questions in the field has been how Las17 is inhibited during the initial ~20 seconds after its arrival to sites of endocytosis.* During this a large biochemically stable complex between Las17 and the clathrin adaptor Sla1 was discovered providing a possible answer to this longstanding question.

To identify this complex, a combination of confocal fluorescence microscopy and biochemical experiments were used to demonstrate that both Las17 and Sla1 are associated in the cytosol and are co-recruited to site of endocytosis. Confocal fluorescence microscopy experiments allowed visualization of the simultaneous recruitment of Sla1-GFP and Las17-RFP to endocytic sites in cells expressing these tagged proteins from the endogenous loci. Mutations affecting the temporal localization of one of the components of the complex were shown to also influence the dynamics of the other, thus corroborating their concomitant recruitment.

To study endogenous Las17, affinity-purified polyclonal antibodies against recombinant Las17 amino- and carboxy-terminal fragments were raised. The use of these antibodies in size exclusion chromatography (SEC) of yeast cytosolic extracts, demonstrated that both proteins co-fractionate consistent with a preformed Sla1-Las17 complex in cytosol. In addition, a combination of SEC and sucrose-gradients were used to estimate the molecular mass for this complex to about 822 kDa. This is considerably large than a 1:1 complex taking to account Sla1 and Las17 are 135 and 68 kDa, respectively. Thus it is possible that these proteins form a

multimeric protein complex containing numerous copies of Sla1 and Las17 or additional proteins. To test the possibility of additional proteins endogenous Las17 complex was isolated from a strain expressing C-terminus tandem-affinity purification (TAP)-tagged Las17 from the *LAS17* locus. Following a TAP purification procedure and validation of proteins detected by mass spectrometry analyses, no additional proteins were identified as part of the SLAC complex. Nevertheless, the possibility of additional subunits that might have failed mass spectrometry detection for reasons such as poor peptide ionization cannot be ruled out.

4.3 Complex formation is mediated by a direct and high affinity SH3:PxxP interaction with a new class of polyproline consensus

Las17 is composed of an N-terminal WH1 domain, a polyproline central region, a C-terminal WH2 domain and an acidic tail (Figure 2.3A). Several studies have shown that the central polyproline stretch of Las17 can interact with proteins containing SH3 domains [4]. Sla1 is composed of three amino-terminal SH3 domains and other domains important for cargo recruitment, and clathrin regulation (Figure 2.3A) [5-8]. Importantly, a study by Rodal et al. (2003) showed that the first and second Sla1 SH3 domains, can inhibit the Las17 NPF activity in pyrene-actin polymerization assays. Therefore the first and second Sla1 SH3 domains are good candidates to mediate a direct interaction with Las17.

Analysis of the central polyproline region of Las17 indicates it can be dissected into 20 separate SH3 binding polyproline motifs (PxxP) (P1 through P20, Figure 2.3A). Yeast two hybrid analysis testing for binding of Las17 polyproline motifs to the first and second Sla1 SH3 domains identified five polyproline motifs in Las17 as the binding site for Sla1 (P8-12) (Figure 2.3A-D). Sequence analysis of these polyproline motifs revealed they conform simultaneously

class I (RxxPxxP) and class II (PxxPxR) polyproline motifs consensus, which are termed classI/II motifs. To confirm the specificity of the interaction, proline-to-alanine point mutations were introduced that selectively destroyed the class I/II motifs, but maintained all other polyproline motifs intact (Figure 2.3D). Mutations of polyprolines sequences spanning P8 to P12 completely destroyed binding to Sla1 SH3 domains (Figure 2.3D). Together, these experiments allowed us to map the interaction of Sla1 SH3 domains to specific sequences in Las17 that belong to a new class I/II motif. To corroborate a direct association between Las17 and Sla1 specifically mediated by these class I/II polyproline motifs, a series of GST-fusion binding assays were performed analyzing the capacity of similar fragment used in yeast two hybrid experiments for binding purified Sla1 SH3 domains. The relative level of binding observed in these assays provides similar conclusions obtained by yeast two hybrid analyses (Figure 2.3) and confirmed a direct association between Las17 and Sla1. It is possible that the presence of five class I/II polyproline motifs in Las17 may mediate a strong binding due to an avidity effect with a divalent Sla1 fragment.

Following a quantitative ligand depletion experiment using increasing concentrations of GST-fusion protein containing all five Las17 class I/II polyproline motifs incubated with Sla1 SH3 domains, a Kd of 56 nM for the Sla1-Las17 interaction was determined (Figure 2.5B). The high affinity interaction between Sla1 SH3 domains 1 and 2 and specific Las17 class I/II polyproline motifs is in agreement with the idea of a stable complex between the full length proteins.

4.4 Mutations in Las17 P8-12 sequence affect the stability of the complex and its regulation *in vitro* and *in vivo*

Purified Las17 is not autoinhibited and effectively activates Arp2/3-mediated actin polymerization [1, 2]. By contrast, addition of the first two Sla1 SH3 domains was shown to inhibit Las17 NPF activity [1]. To investigate if Sla1 inhibition is dependent on the same Las17 class I/II polyproline motifs mediating the Las17-Sla1 association, recombinant full length Las17 containing the same polyproline motif point mutations that abolished binding to Sla1 was purified (Figure 2.3D and 2.5B). Pyrene-actin polymerization assays showed that mutations to the full Sla1 binding site (MP8-12) abrogate the inhibitory capacity of Sla1 SH3 domains on Las17 NPF activity (Figure 2.6C-F). This result indicates that the class I/II polyproline motifs identified here are not only central for Las17-Sla1 strong association but are also essential for Las17 negative regulation by Sla1.

Our results suggest that Las17 and Sla1 arrive to sites of endocytosis in a pre-formed stable complex that keeps Las17 in an inactive state. Furthermore, the specific polyproline motifs in Las17 involved in both the *in vitro* interaction with Sla1 and in its inhibition have been identified. These findings suggest that disrupting the physical interaction between Las17 and Sla1 in live cells may lead to a defect in Las17 recruitment to sites of endocytosis or perhaps lack of inhibition of Las17 NPF activity. These possibilities were tested by tagging Las17 endogenous gene with GFP and subsequently introducing the same polyproline motif point mutations that abolished binding to Sla1 and disrupted its inhibition in actin polymerization assays (Figure 2.3D and 2.5B, Figure 2.6C-F). This strain was crossed with one expressing Sla1-RFP or Abp1-RFP from the corresponding endogenous locus. Haploid cells expressing the mutant Las17-GFP (Las17-MP8-12-GFP) and Sla1-RFP or Abp1-RFP were analyzed by

confocal fluorescence microscopy (Figure 2.8, Figure 2.11). In these cells Sla1 arrived 20s before Las17 could be detected at endocytic sites, whereas in wild type cells their recruitment was simultaneous (Figure 2.8). Additionally, an apparent decreased of Las17- GFP patch intensity of mutant cells was observed when compared to wild type cells (Figure 2.9A). Quantification of the fluorescence intensity ratio of Las17-MP8-12-GFP at endocytic patches to cytosol, confirmed a statistically significant decrease in Las17-GFP patch-localization compared to wild type cells. Analysis of Las17-GFP expression levels, by immunoblotting, ruled out impairment in Las17 expression or its stability in mutant cells (Figure 2.9B). These results are consistent with a defect in Las17 recruitment to endocytic sites when its association with Sla1 is compromised.

Confocal fluorescence microscopy analysis of cells expressing Las17-GFP and Abp1-RFP was used to investigate the effect that mutations in class I/II polyprolines have on Las17 NPF activity. Consistent with published studies, in wild type cells Abp1-RFP was detected at endocytic sites 19 seconds after Las17-GFP (Δ time) (Figure 2.11A) [2]. In contrast, Δ time in cells with mutations in Las17 class I/II polyprolines was 9 seconds, which can be explained by dissociation of the complex leading to lack of inhibition by Sla1 (Figure 2.11B). In cells expressing mutant Las17-GFP the Abp1-RFP patch lifetime was increased from 14 to 20 seconds (Figure 2.11). However, in both mutant and wild type cells the maximum Abp1-RFP fluorescence intensities at endocytic sites were unchanged (Figure 2.10A). These results suggest endocytosis likely requires a given amount of Arp2/3 complex-mediated actin polymerization that in cells expressing the mutant Las17 takes longer to be achieved because there are less Las17 molecules at the patch.

Together, *in vitro* actin polymerization assays and live cell fluorescence microscopy analysis demonstrate that Las17 molecules that are unable to bind Sla1 and therefore not in the native complex have the NPF activity readily manifested but are deficiently recruited to endocytic sites. These results support the idea that in wild type cells Las17 recruitment to sites of endocytosis is facilitated by being in a preformed complex with Sla1 in which the NPF activity of Las17 is inhibited.

4.5 Characterization of <u>L</u>as17 novel <u>G</u>-actin binding <u>m</u>odule <u>1</u> (LGM1)

A recent study by Robertson *et al*. (2009) identified a sequence in Las17 capable of binding monomeric actin, independent of the WH2 domain [9]. This site was located within residues 300-422 of the Las17 central polyproline stretch; however, this novel G-actin binding site was not fully characterized. Interestingly, the region in Las17 identified as Sla1 binding site (P8-12) spans residues 300-404. Evidence is presented showing that monomeric actin and the Sla1 SH3 domains compete for binding to overlapping sequences in Las17 (P8-12) (Figure 2.7). This indicates that Sla1 may inhibit Las17 NPF activity at least in part by disrupting the ability of Las17 to interact with G-actin through this novel binding site. To further characterize this novel G-actin binding site, a series of yeast two hybrid assays were conducted to examine the ability of several Las17 fragments for binding to actin (Figure 3.2A). Results from these analyses show that sequences in P8-12 can bind to actin with a binding strength comparable to that observed for the WH2 domain in VCA (Figure 3.2A).

After inspection of Las17 P8-12 sequence, two sites (PRRG and GRRG) with similar hydropathic amino acid patterns as those observed in Las17 WH2 basic sequence (LRKV) were identified (Figure 3.2B). To test the significance of these sequences for Las17 NPF activity,

pyrene-actin polymerization assays were performed using recombinant full length Las17 with arginine to glycine substitutions to both of these arginine-rich sites (Las17-RR-Mut) (Figure 3.2C). Quantification of relative actin polymerization rates shows the mutations in Las17 arginine-rich sites decreased the NPF activity by 73 % when compared to wild type Las17 (Figure 3.2C right panel). These results parallel observations from pyrene-actin assays in which Sla1 SH3 domains are added to the reaction leading to blockage of G-actin binding and a decrease in Las17 NPF activity by 75 % (Figure 2.6, Figure 2.7). These results suggest that the arginines mutated in these two sites are key components of a site in Las17 require for its NPF function.

Additional yeast two hybrid assays were conducted to determine the contribution of these arginine-rich sites for G-actin binding. The same point mutations were introduced to the arginine-rich sequence flanking P11 or the sequence at P12 (Figure 3.2B, D). This assay reveals that both the site flanking P11 and the site at P12 contribute to actin binding but the former is more important, consistent with the differences in the amino acid hydropathic properties observed between these sites and the WH2 domain (Figure 3.2B, D). These results indicate that two unique sets of arginines within P8-12 are part of a G-actin binding module potentially comprised of two G-actin binding motifs.

Confocal fluorescence microscopy experiments were used to demonstrate the significance of these two arginine-rich sites for regulation of actin polymerization in live cells. Analysis of haploid cells expressing mutant Las17-GFP (Las17-RR-Mut) and Abp1-RFP revealed an increase in patch lifetimes for both Las17-GFP and Abp1-RFP (Figure 3.3). The increase in Abp1-RFP patch lifetime is consistent with a defect in Las17 NPF activity that leads to a reduction in the rate of actin filament formation at endocytic sites. A decrease in the rate of

actin filaments accumulation would likely slowdown the internalization step of endocytosis thus explaining the extended Las17-GFP patch lifetime in Figure 3.3.

Together, my results here define a role for the Las17 novel G-actin binding site in actin polymerization and have identified two sets of arginines in this motif as important components for Las17 NPF activity in live cells, which is termed Las17 novel G-actin binding module 1 (LGM1). In the future, additional mutations to other arginines within LGM1 should be analyzed to determine if these also contribute to G-actin binding.

4.6 Syp1 cooperates with Sla1 to inhibit Las17 NPF activity in *vivo* and *in vitro*

Las17 exists in a large biochemically stable complex with Sla1 in which Las17 NPF activity is inhibited. However, two other components of the endocytic machinery, Bbc1 and Syp1, have been shown to reduce Las17 NPF activity *in vitro* and may also contribute to some extent, during Las17 inhibition *in vivo* [1, 3]. However, since Bbc1 arrives to endocytic sites about 20 seconds after Las17 recruitment it cannot inhibit Las17 during the initial ~20 seconds of its recruitment. This is consistent with the analysis of *bbc1*Δ cells presented in Figure 2.12A. On the other hand, Syp1 arrives to endoytic sites much earlier than Las17 and could therefore be an inhibitor during the initial ~20 seconds of Las17 recruitment [3, 10, 11]. Previous studies found *syp1*Δ cells display a relatively mild defect in growth or endocytic dynamics [3, 10-12].

Here evidence is presented indicating that *syp1*Δ cells display a small but statistically significant reduction in the time from Las17 arrival to detection of actin polymerization, suggesting the possibility that Sla1 and Syp1 cooperate to inhibit Las17 during its initial recruitment (Figure 2.12A). This idea is supported by pyrene-actin polymerization assays showing an additive effect between Sla1-SH3-1-2 fragment and Syp1 to inhibit Las17 (Figure

2.12B). The physical interaction reported between Sla1 and Syp1 argues for a potentially more intertwined relationship between these two Las17 inhibitors [13]. In the future it will be important to better delineate the molecular mechanism of Syp1 inhibition of Las17 NPF activity and its cooperation with Sla1.

4.7 Las17 class I/II polyproline motifs are important for normal patch dynamics and CME

The defects in Abp1-RFP patch lifetime observed in cells expressing Las17-MP8-12-GFP, suggested that overall endocytic patch dynamics may be abnormal and endocytosis may be less efficient in these mutant cells. To investigate these possibilities the patch lifetime of early, intermediate, and late coat components in cells expressing Las17-MP8-12 or wild type Las17 were examined (Figure 2.13). Early and intermediate proteins showed a statistically significant increase in their patch lifetime in mutant Las17 cells, but not in late markers (Figure 2.13A-B). These findings demonstrate that the decrease in actin filament accumulation rate in Las17-MP8-12-GFP cells impairs the normal patch dynamics of early and intermediate endocytic components. In addition, a defect in cell physiology in Las17-MP8-12 cell is evident, as reflected by the inability of these cells to adapt and grow at high temperatures (Figure 2.14A). Furthermore, analyses of bulk endocytosis and CME demonstrate that MP8-12 mutant cells display a defect in global endocytic uptake that could be explained by the misregulation of actin polymerization observed in these cells (Figure 2.11).

Overall, the characterization of Las17-MP8-12 mutant cells presented here indicates this region of interaction with Sla1 is important for normal progression of the endocytic patch and efficient endocytosis. Because this complex between Sla1 and Las17 regulates actin polymerization during clathrin-mediated endocytosis, it has been named SLAC. The SLAC

139

complex is important for controlling the initial stages of actin assembly, and SLAC complex dissociation by mutations in the P8-12 region affects the normal progression of CME.

4.8 SLAC activation *in vitro* requires full length Bzz1 and may not be dependent on complex dissociation

Las17 is kept inactive as part of the SLAC complex. The complex is recruited to endocytic sites where it is inhibited for around 20s before it can activate Arp2/3 to promote actin polymerization. Sla1 can inhibit Las17 by the binding of its first and second SH3 domains to specific polyproline sequences in Las17 that overlap with the actin binding sequence LGM1.

Pyrene-actin polymerization assays performed by Sun et al. (2006) identified Bzz1 as a potential candidate for stimulation of Las17 NPF activity [2]. This suggested that activation of Las17 is driven by binding of Bzz1 C-terminal SH3 domains to the central polyproline stretch in Las17. This idea was tested by conducting a series of yeast two hybrid assays that identified a strong (P1) and weak (P10-11) set of Las17 polyproline motifs as Bzz1 SH3 domains binding sites (Figure 3.4). Furthermore, in glutathione S-transferase (GST)-fusion binding assays Bzz1 was found to interact with Las17 confirming a direct association between both proteins (Figure 3.4C). Together, these experiments allowed the identification of the specific polyproline sequences in Las17 that mediate the interaction with Bzz1 SH3 domains.

During this study, two possible mechanisms were proposed for activation of the SLAC complex mediated by the binding of Bzz1 to Las17 (Figure 3.1). One mechanism requires rearrangement of the complex in which Sla1 is kept bound to Las17. The second mechanism is mediated by dissociation of the SLAC complex by the competition between Bzz1 and Sla1 for binding to the Las17 P10-11 site. To differentiate between these two models, a competition assay

was performed using a truncated version of wild type or mutant (MP1) SLAC complex (mini-SLAC) incubated with increasing concentrations of full length Bzz1 (Figure 3.3A). In these experiments increasing binding of Bzz1 to mini-SLAC at 0, 2, and 5µM concentrations of Bzz1 was observed. By contrast, mini-SLAC containing the P1 mutation in Las17 displayed a remarkable binding defect at all Bzz1 concentrations as reported for constructs with the same point mutation analyzed by yeast two hybrid assays (Figure 3.4E, 3.5A). In addition, analyses of both wild type and mutant (MP1) mini-SLAC showed no significant dissociation of Sla1 SH3 domains when incubated with Bzz1 (Figure 3.5A, right panel). These findings confirm the importance of P1 as the main Bzz1 binding site, and suggest that activation of the SLAC complex is achieved without requiring complex dissociation (Figure 3.5C). These results are in agreement with the four fold difference between the binding affinities obtained for Las17-Sla1 (Kd = 56 ± 8 nM) and Las17-Bzz1 (Kd = 0.2 ± 0.01 µM) interaction (Figure 2.5B and Figure 3.5B).

Additional yeast two hybrid experiments presented in Figure 3.4 indicate that full length Bzz1 associates with Las17 P1-20 fragment more strongly than Bzz1 SH3 domains alone, as reflected by an increased ability of the cells to grow in 5uM 3-AT. This observation suggested that sequences in the N-terminus of Bzz1 contribute to Las17 binding, in addition to the SH3 domains, and may therefore be important for SLAC activation. To determine the relevance of sequences at the N-terminus of Bzz1 for SLAC activation, pyrene-actin polymerization assays were performed incubating full length Las17 and Sla1 SH3 domains with different concentrations of purified full length Bzz1 or purified Bzz1 SH3 domains (Figure 3.6A, B). In the presence of sub-saturating amounts of Sla1 SH3 domains addition of Bzz1 SH3 domains

caused a concentration-dependent inhibition of Las17 function while full length Bzz1 stimulated its activity (Figure 3.6A, B).

In summary, the results in this dissertation demonstrate that inhibition of Las17 NPF activity during the initial 20s of its recruitment is achieved by formation of the SLAC complex. Within the complex, the first and second SH3 domains in Sla1 bind sequences in Las17 overlapping those for LGM1, thus blocking G-actin from binding to Las17. Full length Bzz1 binds to specific Las17 polyproline motifs through its SH3 domains activating the SLAC complex likely by exposing LGM1 but without disassembly of the complex. This would allow for actin monomers to bind to Las17 stimulating Arp2/3-mediated actin polymerization at sites of endocytosis. Additional work is required to elucidate the role of the F-BAR domains and the central region of Bzz1 during the activation of the SLAC complex.

The discovery and characterization of the SLAC complex helps define the negative and positive mechanisms regulating Las17 NPF activity thus answering one of the most outstanding questions in the field. This work could also help decipher the roles of other WASp/WAVE homologues to increase our understanding of how these proteins aid in the control of platelet formation and activation of the immune system, which are processes severely affected in Wiskott-Aldrich syndrome patients.

REFERENCES

1. Rodal, A.A., et al., *Negative regulation of yeast WASp by two SH3 domain-containing proteins.* Curr Biol, 2003. **13**(12): p. 1000-8.
2. Sun, Y., A.C. Martin, and D.G. Drubin, *Endocytic internalization in budding yeast requires coordinated actin nucleation and myosin motor activity.* Dev Cell, 2006. **11**(1): p. 33-46.
3. Boettner, D.R., et al., *The F-BAR protein Syp1 negatively regulates WASp-Arp2/3 complex activity during endocytic patch formation.* Curr Biol, 2009. **19**(23): p. 1979-87.
4. Tong, A.H., et al., *A combined experimental and computational strategy to define protein interaction networks for peptide recognition modules.* Science, 2002. **295**(5553): p. 321-4.
5. Di Pietro, S.M., et al., *Regulation of clathrin adaptor function in endocytosis: novel role for the SAM domain.* EMBO J, 2010. **29**(6): p. 1033-44.
6. Holtzman, D.A., S. Yang, and D.G. Drubin, *Synthetic-lethal interactions identify two novel genes, SLA1 and SLA2, that control membrane cytoskeleton assembly in Saccharomyces cerevisiae.* J Cell Biol, 1993. **122**(3): p. 635-44.
7. Howard, J.P., et al., *Sla1p serves as the targeting signal recognition factor for NPFX(1,2)D-mediated endocytosis.* J Cell Biol, 2002. **157**(2): p. 315-26.
8. Mahadev, R.K., et al., *Structure of Sla1p homology domain 1 and interaction with the NPFxD endocytic internalization motif.* EMBO J, 2007. **26**(7): p. 1963-71.
9. Robertson, A.S., et al., *The WASP homologue Las17 activates the novel actin-regulatory activity of Ysc84 to promote endocytosis in yeast.* Mol Biol Cell, 2009. **20**(6): p. 1618-28.
10. Reider, A., et al., *Syp1 is a conserved endocytic adaptor that contains domains involved in cargo selection and membrane tubulation.* EMBO J, 2009. **28**(20): p. 3103-16.
11. Stimpson, H.E., et al., *Early-arriving Syp1p and Ede1p function in endocytic site placement and formation in budding yeast.* Mol Biol Cell, 2009. **20**(22): p. 4640-51.
12. Kaksonen, M., C.P. Toret, and D.G. Drubin, *A modular design for the clathrin- and actin-mediated endocytosis machinery.* Cell, 2005. **123**(2): p. 305-20.
13. Tonikian, R., et al., *Bayesian modeling of the yeast SH3 domain interactome predicts spatiotemporal dynamics of endocytosis proteins.* PLoS Biol, 2009. **7**(10): p. e1000218.

APPENDIX

IN VIVO AND *IN VITRO* STUDIES OF ADAPTOR-CLATHRIN INTERACTION[3]

A.1.1 Summary

Clathrin-mediated endocytosis depends on adaptor proteins that coordinate cargo selection and clathrin coat assembly. Here we describe procedures to study adaptor-clathrin physical interaction and live cell imaging approaches using as a model the yeast endocytic adaptor protein Sla1p.

A.1.2 Introduction

A major endocytic pathway initiates with the formation of clathrin-coated vesicles (CCVs) that transport cargo from the cell surface to endosomes [1-6]. CCVs are distinguished by a polyhedral lattice of clathrin that coats the vesicle membrane and serves as a mechanical scaffold. Clathrin coats are assembled during vesicle formation from individual clathrin "triskelia", the soluble form of clathrin composed of three heavy and three light chain subunits [7,8]. Because the triskelion does not have the ability to bind to the membrane directly, clathrin-

[3]Daniel Feliciano, Jarred J. Bultema, Andrea L. Ambrosio, Santiago M. Di Pietro
 Department of Biochemistry and Molecular Biology, Colorado State University,
 Fort Collins, Colorado 80523, USA

binding adaptors are critical to link the forming clathrin lattice to the membrane through association with lipids and/or membrane proteins [9]. Adaptors also package transmembrane protein cargo, such as receptors, and can interact with each other and with other components of the CCV formation machinery [9].

Over twenty clathrin adaptors have been described, several are involved in clathrin mediated endocytosis and others localize to the *trans* Golgi network or endosomes [9]. With the exception of HIP1R (yeast Sla2p), all known clathrin adaptors bind to the N-terminal β-propeller domain of the clathrin heavy chain [9]. Clathrin adaptors are modular proteins consisting of folded domains connected by unstructured flexible linkers. Within these linker regions, short binding motifs mediate interactions with the clathrin N-terminal domain or other components of the vesicle formation machinery [9]. Two distinct clathrin-binding motifs have been defined: the clathrin-box and the W-box [9]. The consensus clathrin-box sequence was originally defined as L[L/I][D/E/N][L/F][D/E] but variants have been subsequently discovered [10, 11]. The W-box conforms to the sequence PWxxW (where "x" is any residue).

Sla1p (Synthetic Lethal with Actin binding protein-1) was originally identified as an actin associated protein and is necessary for normal actin cytoskeleton structure and dynamics at endocytic sites in yeast cells [12]. Sla1p also binds the NPFxD endocytic sorting signal and is critical for endocytosis of cargo bearing the NPFxD signal [13,14]. More recently, Sla1p was demonstrated to bind clathrin through a motif similar to the clathrin box, LLDLQ, termed a variant clathrin-box (vCB), and to function as an endocytic clathrin adaptor [15]. In addition, Sla1p has become a widely used marker for the endocytic coat in live cell fluorescence microscopy studies [16]. Here we use Sla1p as a model to describe approaches for adaptor-

145

clathrin interaction studies. We focus on live cell fluorescence microscopy, GST-pull down, and co-immunoprecipitation methods.

A.1.3 Protocol

A.1.3.1 Part 1: Incorporation of a GFP tag and selectable marker in the SLA1 gene

1. Apply the Longtine method [17] in order to fuse a GFP tag directly at the 3' end of the *SLA1* gene open reading frame (Sla1p C-terminus) and simultaneously mark the gene with the *E. coli kan^r* gene that allows for G418 selection.

2. Generate a DNA fragment by PCR using as a template the plasmid pFA6a-GFP(S65T)-kanMX6 [18] and the following primers: forward, 5'-CA AGG CAA GCC AAC ATA TTC AAT GCT ACT GCA TCA AAT CCG TTT GGA TTC CGG ATC CCC GGG TTA ATT AA-3', and reverse, 5'-CA TAT AGC TTG TTT TAG TTA TTA TCC TAT AAA ATC TTA AAA TAC ATT AAT GAA TTC GAG CTC GTT TAA AC-3'. The underlined sequence corresponds to the *SLA1* gene specific segment immediately preceding (forward primer) and following the stop codon (reverse primer). Isolate the PCR product by agarose gel electrophoresis followed by DNA purification.

3. Prepare a 50 ml culture *S. cerevisiae* SEY6210 strain (*MATα* ura3-52, leu2-3,112 his3−Δ200, trp1−Δ901, lys2-801, suc2-Δ9 GAL-MEL) [19] in YPD, growing at early logarithmic phase (OD_{600} =0.2-0.6). Spin at room temperature for 3 min at 2,000 x *g*, wash twice with sterile water.

4. Transform the PCR fragment obtained in step 2 into the cells using the lithium acetate procedure [20]. Wash the cells with 1 ml sterile water, add 1 ml YPD and incubate for 4 h at 30 °C in a shaker.

146

5. Spread the cells on YPD-G418 plates to select for G418-resistant transformants, incubate at 30 °C for 2-3 days. Pick colonies and streak them on YPD-G418 plates.

6. Using colony-PCR, identify transformants in which the GFP-kan module was properly integrated with the *SLA1* gene sequences by homologous recombination. Use a forward primer that anneals within the *SLA1* open reading frame and a reverse primer that anneals inside the GFP-kan module. Identify colonies which PCR products have the expected size and verify by sequencing.

7. Screen the colonies by fluorescence microscopy to confirm they have GFP fluorescence.

A.1.3.2 Part 2: Mutation of the variant clathrin box (vCB) in the SLA1 gene

1. Introduce an LLDLQ to AAALQ mutation in the *SLA1* gene (nucleotides 2407-2415) following a two-step approach [15]. First, amplify *SLA1* nucleotides 1207-1410 and 2427-2589 by PCR and clone the fragments into *Not*I/*Bam*HI and *Eco*RI/*Sal*I sites of pBluescriptKS, respectively.

2. Subsequently subclone into the *Bam*HI/*Eco*RI sites a PCR fragment containing *URA3*. Cleave the resulting plasmid with *Not*I/*Sal*I, isolate the *URA3* fragment by gel purification, and introduce it by lithium acetate transformation into the Sla1-GFP strain generated in Part 1, or into TVY614 (Thomas A. Vida Collection, *MAT*a *ura3-52 leu2-3112 his3-Δ200 trp1-Δ901 lys2-801 suc2-Δ9 pep4*::*LEU2 prb1*::*HISG prc1*::*HIS3*) [21]. This will allow to isolate vCB mutants in step 6.

3. Spread the cells on supplemented SD plates lacking uracil. Confirm by colony-PCR and sequencing that the Ura+ colonies contain properly integrated *URA3* replacing the vCB fragment. We call this intermediate strain SLA1-URA3.

4. In a second step, subclone *SLA1* nucleotides 1207-2589 into *Not*I/*Sal*I sites of pBluescriptKS. Using the QuickChange-XL site-directed mutagenesis kit (Stratagene), mutate the vCB residues LLDLQ to AAALQ. Verify by sequencing.

5. Cleave the resulting construct with *Bsg*I/*Age*I, and isolate the mutant vCB containing fragment by gel purification. Cotransform the *Bsg*I/*Age*I fragment with pRS313 (*HIS3*) [22] into the SLA1-URA3 strain obtained in Part 2.3.

6. Spread the cells on supplemented SD plates lacking histidine. Replica-plate His+ colonies onto agar medium containing 5-fluorotic acid to identify cells in which the mutant sequences replaced *URA3*, thus regenerating the *sla1* gene containing the LLDLQ to AAALQ mutation (*sla1^{AAA}*). Confirm by colony-PCR and sequencing.

A.1.3.3 Part 3: Fluorescence microscopy

1. Grow the yeast strains Sla1-GFP and Sla1^{AAA}-GFP generated in Parts 1 and 2 in 4 ml of supplemented SD media at 30ºC in a rotator in the dark until reaching an $OD_{600} = 0.1$-0.4. Spin 1ml of culture in microcentrifuge at 4,000 x *g* for 1 min at room temperature. Discard ~950 μl of supernatant. Resuspend cells in the remaining liquid (~50 μl).

2. Deposit 3 μl of the cell suspension onto a microscopy slide and cover with a glass coverslip. Protect the sample from light.

3. Mount slide on a 100x oil-immersion objective of a spinning-disc confocal microscope.

4. Locate correct focal plane of cells using brightfield illumination or 488 nm laser with appropriate filters to excite and detect fluorescence from GFP.

5. Capture time-lapse images of Sla1-GFP and Sla1^{AAA}-GFP in cells with exposure time of 500 ms (or appropriate value) at an interval of one image per second for 150 seconds. Expected result: GFP labeled punctae will appear on the inner surface of limiting membrane

of the cell, persist for several seconds, and move toward the center of the cell as the signal quickly disappears (indicating coat disassembly).

6. Select a portion of an image in which spots are seen to appear, remain for several seconds, and disappear. Crop this section of the image for each frame of the time-lapse images.

7. Generate a kymograph representing this section of the image in each frame of the 150 second time-lapse image by aligning the frames along an axis corresponding to time elapsed. We use the automate function in Adobe Photoshop but you can also do it manually.

8. Calculate the duration of each spot by manually counting how many seconds (time-lapse frames) the spot is present in the kymograph. Note that each spot should "curve" toward the interior of the cell as it is disappearing, reflecting endocytosis and disassembly of the coat.

9. Compare wild type Sla1-GFP with Sla1^{AAA}-GFP. Repeat to determine if results are statistically significant. Expected result: Sla1^{AAA}-GFP spots persist significantly longer (~80 sec) than wild type (~30 sec) indicating a defect in coat formation [15].

A.1.3.4 Part 4: Preparation of yeast cytosolic extract and total cell extract

1. Inoculate 3 liters of YPD with an appropriate yeast strain, such as TVY614 [21], and grow at 30 °C in a shaker incubator until reaching an OD_{600} = 1-2.

2. Centrifuge the yeast culture at room temperature for 45 min at 3,700 *x g*. Discard the supernatant, add 3-5 ml of sterile water, and pipet up and down until the pellet is completely resuspended.

3. Pour ~150 ml of liquid nitrogen in a 250 ml plastic beaker. Flash-freeze the yeast by adding dropwise into the liquid nitrogen in a circular pattern to avoid agglutination of the frozen pellets. Do not let the pellets thaw, add more liquid nitrogen if necessary.

4. Chill a stainless steel blender container by pouring liquid nitrogen in it. Allow the liquid nitrogen to almost completely evaporate. Add the frozen yeast pellets to the cold blender container. Close the blender container with a cold rubber stopper and grind the yeast pellets for 10 seconds. Invert the container 3-4 times to mix contents and repeat the grinding step twice. The ground frozen yeast will have a powder-like appearance.

5. Chill a funnel and a 50 ml conical tube with liquid nitrogen. Using the cold funnel, transfer the ground yeast to the tube. The frozen ground yeast can be store at -80 °C or used immediately.

6. To obtain a cytosolic extract for the GST-fusion protein affinity assay (Part 5), weight 3 g of frozen ground TVY614 yeast in a 15 ml conical tube and resuspend in 3 ml of room temperature buffer A (10 mM HEPES, pH 7.0, 150 mM NaCl, 1 mM EDTA, 1 mM DTT) containing protease inhibitor cocktail (Sigma).

7. Cap and invert the tube several times until completely thawed and then put on ice.

8. Ultracentrifuge the extract at 4 °C for 20 min at 300,000 x g. Carefully transfer the supernatant (cytosolic extract) to a conical tube using a pipette without disturbing the pellet. Keep the cytosolic extract on ice.

9. Add 100 µl of a 50% (v/v) glutathione-Sepharose slurry in buffer A. It is convenient to cut the end of the tip in order to facilitate pipeting the beads. Rotate at 4 °C for 15 min, spin-down the beads by centrifugation at 4 °C for 2 min at 1,000 x g, and transfer the supernatant (cytosolic extract) to a fresh tube. Reserve 50 µl of extract for input control.

10. To obtain total cell extracts for co-immunoprecipitation experiments (Part 6), use strain TVY614 (WT *SLA1*), the *sla1^{AAA}* strain carrying an LLDLQ to AAALQ mutation generated in Part 2 in TVY614 background, and a *sla1Δ* strain carrying a deletion of the *SLA1* gene

such as GPY3130 [23]. Weight 2 g of the corresponding frozen ground yeast in conical tubes and resuspend them in 2 ml of room temperature buffer A, containing protease inhibitor cocktail (Sigma) and 1% Triton X-100.

11. Cap and invert the tube several times until completely thawed and then incubate on ice for 10 min, periodically mixing by inversion.

12. Transfer the material to microcentrifuge tubes and spin at 4 °C for 15 min at 16,000 x *g* (top speed in microcentrifuge). Carefully transfer the supernatant (total cell extract) to a conical tube on ice using a pipette without disturbing the pellet.

13. Add 100 µl of a 50% (v/v) protein A-Sepharose slurry in buffer A. Rotate at 4 °C for 15 min, spin-down the beads by centrifugation at 4 °C for 2 min at 1,000 x *g*, and transfer the supernatant (total extract) to a fresh tube. Reserve 50 µl of extract for input control.

A.1.3.5 Part 5: GST-fusion protein affinity assay

1. Amplify by PCR a fragment containing the Sla1p variant clathrin-box (vCB) (residues 803-807), clone it into pGEX-5X to obtain pGEX-5X-vCB. Verify by sequencing.

2. Using pGEX-5X-vCB as a template and the QuickChange-XL site-directed mutagenesis kit (Stratagene), mutate the vCB residues LLDLQ to AAALQ to obtain pGEX-5X-vCBmut. Verify by sequencing.

3. Express GST and the fusion proteins GST-vCB and GST-vCBmut in *E.coli* (BL21 DE3), purify using glutathione-Sepharose, elute from the beads with reduced glutathione, dialyze against PBS, and determine protein concentration.

4. Label 3 microcentrifuge tubes: GST, GST-vCB, and GST-vCBmut, and add 1 ml of PBS, 30 µl of a 50% (v/v) glutathione-Sepharose slurry in buffer A, and 50 µg of dialyzed GST, GST-vCB, or GST-vCBmut fusion proteins.

5. Rotate at room temperature for 30 min to allow for binding.

6. Wash the beads 2 times with PBS and 1 time with buffer A. Add 1 ml of yeast cytosolic extract – prepared as described in Part 4 – to each tube.

7. Rotate the tubes 1 h at 4 °C, spin 10 sec at 5,000 x g to pellet the beads, discard supernatant, and quickly wash the beads 3 times with buffer A containing 0.1% Triton X-100, and 1 time with buffer A.

8. Spin down the beads one more time and using a gel loading tip remove as much liquid as possible. At this point the samples can be stored at -20 °C to continue at a later time.

9. Add 15 µl of 2x Laemmli sample buffer to each tube, incubate at 95 °C for 5 min, and spin 10 sec at 5,000 x g.

10. Analyze the samples by immunoblotting using an antibody to the clathrin heavy chain. Expected results: clathrin binds to GST-vCB but not to GST or GST-vCBmut. Also analyze the samples by SDS-PAGE to confirm similar loading of the GST fusion proteins.

A.1.3.6 Part 6: Co-immunoprecipitation assay

1. Label 3 microcentrifuge tubes: WT (wild type *SLA1*), *sla1^{AAA}*, and *sla1Δ*, and add 1 ml of PBS, 30 µl of a 50% (v/v) protein A-Sepharose slurry in buffer A, and 2 µg of a rabbit anti-Sla1p antibody.

2. Rotate at room temperature for 30 min.

3. Wash the beads twice with PBS and 1 time with buffer A containing 1% Triton X-100.

4. Add 1 ml of the corresponding total yeast extracts prepared in Part 4: *SLA1*, *sla1^{AAA}*, and *sla1Δ*. Rotate 1 h at 4 °C.

5. Spin 10 sec at 5,000 x g to pellet the beads, discard supernatant, and quickly wash the beads 3 times with buffer A containing 0.1% Triton X-100, and 1 time with buffer A.

6. Spin down the beads one more time and using a gel loading tip remove as much liquid as possible. At this point the samples can be stored at -20 °C to continue at a later time.

7. Add 15 µl of 2x Laemmli sample buffer to each tube, incubate at 95 °C for 5 min, and spin 10 sec at 5,000 x g.

8. Analyze the samples by immunoblotting using an antibody to the clathrin heavy chain. Expected results: clathrin co-immunoprecipitates with wild type Sla1p but not to with sla1^{AAA}, or in the sla1Δ sample.

A.1.4 Representative Results:
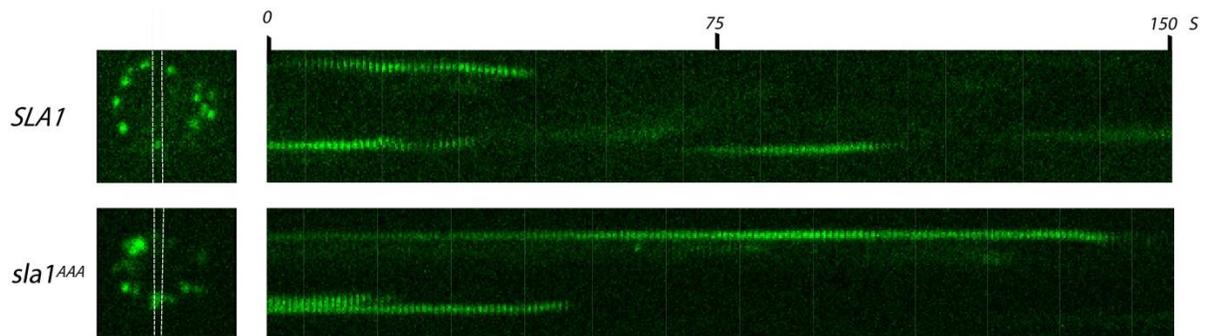
Figure A. 1
Analysis of Sla1p clathrin adaptor at endocytic sites by live cell fluorescence microscopy. One frame (left) from a video and corresponding kymographs (right) of yeast cells expressing Sla1-GFP or Sla1AAA-GFP carrying an LLDLQ to AAALQ mutation. Both wild type and mutant Sla1-GFP were expressed from the endogenous SLA1 locus. Endocytic sites are observed as bright spots distributed in the cell periphery (left images). The area between white lines corresponds to the region from which kymographs were generated. Movies were taken at a frame rate of 1 frame/sec. Notice the longer lifetime of Sla1-GFP in the LLDLQ to AAALQ mutant (sla1AAA) compared to wild type (SLA1).
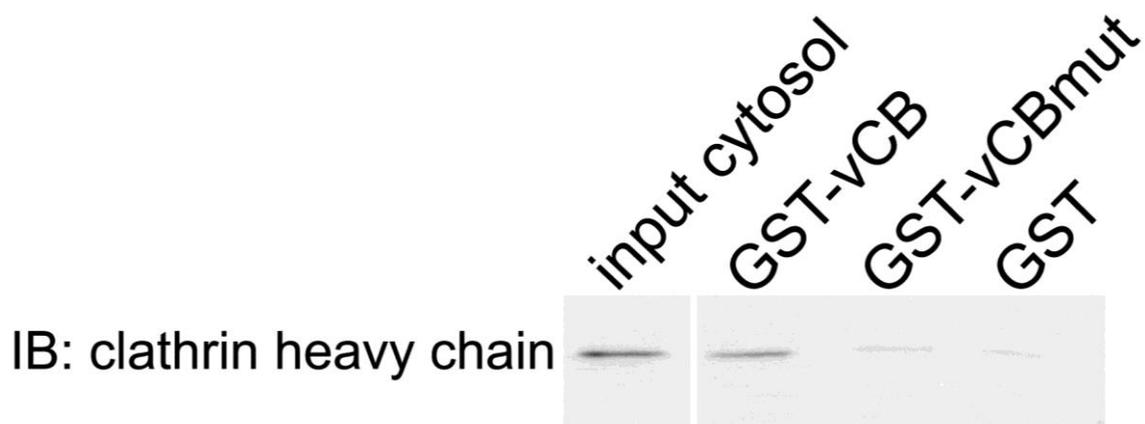
Figure A. 2
Physical interaction between clathrin and the Sla1p-variant clathrin box. GST fused to Sla1p fragment aa798–813 containing the sequence LLDLQ (GST-vCB), the corresponding AAALQ mutant (GST-vCBmut), or GST alone (GST) were bound to glutathione–Sepharose beads and incubated with a cytosolic extract from wild-type yeast cells. The associated proteins were eluted and analysed by immunoblotting (IB) for clathrin heavy chain.

A.1.5 Discussion

Clathrin-coated vesicles (CCV) participate in endocytosis and transport from the *trans* Golgi network and endosomes, conserved pathways that are fundamental to eukaryotic cell biology. The approaches described in this methods paper are useful to study the molecular mechanisms responsible for CCV formation, in particular interactions between adaptor proteins and clathrin. GST-fusion protein affinity and co-immunoprecipitation assays allow testing for physical association between an adaptor (candidate) and clathrin. GFP-tagging and fluorescence microscopy imaging permit dynamic studies in live cells. Yeast cells in particular offer the advantage of easy genetic manipulation to introduce tags and mutations in the adaptor endogenous gene thus maintaining normal expression regulation of the tagged/mutated protein. Similarly, clathrin or other components of the CCV can be tagged with RFP or other fluorescent proteins to facilitate dual imaging studies in living cells [16].

REFERENCES

1. Mellman, I. and Warren, G. (2000) The road taken: past and future foundations of membrane traffic. *Cell* 100, 99-112.
2. Engqvist-Goldstein, A.E. and Drubin, D.G. (2003) Actin assembly and endocytosis: from yeast to mammals. *Annu Rev Cell Dev Biol* 19, 287-332.
3. Conner, S.D. & Schmid, S.L. Regulated portals of entry into the cell. *Nature* **422**, 37-44. (2003).
4. Bonifacino, J.S. and Traub, L.M. (2003) Signals for sorting of transmembrane proteins to endosomes and lysosomes. *Annu Rev Biochem* 72, 395-447.
5. Ungewickell, E.J. & Hinrichsen, L. (2007) Endocytosis: clathrin-mediated membrane budding. *Curr Opin Cell Biol* 19, 417-425.
6. Doherty GJ, McMahon HT. (2009) Mechanisms of endocytosis. *Annu Rev Biochem.* 78, 857-902.
7. Kirchhausen T. (2000) Clathrin. *Annu Rev Biochem.* 69, 699-727.
8. Brodsky FM, Chen CY, Knuehl C, Towler MC, Wakeham DE. (2001) Biological basket weaving: formation and function of clathrin-coated vesicles. *Annu Rev Cell Dev Biol.* 17, 517-568.
9. Owen DJ, Collins BM, Evans PR. (2004) Adaptors for clathrin coats: structure and function. *Annu Rev Cell Dev Biol.* 20, 153-191.
10. Dell'Angelica EC, Klumperman J, Stoorvogel W, Bonifacino JS. (1998) Association of the AP-3 adaptor complex with clathrin. *Science* 280, 431-434.
11. Dell'Angelica EC (2001) Clathrin-binding proteins: got a motif? Join the network! *Trends Cell Biol.* 11, 315-318.
12. Holtzman DA, Yang S, Drubin DG. (1993) Synthetic-lethal interactions identify two novel genes, SLA1 and SLA2, that control membrane cytoskeleton assembly in Saccharomyces cerevisiae. *J Cell Biol.* 122, 635-644.
13. Howard, J. P., Hutton, J.L., Olson, J.M. and Payne, G.S. (2002) Sla1p serves as the targeting signal recognition factor for NPFX$_{(1,2)}$D-mediated endocytosis. *J. Cell. Biol.* 157, 315-326.
14. Mahadev RK, Di Pietro SM, Olson JM, Piao HL, Payne GS, Overduin M. (2007) Structure of Sla1p homology domain 1 and interaction with the NPFxD endocytic internalization motif. *EMBO J.* 26, 1963-1971.
15. Di Pietro SM, Cascio D, Feliciano D, Bowie JU, Payne GS. Regulation of clathrin adaptor function in endocytosis: A novel role for the SAM domain. *EMBO J.* 29, 1033-1044.
16. Kaksonen M, Toret CP, Drubin DG. (2005) A modular design for the clathrin- and actin-mediated endocytosis machinery. *Cell* 123, 305-320.
17. Longtine MS, McKenzie A 3rd, Demarini DJ, Shah NG, Wach A, Brachat A, Philippsen P, Pringle JR. (1998) Additional modules for versatile and economical PCR-based gene deletion and modification in Saccharomyces cerevisiae. *Yeast* 14, 953-61.
18. Wach A, Brachat A, Alberti-Segui C, Rebischung C, Philippsen P. (1997) Heterologous HIS3 marker and GFP reporter modules for PCR-targeting in Saccharomyces cerevisiae. *Yeast* 13, 1065-75.
19. Robinson JS, Klionsky DJ, Banta LM, Emr SD (1988) Protein sorting in Saccharomyces cerevisiae: isolation of mutants defective in the delivery and processing of multiple vacuolar hydrolases. *Mol Cell Biol* 8, 4936-4948.
20. Ito H, Fukuda Y, Murata K, Kimura A (1983) Transformation of intact yeast cells treated with alkali cations. *J. Bacteriology* 153, 163-168.
21. Vida TA, Emr SD. A (1995) new vital stain for visualizing vacuolar membrane dynamics and endocytosis in yeast. *J Cell Biol.* 128, 779-792.
22. Sikorski RS, Hieter P (1989) A system of shuttle vectors and yeast host strains designed for efficient manipulation of DNA in Saccharomyces cerevisiae. *Genetics* 122, 19-27.

23. Piao HL, Machado IM, Payne GS (2007) NPFXD-mediated endocytosis is required for polarity and function of a yeast cell wall stress sensor. *Mol Biol Cell* 18, 57-65.

LIST OF ABBREVIATIONS

AP: Adaptor Protein

APP: Amyloid precursor protein

Arp: Actin related protein

BAR: Bin/Amphiphysin/Rvsp

CA: Cofilin homology domain/ acidic domain

CB: Clathrin box

CCP: Clathrin coated pit

CCV: Clathrin coated vesicle

CDE: Clathrin-dependent endocytosis

CIE: Clathrin-independent endocytosis

CME: Clathrin-mediated endocytosis

CRIB: CDC42/Rac-interactive binding

EHD: Eps15 homology domain

ESCRT: Endosomal Sorting Complex Required for Transport

F-actin: Filamentous actin

F-BAR: Fes/CIP4 homology-Bin/Amphiphysin/Rvsp

G-actin: Globular actin

GBD: GTPase-binding domain

GST: Glutathione S-transferase

ITP: Immune Thrombocytopenic Purpura

Kd: Dissociation Constant

LDLR: LDL receptor

LGM1: Las17 novel G-actin binding module 1

MVB: Multivesicular bodies

NPF: Nucleation promoting factors

N-WASp:

PtdIns3P: Phosphatidylinositol-3-phosphate

PxxP: Polyproline motif

SH3: Src homology 3

SHD: Scar homology domain

SLAC: Sla1 and Las17 regulate actin polymerization during clathrin-mediated endocytosis

TAP: Tandem affinity purification

Tβ: Thymosin beta

Toca: Transducer of Cdc42-dependent actin assembly

VCA: verproline homology domain/ central domain/ acidic domain

vCB: Variant clathrin box

WAS: Wiskott-Aldrich syndrome

WASp: Wiskott-Aldrich syndrome protein

WASH: Wiskott–Aldrich syndrome protein and SCAR homologue

WAVE: WASP family Verprolin-homologous protein

WB: W-box

WCA: WASp homology domain 2/ central domain/ acidic domain

WH1: WASp homology domain 1

WH2: WASp homology domain 2

WIP: WASp interacting protein

WRC: WAVE regulatory complex